Wearable Optical Biometric Tracking System

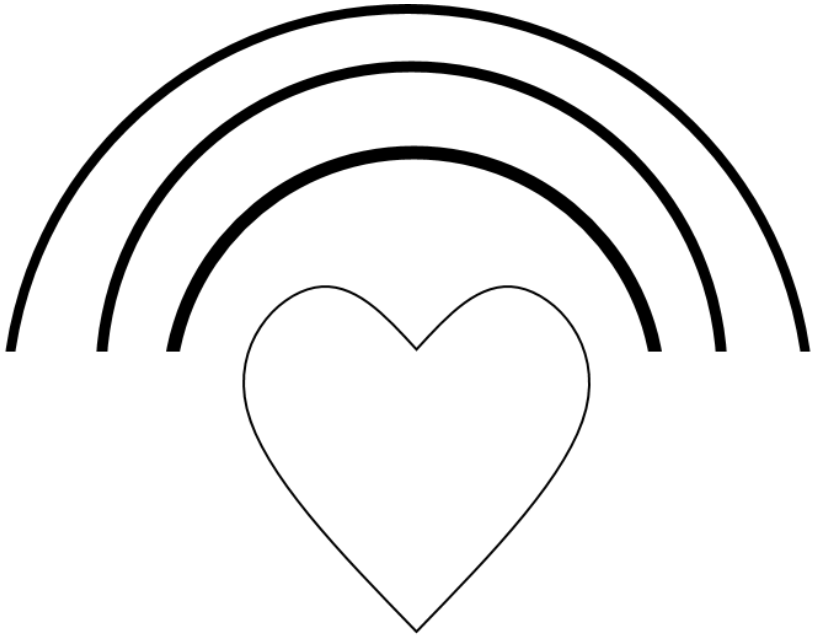

Figure 1.0-1.

Group 2

Tyrone Morales	PSE
Christopher Bormey	EE
Scott Perryman	EE/CpE
Cody Showers	CpE

University of Central Florida
College of Engineering and Computer Science

Senior Design 1
EEL4914 Spring 2022
Dr. Lei Wei, Dr. Samuel Richie, and Dr. Aravinda Kar

Project Documentation

Table Of Contents

1.0 Project Executive Summary

The wearable optical biometric tracking system proposed by our group was a mobile friendly, and easy-to-use device that enables users to monitor their cardiovascular health in their day-to-day life. The device utilizes PPG technology, interfacing with a user's personal device, such as their smartphone, to collect and store biometric data for an extended period of time such that a user can observe their progress with respect to their cardiovascular health with ease. With our device, we hope to enable users to take charge of their cardiovascular health and make improvements by providing them a method for benchmarking their cardiovascular performance and facilitating the access to health feedback.

This project had a few goals in mind. First and foremost being the ability to measure and provide feedback on the 4 following biometrics: Heart-rate, Heart-rate variability, Blood oxygenation, and skin temperature. All of the biometrics are tied to cardiovascular health as will be explained later in the document. Another basic goal this project intended to achieve is to wirelessly communicate with a personal device to facilitate the system's operation. Further the project it was our intention to construct a highly efficient optical sensor that collects the PPG signal with the least amount of noise and errors possible. The advanced goals of our group include providing a high-level of accuracy with respect to marketplace ready products, and the reduction of common sources of errors present in PPG signals, such as, motion artifacts and light-attenuation related issues from the variation of people's skin. The stretch goals for our group include deriving advanced biometrics embedded in the PPG signal such as blood pressure and blood glucose although these were not realized. These are biometrics that are particularly difficult to extract and only recently in academia have reached moderate levels of accuracy with respect to alternative technologies.

The objectives of our group were divided according to the necessary modules for the device to function. The objectives include the design and construction of; a sensor module to generate a PPG signal from a user's skin, a signal processing module to extract the necessary biometric via signal analysis, a communication module to send data to and from the person device, and a power system to supply the necessary energy to system in a compact and efficient manner. All these objectives have an additional consideration for size due to the planned wearable nature of the device. All of these were successfully realized individually however integration proved challenging and issues cropped up for the final implementation. Specifically the bluetooth module would connect but no read data, board issues and shorts prevented the use of our primary and most complicated custom pcb. Although we utilized our custom sensing pcb, we did not have as many sensing photodiodes as originally planned and the thermal sensor gave us problems with the final implementation.

2.0 Project Description

2.1 Project Motivation and Goals

Mindful monitoring of one's cardiovascular health is a useful habit to establish in the modern day as cardiovascular disease (CVD) is the leading cause of death worldwide. Identifying an individual's personal cardiovascular biometrics, such as heart rate, is a good approach towards analyzing their risk for CVD, as well as monitoring progress towards better cardiovascular endurance. There currently exist a few different methods to extract cardiovascular biometrics, with one of the most popular being an EKG system, in which multiple electrodes generate an electric signal with embedded cardiovascular information. While this method is considered the gold standard by the medical community, it offers disadvantages with regard to personal health tracking as using EKG systems can be cumbersome to implement in day-to-day life due to the need for various probes for measurement. Optical sensors provide a significant advantage in this regard due their ability to be implemented in small dimensions that facilitate casual wearable designs. An opto-electronic technique that is becoming increasingly used in personal biometric tracking systems is the generation of a PPG signal via an optical sensor system, and subsequent processing by an electronic system.

A PPG sensor system obtains information about a person's cardiovascular system by measuring the change in volumetric blood flow from blood vessels in the skin. Given that the PPG signal is derived from a person's blood flow, various biometrics that could not be extracted from techniques like an EKG are potentially possible given careful enough analysis of the PPG signal. It is not unusual to derive biometrics such as heart-rate, heart-rate variability, and blood oxygenation from the PPG signal. In addition to the previously stated biometrics, other critical health-related biometrics such as blood pressure (diastolic and systolic), blood glucose, and arterial stiffness can be derived from the PPG signal and are currently the focus of various biomedical engineering researchers. Research in this academic field has also focused on the reduction of errors that affect the signal quality of PPG signal as it is a prerequisite to accurate extraction of biometrics, although a noticeable amount of developments done in these studies has yet to be implemented in commercially available devices.

Due to the great potential that PPG technology offers in the future and the advantages it currently offers in mobile health monitoring, a large number of commercial PPG-based devices have been developed and sold in the health device industry. A push for more fitness-oriented PPG-based health tracking devices can be seen in the marketplace from such companies as Fitbit and Polar via their mobile-device compatible products.

Our group's motivations for this project were to develop a biometric tracking system that is convenient to use for the majority of people so that they can accurately know their cardiovascular health within their day-to-day life. An additional motivation of our group is to attempt to bridge the current gap between the academic developments of PPG system designs and the marketplace-friendly designs that are commonplace of commercial products. This second motivation is meant to assess the feasibility of optimized PPG system designs with consideration to cost, time and practicality.

Our group's basic project goals were to design and construct a non-invasive wrist-worn biometric monitoring device via the processing of optical bio-signals. The optical sensor will ideally be designed such that notable sources of errors with respect to signal acquisition are considered and mitigated as best as possible given present constraints. The proposed device will be able to interface wirelessly with a personal device via a health monitoring application that will store biometrics for an extended period. The long-term storing of biometric information enables a user to observe trends with respect to their biometrics to assess their cardiovascular health's improvements or deterioration. The principal biometrics that are to be collected for the basic design goals are the following: Heart rate, Heart Rate Variability (HRV), Blood oxygenation concentration (SpO2), and Skin temperature. The ability to monitor heart rate, in particular resting heart rate, is important for diagnosing conditions such as tachycardia (>100 bpm) which can lead to cardiac arrest if left untreated. HRV is important to monitor as it provides information about the body autonomic nervous system which regulates a large number of important cardiovascular tasks. Typically, a high variability is associated with better cardiovascular health and, to a lesser degree, mental health as it gives insight to a person's stress levels. Blood oxygenation levels give insight into the health of the body's organs and tissues. When insufficient oxygen is transported to a person's tissues, the cells that comprise them begin to suffer, leading to difficulty of function for that particular organ. Often respiratory issues can be diagnosed via oxygen levels before such symptoms as difficulties of breathing manifest. There is an established correlation between the development of congestive heart failure and the body's ability to thermoregulate, often indicated by lower temperatures. Skin temperature is able to be measured via optical sensors and thus can give an insight into the body's thermoregulation.

The advanced design goals of our project include improvements in the accuracy of the principal biometrics collected such that they meet the relative accuracy standards. It is worth noting that for PPG devices there are no officially established standards for accuracy given the recent implementation of the technique. For this reason, the standards we are using for comparison are that of commercially available devices. Another advanced goal is the reduction of motion artifacts in the PPG signal. Motion artifacts are common signal noise resulting from movement of the sensor during signal acquisition and processing. By mitigating motion artifacts, the device will not be accuracy limited for non-resting measurements during exercise. The final advanced goal of the

device will be to provide the same level of accuracy for people who have darker skin tones, high BMI, and have dark tint tattoos. This goal arises from the base decrease in accuracy of the PPG system due to the interaction of light and skin when certain parameters are increased (in these cases, absorption and thickness).

The stretch goals that our group were to tackle if enough time is allocated include the collection of more difficult to obtain cardiovascular biometrics such a blood pressure (diastolic and systolic), and blood glucose. Hypertension (high blood pressure) is often referred to as “the silent killer” due to its fatal consequences when left unchecked along with its lack of symptoms. Monitoring blood pressure levels is paramount to avoiding hypertension, but often requires bulky and uncomfortable methods for acquisition. In the last few years, researchers have been able to design and construct PPG systems that measure both types of blood pressure to varying levels of accuracy by utilizing advanced machine learning techniques that assess subtle features of the PPG signal and its higher order derivatives. The stretch classification of this goal arises from the complexity of the software aspect of these designs. Blood glucose levels are of concern for people with diabetes and ultimately induce damage to your body’s blood vessels. Convenient and cost-effective blood glucose monitoring methods are often invasive and can cause varying levels of pain. Similar to blood pressure methods, blood glucose can be derived from the PPG signal given the proper identification of signal features and analysis algorithms.

2.2 Project Objectives

The project objectives this group set were divided into two subsections: current objectives for which defined courses of action have been devised and are essential to the fundamental functions of the project; and long term objectives where the course of action is less defined and still in a more conceptual stage of development. The classification of objectives are subject to change as progress is made through project development.

2.2.1 Current Objectives

Our group’s initial objectives were related to the current proposed design as well as market-research methods of how to cost-effectively implement the necessary modules for the construction and function of the device.

To achieve the goal of error-minimized signal acquisition from the optical sensor, we planned on carefully designing the sensor’s parameters by taking into consideration the expected light-skin interactions and optical characteristics of the photonic components. The light-skin interactions are going to be modeled via rough calculation through python code and possible simulation softwares, such as COMSOL Multiphysics, to get a workable range of needed optical power illumination on the skin. The coupling of back reflected light from the skin to the

detector is also of interest for optimized sensor design and will be considered when setting the separation parameters of the sensor to skin, as well as the components themselves. Further optimization of the optical sensor is being considered with respect to refractive index matching to reduce Fresnel losses.

To achieve the goal of having the device be relatively low-profile and wearable, we took into consideration the size of our components and overall design at each step of the project. We planned on designing an integrated schematic that connects all the PCB-compatible modules in a space efficient manner. Spatial consideration for the mechanical designs must be also made, as the final product included solid and encapsulating casings to provide structural support and optomechanical functions. Limiting the dimensions of each module to an arbitrary but reasonable cubic measurement is the current approach our team is taking to consider this objective. The modification of the cubic measurements as components are selected or substituted was an ongoing process as the project progressed. Even though we had component failures, the final design was wearable and light although a bit bulkier than originally imagined.

Our implementation plan for the wireless communication system had to wait until we had a module that we could work with to test the system. Bluetooth development was supposed to be straightforward according to our research. Although we have begun planning the structure of the data to be transmitted, we were counting on the pairing procedures and two way communications work as intended before moving forward. Testing and further development on this system was reliant on waiting for the BLE module enabled system on chip to arrive. It turned out to be much more complicated than originally advertised and was one of the major sticking points for failure in this project.

As for the external application development, there are some active items we are currently fleshing out. First, we have allowed the data requirements and biometrics which we want to measure to inform the database design. Early on with a blueprint in hand, we are in the phase where a database schema could be prototyped from this design and begin logical unit testing. This data organization also informs a logical organization to the UI of the application. We then used this rough framework to inform the UI flow from this data organization. Once the UI framework was up in very early stages the midterm demonstration provided some feedback about the original design. This helped inform us on the application UI flow to verify it made sense and all data was presentable. Using this back to front design required us to update UI elements and polish the look later. Based on this feedback nearly the entire UI was redesigned. This was to accommodate our likely audience of reviewers criticizing the functionality of the design from the perspective of a video likely on a small screen. This meant large UI elements to enhance clarity. Finally, at this point we were in the process of taking the MATLAB Prototype of the signal analysis algorithms and converting them to a language that the hardware can understand. This will have to be implemented inside the app to be utilized.

As a biometric extraction device the signal processing methods and techniques will be a weight bearing piller for the success of this project. By pulling from Communication and sampling theory, it is possible to design and rigorously prove that our techniques are best in slot. Abstractly, this portion of the project can be broken up into three main objectives. First, sample without losing any information pertaining to the biometrics we would like to measure. Second, filter the digital signal to attenuate any additive white gaussian noise present. Third, extract the key features of the signal to make the prediction.

Sampling at two times the highest frequency component of a band limited signal has been proved by Nyquist to result in a lossless translation to a digital signal. The human body is a relatively low frequency system so to meet this objective sampling at 1kHz. To achieve our second goal we will use a integrate and dump low pass filter to remove all noise above 100Hz. This will also allow us to downsample, reducing the memory usage of the signal by a factor of 10. This will also increase our signal to noise ratio by a factor of 10. Lastly we must extract the key characteristics. To do this we will implement a peak detection algorithm that will approximate the time that each peak occurs to make the best possible predictions for heart rate and heart rate variation. Next, we will perform a fast fourier transform of the signals to predict the blood oxygen percentage.

When devising a power delivery system for the device, staying within size constraints is of utmost importance. To make the device wearable and portable, it must be battery powered, and to make it utilitarian, it must be ergonomic and avoid an overtly bulky battery. The battery itself will not occupy enough space on the wrist to make its presence felt while in use, and to achieve that a small form factor battery that can output high currents for several seconds will be implemented. The latest battery technologies must be employed to ensure the device could be powered for at least an hour continuously while outputting high current levels whilst being powered by a battery comparable in size to a quarter.

2.2.2 Future Objectives

Our group's future objectives and stretch goals were all pushed out beyond the end of the semester. What was functioning for the final demonstration did not include any of our advanced or stretch goals unfortunately. These objectives related to advanced and stretch goals that require multiple device modules to already be established and functional. Their implementation would have provided the system a competitive edge with other market available devices.

The advanced goal of implementing a dynamic illumination scheme for the emitter system requires consideration with regards to the on-device computational capabilities, as well as the sensor illumination characteristics. To develop a dynamic illumination algorithm, we planned on establishing 3-4 possible optical power levels of illumination that will correspond to different amounts of acceptable attenuation resulting from the wide variation of optical properties of skin in a large population. The algorithm will adjust the level of

optical power output depending on the quality of the previously collected signal right after signal acquisition, therefore a control condition must be set between the microprocessor and the LED drivers. This was ultimately not implemented due to issues programming a calibration algorithm for the AFE.

The advanced goal of having the device be motion resilient is a challenge with respect to quantifying what 'motion resilience' is, as well as deciding on a method for implementation. The ideal implementation of this goal is based on a method proposed by a research paper in which multiple sensor channels were used in conjunction with an inertial motion unit (IMU) to determine and attempt to correct motion artifacts at the presence of motion. This method uses individual analysis and processing of each channel collected signal and recreates a 'cleaned' PPG signal using sections of the collected signals. Due to the complexity of the algorithm, our group might use alternative methods of providing motion resilience, such as selecting the least affected channel and possibly indicating a resampling if none of the channels are usable.

2.3 Requirements Specifications

The purpose of this chapter will be to review the specifications outlined that informed design decisions for the project. Initially this will review general project specifications. It will then continue into the specifications for specific modules as they are applicable to the system.

2.3.1 General Project Specifications

General project specifications refer to broad requirements of the project that may not cleanly fit into a specific category but may be essential to the design. These specifications can be found in the table below (Table 2.3.1-1)

Number	Description	Magnitude	Units
1	The device shall have multiple modes of operation: Off, ON: Stand-by, ON: Data Acquisition, ON: Data Transmission & Presentation.	4	Modes
2	Device shall produce predictions for the following biometrics: Heart Rate, Heart Rate Variability, Blood Oxygenation, Temperature.	4	Biometrics

3	The device size should be compact for the contact design (WxLxH)	~8x4x4	cm
4	The device size should be compact for the non-contact design (WxLxH)	~18x24x30	cm

Table 2.3.1-1. General Specifications

2.3.2 Photonic Specifications

Photonics Specifications refers to the requirements of the hardware relating specifically to the photonics modules required for the device's operation. These specification can be observed in the table below (Table 2.3.2-1)

Number	Description	Magnitude	Unit
1	The wavelength range of the illumination source should be in the VI spectrum to IR spectrum.	500 - 1000	nm
2	Photodetector(s) should have a high responsivity at the selected wavelengths of the illumination source(s).	>0.25	A/W
3	The emission spectrum of the illumination source should not vary from it's characteristic wavelength by more than 20 nm	<20	nm
4	The detection module must be designed such that ambient light only comprises less than 5% of detected light.	5%	W

Table 2.3.2-1. Photonic Specifications

2.3.3 Signal Analysis Specifications

Signal Analysis specifications refers to the specific metrics of the performance and application of signal analysis in the system. These specifications can be seen in the table below (Table 2.3.3-1)

Number	Description	Magnitude	Unit
1	A/D converter shall sample at a rate of at least.	100	Hz
2	Signal to noise ratio shall be at least.	30	dB
3	Hardware latency should be less than	0.5	s
4	This process shall produce an estimation of heart rate, heart rate variability, blood pressure, blood oxygen content, and temperature no less than once every second when in data transmission and presentation mode.	1	s
5	The bias of the distribution of any of the biometric predictions on any single user should not be more than away from the true value.	5	%
6	The variance of the distribution of any of the biometric predictions on any single user should be less than.	5	Unit^2

Table 2.3.3-1. Signal Analysis Specifications

2.3.4 Physical/Power Specifications

Physical/Power specifications refers to the overall physical design of the device in the system and the power requirements of the external device. These specifications can be seen in the table below (Table 2.3.4-1)

Number	Requirement	Magnitude	Unit
1	Compact PCB that can fit on the wrist	2000	mm^2
2	Enough battery life to withstand a presentation and testing	3600	s
3	Low Power Consumption	<200	mA
4	Light weight	<500	g

Table 2.3.4-1. Physical/Power Specifications

2.3.5 Software Specifications

This section refers to the requirements of the design related to the transmission and the application's ability to receive, display, and store the data for the system. The software system will be responsible for displaying the measurements and will be constrained by these measurements. The specifications can be seen in the table below (Table 2.3.5-1). The first two of these specifications were met by the BLE standard. Data rates can be larger for this medium and transmission range of 3ft or just outside one's person reach are exceeded by this medium assuming there is not too much interference. The long term data storage was more a testament of the size of the data required to mee this. As it turns out with nearly 10 times the desired metrics the storage space used does not exceed 0.5MB. This is on the order of 1/10000th of the smaller storage capabilities of these mobile platforms. There is more information on this topic in the Software Testing section.

Number	Description	Magnitude	Unit
1	Transmission range	3	ft

2	Data Transmission Rate	1	Mbps
3	Store User Data Long Term	365	day

Table 2.3.5-1. Software Specifications

2.3.6 Biometric Measurement Specifications

This tool is intended to provide an inexpensive tool for the purposes of education rather than a diagnostic tool. To that end we can make some reasonable assumptions about the ranges of the metrics we are trying to measure. Anything outside of these ranges will not be considered when designing the display of the application or notifications inside the application. Minimums and maximums of the metrics are included in Table 2.6

Heart rate refers to the number of times a heart pumps blood during a fixed period. In this case the standard is measured in beats per minute. Although a low resting heart rate can be an indicator of cardiovascular fitness and strength, too low can be detrimental to health or even mean death.

Heart rate variability refers to the difference in time between beats of heart. Although the rate of a heart beat may be fixed, this is an average which can have a variable interval between. This metric is identified by the difference in timing between beats during a fixed period. This measurement is most accurate over long periods however, an estimation can be made by a much smaller window.

Skin Temperature refers to the amount of heat emitted by the skin of the user. This can be affected by the environment and go beyond reasonable health ranges. Operation of this device will assume that skin temperature does not go below freezing or above a temperature where fever would likely induce brain damage. Either of these cases would go beyond reasonable bounds for a tool like this one and medical attention should be sought immediately.

Arterial Oxygen Saturation refers to the percentage of oxygen concentration in the bloodstream. A healthy oxygenation level will approach 100% but excess will escape the blood into the environment. Below 95% often users should be seeking medical attention but this does not represent a good lower bound of the reading. Oxygenation can vary due to a number of factors but cannot possibly be lower than 0%. These biometrics are outlined Table 2.3.6-1 below.

Number	Description	Magnitude	Unit
1	Heart Rate Min	0	bpm
2	Heart Rate Max	600	bpm
3	Heart Rate Variability Min	0	ms
4	Heart Rate Variability Max	1000	ms
5	Skin Temperature Min	0	C
6	Skin Temperature Max	60	C
7	Arterial Oxygen Saturation(SaO2) Min	0	%
8	Arterial Oxygen Saturation(SaO2) Max	100	%

Table 2.3.6-1. Biometric Measurement Specifications

2.4 Quality of House Analysis

The house of quality below (Figure 2.4-1) shows the sacrifice of parameters in developing this device. The legend for this figure is found in the table below that (Table 2.4-1). By using this form of analysis we plan to optimize the balance between the customer's and engineering requirements.

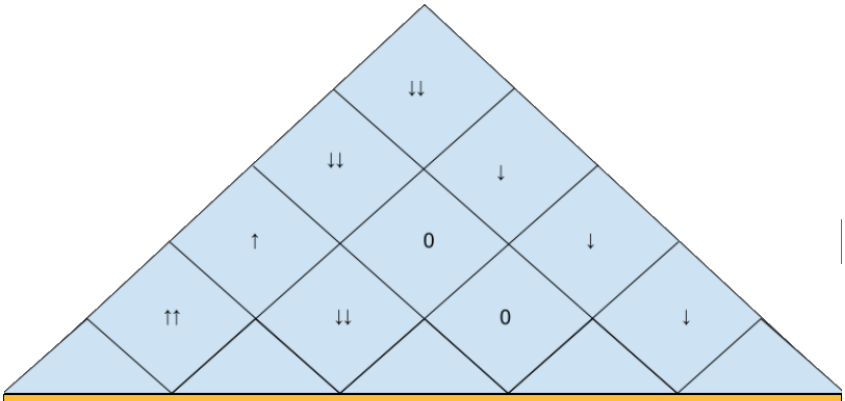

			Engineering Requirements				
			Power consumption	Power Storage	Dimensions	Data-Rate	Range of Connectivity
			-	+	-	+	+
Market Requirements	Ease-of-use	+	0	↑	0	0	↑
	Interconnectivity	+	↓	0	↓	0	↑↑
	Cost	-	0	↓↓	↑↓	↓	↓
	Ergonomics	+	↑	↓	↑	0	↓
	Accuracy	+	↓	0	↓	↑↑	0

Figure 2.4-1. House of Quality

Legend	
+	Positive Polarity
-	Negative Polarity
↑	Positive Correlation
↑↑	Strong Positive Correlation
↓	Negative Correlation
↓↓	Strong Positive Correlation
0	Neutral Correlation
↑↓	Complicated/Nonlinear Correlation

Table 2.4-1.

Due to the many components that change with size, a nonlinear correlation appears with size and cost. As you increase the size of the device, the cost for the wearable casing will increase but the cost for the semiconductor components will decrease. Inversely, as you decrease the size of the device, the cost of the casing will decrease but the cost of smaller integrated circuits will increase.

The red line is the cost of the wearable case as we increase the device size and the blue line is the cost of the Integrated circuits that build the device. The green

line is the summation of the two components representing the total cost of the device. This relation is outlined by the graph below in figure 2.4-2.

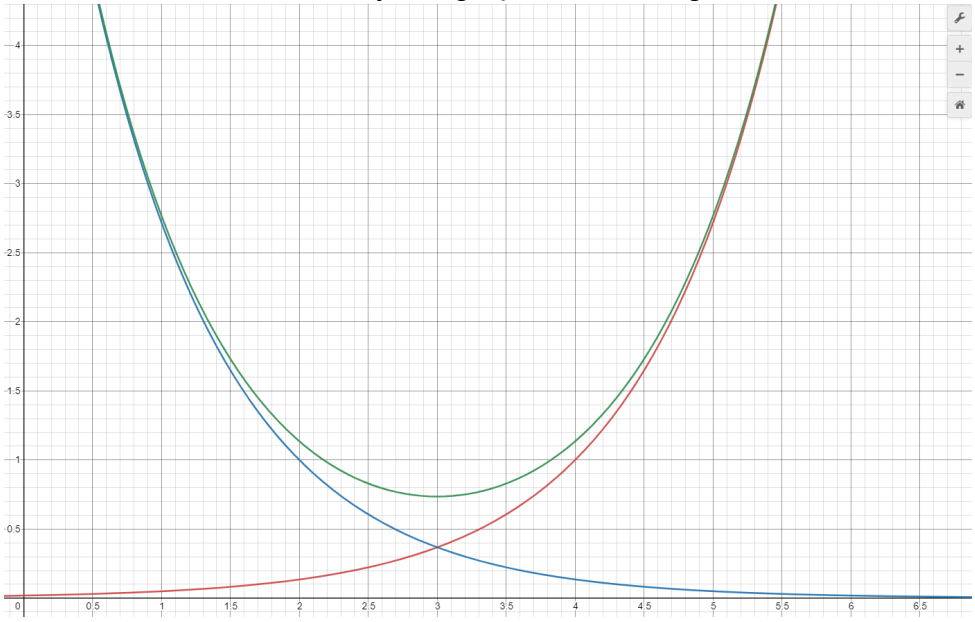

Figure 2.4-2.

3.0 Research related to Project Definition

3.1 Existing Similar Projects and Products

This proposed system aligns clearly with the market demand as there are several applications in research, design classes such as this one, and active market products. Reviewing these existing and proposed systems is integral to informing design and setting benchmarks for the design and specific requirements to achieve.

3.1.1 PetAid Harness

The PetAid Harness is a senior design project completed in the summer of 2020 which focuses on offering a similar device except this one would monitor biometric signals extracted from a pet dog or cat. This project also utilizes optical sensing for the derivation of biometrics such as heartbeat, albeit in an integrated pre-purchased solution since it fills a different niche. The sensors and microcontroller of this device were powered by a different set of batteries than the GSM module, which used its own battery for power, an idea which we have considered since we also have a specific module that is very power hungry, namely the sensors because of all the LEDs.

3.1.2 GOLD

A previous senior project by the name of GOLD appears to be very relevant due to its similarity in goals. Though it is proposed to detect a different biometric, the

similarity comes with the intent of making the prediction non-invasively. GOLD, or Glucose Optic LED Detector, works by taking advantage of the changing frequency response of skin and blood. Because this channel's response changes as a function of the oxygen, glucose, etc. one can extract these parameters by probing the channel with different frequencies and measuring its response. This is mainly where our project and GOLD express similarities.

3.1.3 Consumer Device comparison

In the realm of wearable devices designed for health monitoring marketed as fitness or wellness devices which monitor health statistics with these sorts of sensors the number of options is continually expanding. Many of these options fall into one of two camps, either as fitness or wellness monitoring devices or precision medical devices marketed to clinicians and medical professionals. The market seems to have settled on some standards which also align with this proposed design.

When reviewing the market leaders on wearable devices it would be negligent to not mention the current and recent market leaders of this field. Statista (Laricchia, 2022) organizes this data on their site by quarterly shipments and has a breakdown of the top contributors of the market since 2014. Apple has held a market share of over 30% since 2019 and was a significant portion of the market since 2015. Prior 2020 one could not ignore the influence of FitBit either. In 2014 they held over 38% of the market share, although this has dwindled their influence on the market they are a household name and have been a major player for most of the decade.

The Apple Watch Series 5 is a good example of one of the products that Apple has developed for its wearable fleet. This wearable device fits on a user's wrist and incorporates both an ECG as well as a PPG in order to extract biometrics for its users. These devices retail for nearly $200 and can range depending on features to nearly $400.

Fitbit's showing in the market isn't what it used to be but they still are releasing productions such as the Fitbit Versa 2. This platform uses a PPG to extract blood oxygenation, heart rate, skin temperature, and heart rate variability. This model is a little lower on the market price range coming in below $200 slightly. A comparison table of some of the market leaders is below in table 3.1.3-1.

Product	Features	Price
Apple Watch Series 5	• PPG sensor +ECG sensor • Heart Rate & Heart-Rate	$400

	Variability Measurements	
Fitbit Versa 2	• PPG sensor • Blood Oxygenation, Heart Rate, Heart-Rate Variability, & Skin Temperature	$179.95
Polar M600	• PPG sensor • Blood Oxygenation & Heart-Rate Measurement	$179.95

Table 3.1.3-1.

Some market push and innovations are something to the wellness and fitness market are also coming from lesser known competitors or competitors with a more focused market. One such example of such a consumer device is the Oura ring. This device is designed to fit in the formfactor of a wearable ring. The device tracks blood oxygenation, heart rate, and heart rate variability as is becoming more standard with PPG sensors. They also track respiration, temperature, and sleep patterns. The gathered data is transmitted to an application designed for mobile devices through a Bluetooth connection. There is significant documentation on their marketing page indicating their accuracy for heart rate and heart rate variability but much less on the other metrics they advertise. They boast a battery life of nearly a week, water resistance up to 100m, and a much smaller form factor than most of their competitors.

Similar devices are also common in the medical field such as Masimo's Radius PPG Tetherless Pulse Oximetry system. This product is marketed less to a consumer market and more towards clinicians and other healthcare professionals. Despite this there are similarities with this proposed design. Despite being medical grade equipment they also use bluetooth wireless receivers to establish connections with their monitoring devices. However unlike the consumer products there is a physical piece of hardware dedicated to monitoring. Although consumer products might attempt to measure or document other biometrics the Masimo PPG tetherless system focuses more on the strengths of PPG and advertises its ability to help keep track of patients, easing the processes of health practitioners rather than the wearer of the device. Being a medical grade device, the sensing limit still is comparable with approximately 96 hours of monitored time. One of these systems including a monitor can end up well over 10 times what some of the consumer options cost at nearly $4000.

In this design the goal is to implement comparable features to a lot of the market, hopefully at a potentially reduced cost. At least one area, the form factor of this device will be larger than all of the market examples listed here. This is partially to reduce cost, because as the components get smaller with the same capacity their price tends to increase quickly. However this also will allow the design to incorporate multiple PPG sensing modules to confirm accuracy. Many of the market designs also imply readings during heavy motion and activity, but this can introduce significant noise. The device proposed will likely have a weakness in this area, as mitigating this noise is an active research topic and is not completely solved yet.

3.2 Relevant Technologies

The relevant technologies presented in this chapter provide similar or alternative methods to measure the basic biometrics our system shall retrieve. Certain technologies outlined in this chapter will be used as benchmarks for the levels of accuracy provided from our group's design.

3.2.1 Heart-Rate Measurement Technology: Electrocardiograms

Electrical impulses are generated and dissipated from specialized tissues in order to stimulate the heart to pump blood from the rest of the body. Electrocardiograms, often abbreviated ECG or EKG, take measurement of this electrical activity in the body. Measurements are taken generally by attaching electrodes to a patient's chest, arms, and leg. These electrodes are sent to a machine in order to print and interpret the readings. This is generally considered a noninvasive procedure as it rarely requires much more than possible shaving of areas where the electrodes need to be attached. There is sometimes discomfort when removing these electrodes but otherwise should not require any other procedures or recovery upon completing the test. Often this test requires the patient to not move or talk and to remove clothing and jewelry from their upper body to prevent influencing the results. This test measures several cardiovascular biometrics including heart rate, and rhythm irregularities, heart oxygenation, and detecting heart attack; Often this test informs doctors if further testing or care is required.

3.2.2 Blood Oxygen Measurement Technology: Pulse Oximeter & Blood Oxygen Analyzers

The Pulse Oximeter is one of the leading competitors in oxygen reading medical devices. There are two main ways Pulse Oximetry is conducted, transmissive and reflective. The most common method used is transmissive, where two wavelengths are passed through a thin part of the body and received by a photodetector on the other side. This method tends to be slightly more accurate. Reflective pulse oximetry works by letting the two wavelengths penetrate into the skin and reflect back out where the photodetectors. Because our product is a wrist wearable it was necessary to take the reflective approach. In fact our

product utilizes reflection exactly. The signal processing section of this documentation explains exactly how pulse oximetry is done using red and infrared wavelengths.

Blood Gas Analyzers (BGA) are a medical technology that can provide high-level accuracy measurements of the concentration of gasses, such as oxygen, in a person's blood. These devices function by measuring the partial pressure of oxygen in a person’s arterial blood sample to generate a level of oxygen concentration. This process requires a blood sample from the person whose level is to be tested, therefore is an invasive method of analysis. The blood sample is often processed to remove any additional air bubbles or possible gasses that would be present in the sample. The implementation of this technology is usually found in clinical, or research environments due to their high costs and bulky nature. The benefits to this device include much higher levels of accuracy with regards to concentration levels of oxygen and other gasses, as well as the ability to measure other properties of blood such as pH and carbon dioxide levels within the same sample.

3.2.4 Skin Temperature Measurement Technology: Digital Infrared Thermometers

Infrared Thermometers are an established technology which allows temperature to be taken at range. They work off the principle that every substance emits an amount of infrared radiation which directly correlates with the temperature of that substance. Infrared thermometers focus the infrared light which is emitted by these substances into a specialized component referred to as a thermopile. Thermopiles generate electricity when heated by the infrared light and the amount is directly related to the amount of infrared radiation coming off the substance the thermometer is pointed at.

This technology can be implemented for a variety of reasons, such as cooking or other industrial applications where the temperature needed may be detrimental or even dangerous to touch. This could be because the surface is fragile, like an inner ear thermometer for an infant, or because the surface temperature is dangerously hot like a cooking surface. This technology is relevant to this design as it works on the same principle, sensing infrared radiation, to measure temperature of a surface as the thermal sensor which will be included in the system.

3.3 Strategic Components and Part Selections

In this chapter multiple components essential to our project’s required modules were researched and considered on a module by module basis. Explanations of theory and design considerations were also presented were applicable.

3.3.1 Optical Sensor

[Background] - The quintessential function of the PPG sensor is to utilize the dynamics of light-skin interactions to gather information about a subject's cardiovascular system. When light illuminates a turbid medium, such as skin, it will experience attenuation resulting from two dominant types of optical interactions: absorption and scattering. These processes of light are dependent on the optical properties of the propagation medium, as well as its interface with another medium (such as a skin to air interface). A useful and efficient optical property to use is the complex refractive index which conveys the medium's effect on the "bending" of light which dictates transmission and/or reflection, as well the amount of attenuation that occurs due to absorption for a given wavelength. Skin is considered an inhomogeneous medium due to its layered medium structure and variation of chromophore absorbers and cellular microstructures that influence scattering. Due to the inhomogeneity, the optical properties of skin can be modeled by using layered structures that average the refractive index over a period of layers. It is often beneficial to use a 3 -layered medium structure (Stratum corneous, Epidermis, Dermis) which provided average refractive index of each layer for simplified calculation, although more refined models can be used to account for more parameters, such as thinner layers and subcutaneous fat. The epidermis and dermis are of particular interest with regards to absorption due to its variation with time. This temporal variation is due to the fact that the dermis layer and the epidermis-dermis interface contains blood vessel structures which transport Hemoglobin molecules, a chromophore absorber, in blood. Volumetric changes of hemoglobin in the vascular tissue, such as blood vessels, causes a variation of absorption characteristics for that region of interest. This property of absorption variation as a function of time is the principal parameter which enables the measurement of blood flow via optical interaction. The emission, transmission, and subsequent collection of the scattered light via photodetector from the epidermal and dermal layers over a given period of time provides a bio-signal known as a PPG.

The PPG signal is composed of a DC component which relates the time independent attenuation of the emitted light signal after traversing through the skin which can be explained via the Beer–Lambert law.

$$\frac{I_1}{I_0} = exp(- c\kappa d)$$

Where c is the time-independent concentration of absorbers,
κ is the molar absorbance, and d is the distance the light traverses.

While the AC component of the signal relates to time-dependent attenuation caused from volumetric blood flow, and therefore conveys information about the cardiovascular system of the person whom the signal was collected. A set of graphs of the represented ppg signal and its absorption can be found below mapping the AC and DC components of the signal (figure 3.3.1-1)

$$\frac{I_1}{I_0} = exp(- c(t)\kappa d)$$

Where c is the time-dependent concentration of absorbers,

κ *is the molar absorbance, and d is the distance the light traverses.*

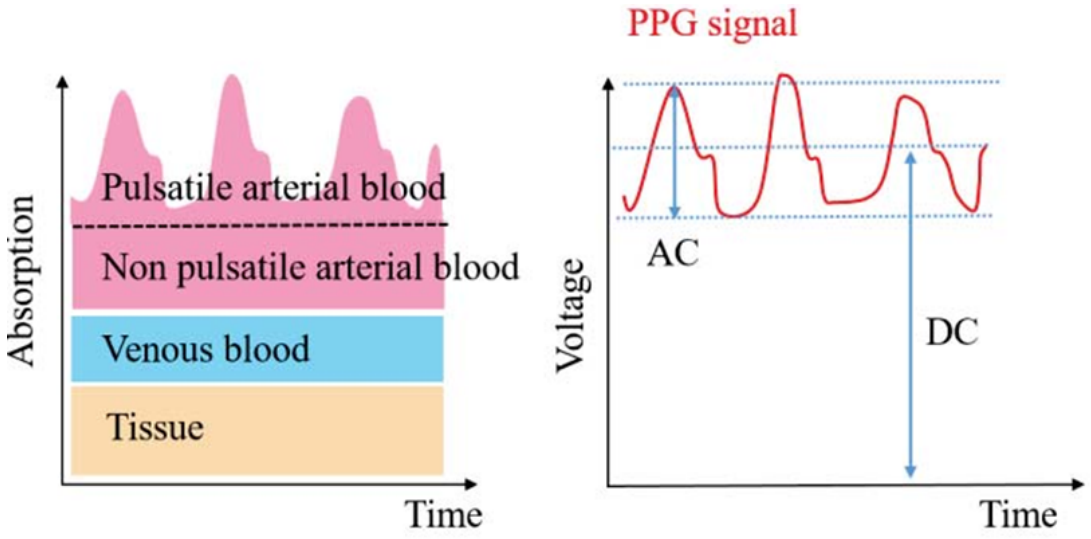

Figure 3.3.1-1. (Taken from Yabuki, Ryosuke et al, 2019)

[Sources of Inaccuracies from Signal Acquisition] - The acquisition of a PPG signal with as little noise as possible is essential to the derivation of biometric measurements with high levels of accuracy. The most common sources of acquisition-related artifacts are ambient light interference, motion artifacts, illumination cross-talk, and substantial attenuation from thick dermal layers and/or higher melanin concentrations. *Ambient light interference (ALI)* is an artifact that results from improper structural design of the PPG sensor resulting in ambient light detection via the photodetector. ALI creates a large DC offset of the detected signal due to crosstalk of ambient light which conveys no biometric information. ALI can be reduced or canceled via the use of sampling and feedback techniques, and the use of opto-mechanical structures to isolate the detector from ambient light. *Motion artifacts* are signal distortions that affect a PPG signal due to the movement of the optical sensor. This distortion leads to an

addition of noise to the signal with a frequency ranging from 0.10 to 10 Hz that can significantly vary both AC and DC components of the waveform. Methods to mitigate motion artifacts are vast and heavily researched, but a common method used is to use of an accelerometer or motion detection unit to identify the periods of the waveform for which the artifact is present and utilize an algorithm to reduce the distortions or retake measurement once the motion has ended or been reduced substantially. *Illumination cross talk* (ICT) is an artifact, similar to ALI, that is caused from improper structure design of the PPG sensor resulting in detection of local light from the source that has not interacted with the user's skin. ICT causes a more prominent DC offset than ALI due to the responsivity photodetector being usually chosen to be more sensitive to the wavelength of the source than ambient light. The most common method to reduce this issue is to account for the radiative patterns of the source and utilize optical barriers to mitigate possible angles that lead to ICT. *Substantial attenuation* of the emitted light leads to a low SNR of the retrieved signal. People who have thicker dermal layers due a large body mass index (BMI) tend to attenuate more light due to an increased optical path length the light must traverse. Attenuation can also occur from people who have a large number on the Fitzpatrick scale, a dermatological scale for human skin pigmentation. A darker skin pigment corresponds to an increased concentration of melanin, a chromophore absorber, resulting in higher attenuation from increased absorption. Methods to a low SNR from both of these instances include different illumination schemes varying from different types of wavelengths, as the travel distance for shorter wavelengths is less, to increasing the amount of emitted light to compensate for the expected loss. A graph showing this artifacting below is found in figure 3.3.1-2.

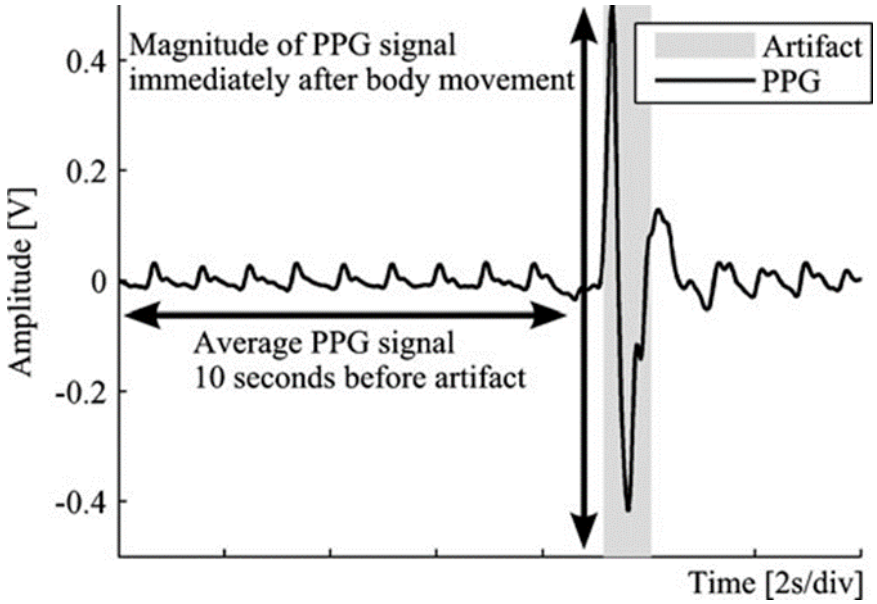

Figure 3.3.1-2. (Taken from Maeda, Y., Sekine, 2011)

[Locations of Sensor and Configuration] - Due to the variation of skin thicknesses for different parts of the human body, a PPG sensor should be designed with the region of collection in mind and is therefore one of the first considerations to make when planning to design such a sensor. Common sites for PPG sensor placement include the torso, ankle, earlobe, fingertip, and wrist; with the last three sites being the most commonly implemented locations due to the low thickness of skin tissue relative to the other sites. The wrist and fingertip position are often the two sites used in most commercial devices for PPG sensors due to their ease of use and offer pros and cons with respect to each other. The fingertip position is commonly used in pulse oximeters due to it offering the second lowest amount of attenuation (first being the earlobe) and providing an accessible area of placement. The *fingertip* position often utilizes a transmissive configuration where the emitter and detector are placed on opposite sides of the finger. The transmissive mode is useful for the finger due to the large capillary density present. The benefits of the transmissive mode are that motion artifacts and ICT are less prominent due to the static separation between the light source and photodetector. A downside of the transmissive fingertip operation is its usability in day-to-day use given that having a device clipped to a user's finger will complicate tasks that require the use of fingers. For this reason, transmissive fingertip operation is often only used in medical establishments and research laboratories. The wrist position is commonly used by commercial smartwatches for calculating heart rate due to its practicability in daily life and possible low

profile facilitating aesthetic design of a larger product. The wrist position requires that a reflective configuration be used due to the unworkable amounts of attenuation that would result from a transmissive operation. In a reflective configuration the emitter and detector are placed on the same plane on the wrist, therefore light is collected as it backscatters from the area of interest. One of the drawbacks of the reflective configuration is that it is more subject to motion artifacts due to less static position of the sensor relative to the area of interest. Another drawback is that due to the close proximity of the emitter and detector, ICT is usually present in the collected signal to some extent. Figure 3.3.1-3 depicts both of these methods for measuring transmission vs reflection methods.

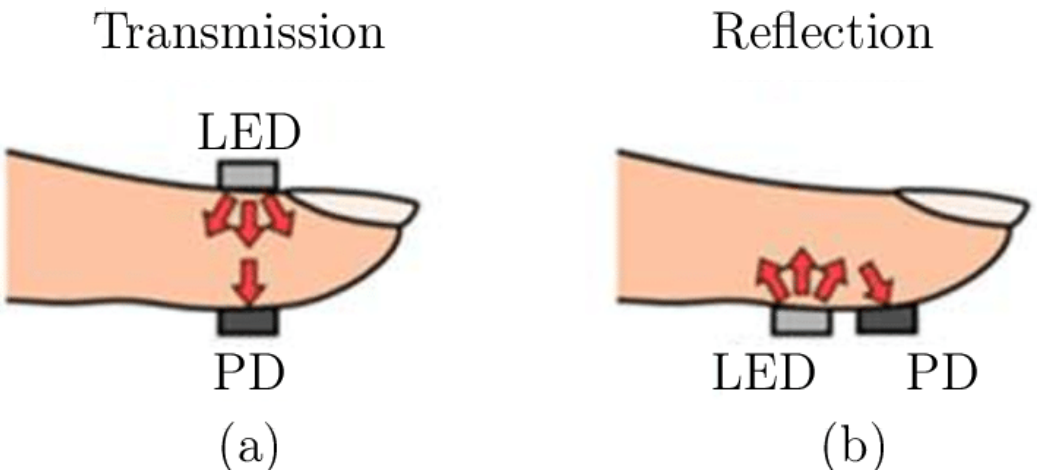

Figure 3.3.1-3. (Taken from Bestbier. A, 2017)

[Wavelength(s) of Operation] – Given that a medium's optical response is dependent on the wavelength, consideration must be made to the wavelength for which the sensor will operate. A functional wavelength window can be derived by taking into account the wavelengths for which hemoglobin, our principal absorber, has a workable absorption response. The functional wavelength window has been found by various studies and product research to be between 500 nm to 1000 nm. Operating at a longer wavelength, closer to the near infrared spectrum, has the advantage of having the deepest penetration depth due to the lower absorption. One of the downsides of operating at the NIR range of the spectrum is the decrease in hemoglobin absorption which results in a smaller AC component of the PPG signal. Operating at the center of the wavelength window, around the red range of the visible spectrum, has the advantage of providing a good balance of penetration depth and hemoglobin absorption with regards to NIR wavelengths. Operating near the blue/green region of the visible spectrum benefits from being more resistant to motion artifacts resulting from it having to traverse less of a distance with respect to optical path length (OPL). The caveat

of these shorter wavelengths is that they experience attenuation from the chromophore absorbers much more strongly than the other wavelengths in the window, therefore their penetration depth is often limited to the epidermal level. Penetration levels depending on the bandwidth of the signal wavelength depicted in Figure 3.3.1-4.

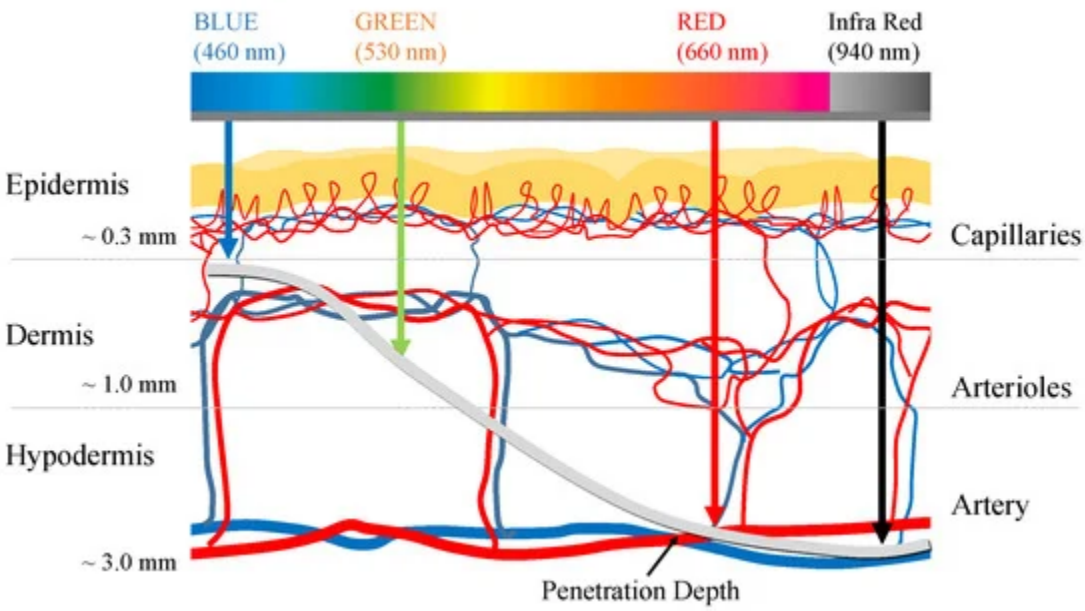

Figure 3.3.1-4. (Taken from Han, S et al 2019)

Another consideration to be made when deciding on the possible wavelength operation is the option of using multiple wavelengths instead of designing the system for one wavelength. Implementing an emitter array with multiple wavelengths enables a sensor to collect multiple PPG signals from different depths of the user's skin. Multiple PPG signals from different parts of the skin's layers enables the possibility of preprocessing algorithms to enhance the final processed PPG signal. When implementing a multiwavelength PPG, special consideration must also be made with respect to the detection scheme. Spectrometric arrays might be used to collect all the different wavelengths at once and processed simultaneously. The benefits of this method is that it allows for synchronous sampling of the multiple PPG signals, as well as facilitates the possibility of utilizing a large number of wavelength channels for high resolution information about cardiovascular dynamics. The downside of this method is that it is impractical to implement in wearable devices due to the price and size constraints of spectrometers. Another method for collecting multiple wavelength PPG signals is to utilize a sampling architecture in which each emitter of a given

wavelength is modulated and the detection of the captured light is asynchronously sequentially sampled to reconstruct the PPG signals. The benefit of this method is that implementation is practical due to the broadband response and high modulation speeds of current photodetectors, as well as their inexpensive price and compact dimensions. The downside of this method is the complexity of a sampling architecture can make it impractical to implement a large number of wavelength varying channels.

[Optomechanical Considerations for Reflective PPG Configurations] – Designing a PPG sensor for a wearable device often requires that certain considerations be made towards the structural layout of the sensor. An important consideration that applies mainly towards wrist-worn reflective PPG sensors is the possible use of optical barriers to prevent ICT artifacts from being introduced to the recovered signal (figure 3.3.1-5). These barriers can often be designed into the outer frame of the wearable device. Typically, these barriers are required to be composed of an opaque and sturdy material, as well as have a height that essentially limits any angle of radiation from the emitter that might leak into the detector. Another useful consideration for reflective configured PPG sensors is the use of an encapsulating sealant on the exposed surface of the optoelectronic components. Utilizing an encapsulating sealant one can achieve sensor protection from common hazards such as water, but also allow for a reduction of transmission losses if the sealant used is of a similar refractive index to the outer layer of human skin. This reduction of transmission losses is due to the principle of Fresnel reflection interactions that dictates the type of backscattering that occurs at an interface with varying refractive indices.

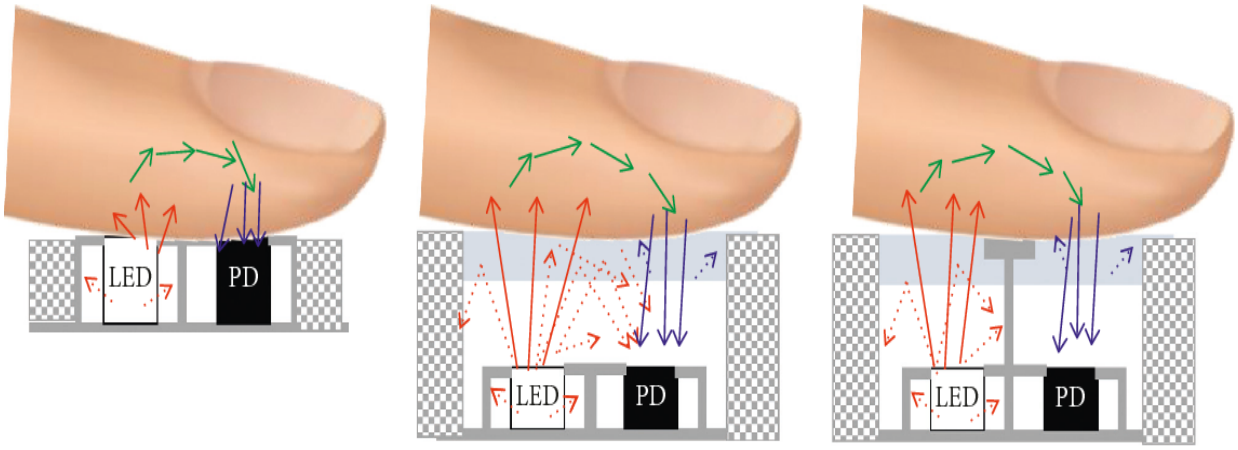

Figure 3.3.1-5. (Taken from Baek, H. J et al, 2018)

[Optical Component Selection: Preliminary] – The PPG sensor is essentially composed of two components: a light source and photodetector. The possible

choices for an emitter are limited to electroluminescent sources due to their integrability to a larger device, and an emission spectrum that is somewhat monochromatic. The two possible electroluminescent source technologies which achieve these properties are the LED and the laser diode. LEDs are semiconductor devices which produce spontaneous emission of light at characteristic wavelength with a moderate linewidth when powered with injection current. LEDs tend to be able to operate at low current density compared to laser diodes, as well as are generally more inexpensive. Laser diodes are semiconductor devices which produce light via stimulated emission at a characteristic wavelength with very narrow linewidth. Laser diodes are able to output larger amounts of optical intensity due to optical gain. Laser diodes also have a faster response time to modulation, thus being useful for faster sampling. For the application of a PPG sensor, LEDs are often chosen over LDs in many designs due to its ability of providing illumination at an inexpensive level for both power consumption and monetary investment. The advantages for which LDs offer are not considered to be vital for a majority of designs. The higher levels of illumination and faster modulation speeds for which the LDs can provide are unnecessary for typical designs and uses. Another limitation is that the larger amounts of injection current typically required by LDs puts a constraint on the Analog Front End ICs (AFE) we must use, as the current drivers of such ICs are often designed for LED current levels.

For the selection of the photodetector, there are three possible components that could be used: photoconductors, photodiodes, and phototransistors. Photoconductors offer a larger responsivity over a range of wavelength compared to photodiodes and phototransistors, although this often comes at a price of larger noise present in the generated signal for relatively low intensity applications. Photodiodes are similar to photoconductors in principle but their doping processes allow for faster modulation speeds, as well as a reduction of noise present due to the process for generation of carriers being that of a diode. Phototransistors are essentially photodiodes with a transistor stage built in to amplify the generated signal. Benefits of phototransistors over photodiodes is the increased responsivity due to amplification, although this often comes at the cost of lower modulation speeds as the capacitance is increased due to the configuration. Photodiodes are often chosen as a photodetector as the benefits of a phototransistor can be achieved via a transimpedance amplifier, which are commonly implemented in AFEs, without the slow modulation issues.

[Optical Component Selection: Criteria] - The selection of the illumination LED(s) was the most important process for the design of the sensor modules as it dictated the criteria for the photodiode. We utilized a multiwavelength

illumination scheme for LED arrays. The LEDs characteristic ranges were chosen to be Green (520 - 565 nm), Red (625 - 740 nm), and Near Infrared (760 – 900 nm). These characteristic wavelengths serve as the first principal criteria for LED selection. The second principal criteria are the linewidths of the LEDs with respect to the characteristic wavelength. The linewidth and characteristic wavelengths must be chosen in such a manner there is no overlap between any of the LED spectrums, as well as a 30-50 nm distance between each LED spectrum. The third principal criterion for choosing the illumination LEDs are the modulation speeds arising from the rise and fall times. This criterion is required for the required sampling architecture of multiwavelength collection. It is worth noting that it is not hard to satisfy this requirement as LEDs have rise and fall times in the nanosecond range. The fourth principal criterion is the radiative characteristics of the LEDs. Half angle values convey the limits of the emission pattern of the LED. For applications such as PPG sensing where the sensor will be constructed in a SM-PCB and will be in contact with the skin, a large half angle will be considered useful.

Using the spectral characteristics of LEDs, a principal criterion for the spectral responsivity of the photodiode can be established, namely, it must have notable (above 25% relative responsivity) for green, red, and NIR wavelengths. The second principal criterion for the selection of a photodiode is the frequency response with regards to modulation. The rise and fall times must be chosen such that any limitations on sampling rates arise from the processing requirements of the microprocessor rather than the photodiode modulation capabilities. The third principal criterion is the signal quality of the photodiode with respect to the Noise Equivalent Power (NEP). Minimizing the amount of NEP present at our desired wavelengths enables us to achieve a higher SNR which facilitates the processing of the PPG signal. Secondary criterion to consider is the acceptance half angle of the photodiode. Similar to the LED selection, we required that the photodiode have a complimentary or at the very least comparable half angle of the LED for optimal detection.

Secondary criteria for both components are that they have compact dimensions and be SM devices for ease of integration and design. Through-hole components will be considered for the Optics Demo showcase to demonstrate the function of the device.

[Optical Component Selection: Comparison] – Utilizing the criterion set in the previous section, a number of components were selected for the full sensor system, and the optics demo partial system. The relevant characteristics of each

component are listed in tables 3.3.1-1 and 3.3.1-2 for both designs. The components were found using the websites Mouser, Digikey, and Thorlabs.

For the LEDs to be used for the full sensor system, two options were present. The first option utilized a singular green LED, the *DBLP31.12* by *OSRAM*, in conjunction with a multichip LED, the *SFH 7015* by *OSRAM*, that contain two emission wavelengths (Red and IR). The second option utilized a singular multichip LED that has all the required LEDs wavelengths on the device. The benefits to the first configuration are that the green LED has a noticeable higher amount of output intensity compared to the other device, leading to a higher possible SNR. Another benefit could arise from the degree of freedom one would get with regards to LED placement and overall configuration, as it is not integrated into a single chip. The downsides to the two-chip option are the increase in size of the sensor, as well as the non-specified dimensions of the active area which could complicate radiation pattern modeling. The benefits of the second option are the simplifications to PCB design as all LEDs are integrated, as well as the reduction of expense as one device would need to be purchased per individual sensor.

For the photodiode to be used in the system, two options were present. The first option utilizes the *SFH 2200* by *OSRAM.* The second option utilizes the *VEMD1060X01* by *Vishay Semiconductors.* The spectral response for OSRAM photodiode can be seen in figure 3.3.1-6 respectively. The benefits of the first option is the stated NEP as it allows us to model and compensate for the possible noise we will encounter during its use. The benefits of the second option is the faster modulation time of the device, along with a larger half angle. The downsides to the second option mainly arise from the lack of specifications for important parameters such as the maximum sensitivity value of the device, as well as the NEP. Without these values, it is hard to compare any possible advantages or disadvantages it might have with regards to the other photodiode. For the previous reason, we plan on using the SFH 2200 photodiode for our design.

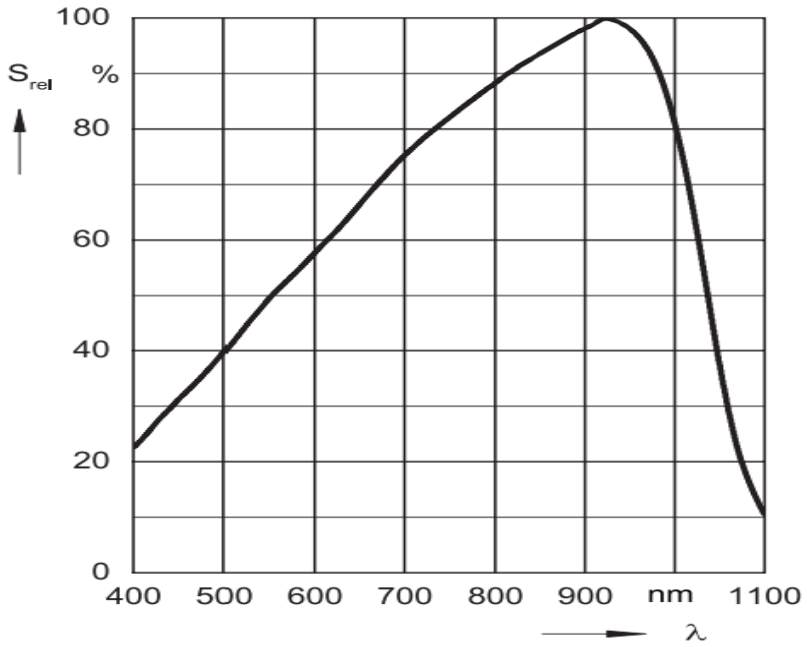

Figure 3.3.1-6. Taken from SFH 2200 - OSRAM datasheet (PENDING PERMISSION)

Component Name	Spectral Characteristics	Radiative Characteristics	Modulation Characteristics	Component Dimensions	Output Characteristics
FIREFLY® CT DBLP31.12 - OSRAM	**[Peak Wavelength]** *536.0 nm* **[FWHM]** Green: *26.0 nm*	**[Half Angle]** *60* **[Dimensions of Active Area]** Not Specified	[**Rise Time & Fall Time]** Not Specified	**[Device Dimensions]** Length: *1.80 mm* Width: *2.20 mm* Thickness: *0.6 mm*	**[Radiant Intensity@ 20mA]** *5.0 mW/sr*
Multi Chip LED SFH 7015 - OSRAM	**[Peak Wavelength]** Red: *660.0 nm* Infrared: *950.0 nm* **[FWHM]** Red: *17.0 nm* Infrared: *42.0 nm*	**[Half Angle]** Red: *60* Infrared: *60* **[Dimensions of Active Area]** Red: *0.3 x 0.3* Infrared: *0.3 x 0.3*	[**Rise Time & Fall Time]** Red: *17 ns* Infrared: *16 ns*	**[Device Dimensions]** Length: *2.00 mm* Width: *0.80 mm* Thickness: *0.6 mm*	**[Radiant Intensity@ 20mA & 20ms]** Red: *4.2 mW/sr* Infrared: *3 mW/sr* **[Total Radiant Flux]** Red: *14 mW* Infrared: *11 mW*
Multi-Chip LED SFH 7016 - OSRAM	**[Peak Wavelength]** Green: *526.0 nm* Red: *660.0 nm* Infrared: *950.0 nm* **[FWHM]** Green: *32.0 nm* Red: *17.0 nm* Infrared: *42.0 nm*	**[Half Angle]** Green: *60* Red: *60* Infrared: *60* **[Dimensions of Active Area]** Green: *0.5 x 0.5* Red: *0.3 x 0.3* Infrared: *0.3 x 0.3*	[**Rise Time & Fall Time]** Green: *59 ns* Red: *17 ns* Infrared: *16 ns*	**[Device Dimensions]** Length: *1.85 mm* Width: *1.65 mm* Thickness: *0.6 mm*	**[Radiant Intensity @ 20mA & 20ms]** Green: *4 mW/sr* Red: *4.2 mW/sr* Infrared: *3 mW/sr* **[Total Radiant Flux]** Green: *14 mW* Red: *14 mW* Infrared: *11 mW*

Table 3.3.1-1.

Component Name	**Spectral Characteristics**	**Radiative Characteristics**	**Modulation Characteris-tics**	**Component Dimensions**	**Signal Quality Characteri-stics**
TOPLED® Silicon Photodiode SFH 2200 - *OSRAM*	**[Spectral Range & Maximum Sensitivity]** Range: 300 – 1100 nm Maximum: 0.7 A/W @ 940nm **[Relative Sensitivity at Interested Wavelengths]** Green (530 nm): ~45% Red (660 nm): ~67.5 % Infrared (950 nm): ~95%	**[Half Angle]** *60* **[Dimensions of Active Area]** 2.65 x 2.65	[**Rise Time & Fall Time]** 0.04	**[Device Dimensions]** Length: 5.1 mm Width: 4 mm Thickness: 0.85 mm	**[Noise Equivalen t Power]** 0.026 pW/Hz when
Silicon PIN Photodiode VEMD1060 X01 Vishay Semiconduc tors	**[Spectral Range & Maximum Sensitivity]** Range: 350 – 1070 nm Maximum: Not specified @ 890nm **[Relative Sensitivity at Interested Wavelengths]** Green (530 nm): ~45% Red (660 nm): ~70% Infrared (950 nm): ~75%	**[Half Angle]** *70* **[Dimensions of Active Area]** 0.23x0.23	[**Rise Time]** *60 ns* **[Fall Time]** *70 ns*	**[Device Dimensions]** Length: 2 mm Width: 1.25 mm Thickness: 0.85 mm	**[Noise Equivalen t Power]** Not specified

Table 3.3.1-2.

As stated before, for the optics demo through-hole components must be selected in such a way to mimic a portion of our complete system. For this we decided to focus on the singular wavelength LED (~530 nm) and a photodiode that would yield a considerable response at this wavelength. Certain criteria previously stated, such as modulation and dimension characteristics, were

deemed unnecessary for this selection due to lack of need for them with respect to the demo.

For the LED selection, two possible options were considered, as seen in table 3.3.1-3. The first option utilizes the LED525L by Thorlabs. The second option utilizes the LED528EHP by Thorlabs. The benefits of the first option are the larger and more uniform viewing half angle of its radiation pattern (seen in figure 3.3.1-7), as well as its relatively small FWHM. The relatively large viewing angle is beneficial to the demo as a means to replicate the larger viewing angle that will be observed in the actual device. The downside to this option is the relatively low optical power output at continuous operation. The benefits of the second option are a higher power output at efficient current injection, as well as the convenience of being available to our group via the undergraduate photonics laboratory. It is worth noting that at this moment it is currently in stock at the undergraduate's lab, but that is subject to change. The downside to this option is the smaller and skewed half angle of the device that arises from not utilizing any lenses. We plan on utilizing the LED525L for the demo, although we will use the LED528EHP to practice setting up the experiment in the meantime while the LED525L ships, so long as it was available in the undergraduate lab.

For the photodiode, two possible options were considered. The first option is the FDS100 silicon PIN photodiode by Thorlabs. The second option is the BPX 61 silicon PIN photodiode by OSRAM. The benefits of the first option include a higher responsivity for the wavelength of interest (figure 3.3.1-8), as well as a larger active area and lower NEP. The main downside of this device is that it is currently not in-stock on the Thorlabs. It is available via the undergraduate photonics laboratory but, similarly to the previous component, is subject to change and the group cannot be fully dependent on. The benefits of the second option are essentially its availability in the marketplace and comparable performance to the previously stated photodiode. Our group purchased the BPX 61 as a back up device for the optics demo, but ideally will use the FDS100.

Component Name	Spectral Characteristics	Radiative Characteristics	Component Dimensions	Output Characteristics
LED525L - Thorlabs	**[Peak Wavelength]** *525 nm* **[FWHM]** *25 nm*	**[Half Angle]** *20*	**[Device Dimensions]** Length: *6.4 mm* Width: *4.7 mm* Thickness: *4.7 mm*	**[Optical Power]** 4 mW @ 50 mA
LED528EHP – Thorlabs	**[Peak Wavelength]** *525 nm* **[FWHM]** *35 nm*	**[Half Angle]** 9	**[Device Dimensions]** Length: 9 mm Width: 5.8 mm Thickness: 5.8 mm	**[Optical Power]** 7.0 mW @ 20 mA

Table 3.3.1-3.

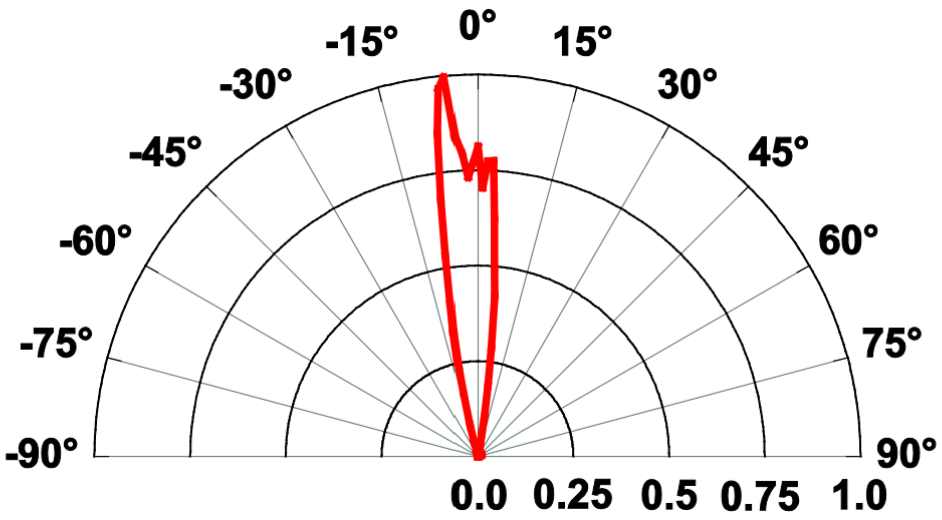

Figure 3.3.1-7. Taken from LED528EHP-Thorlabs datasheet (PENDING PERMISSION)

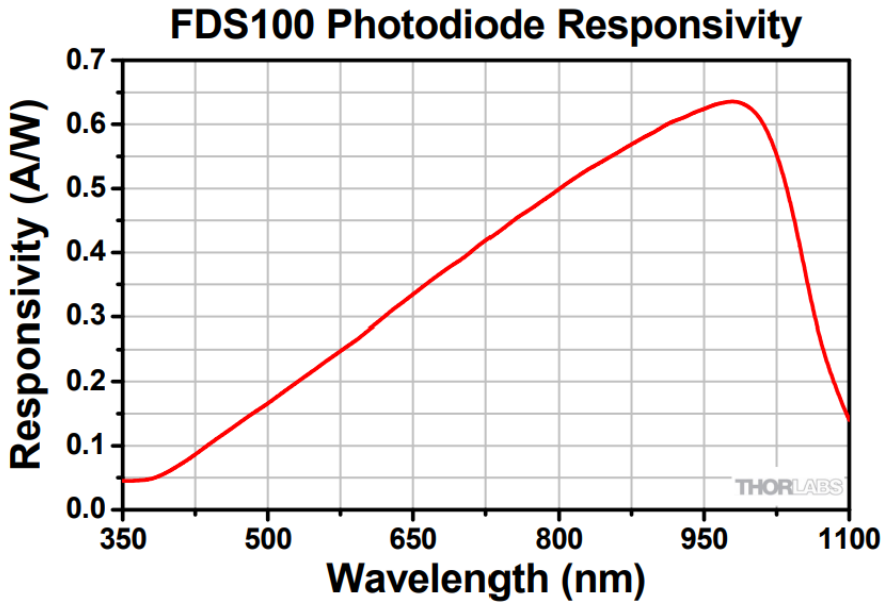

Figure 3.3.1-8. Taken from FDS100-Thorlabs datasheet (PENDING PERMISSION)

Component Name	**Spectral Characteristics**	**Radiative Characteristics**	**Component Dimensions**	**Signal Quality Characteristics**
FDS100 - Thorlabs	**[Spectral Range & Maximum Sensitivity]** *Range:* 350 - 1100 nm *Maximum*:0.65 A/W @ 980 nm **[Relative Sensitivity at Interested Wavelengths]** 30%	**[Half Angle]** Not specified	**[Device Dimensions]** 13 mm^2	**[Noise Equivalent Power]** 0.012 pW/ Hz
BPX 61 – OSRAM	**[Spectral Range & Maximum Sensitivity]** *Range:* 420 - 1120 nm *Maximum*:0.62 A/W @ 920 nm **[Relative Sensitivity at Interested Wavelengths]** 30%	**[Half Angle]** 55	**[Device Dimensions]** 7.02 mm^2	**[Noise Equivalent Power]** 0.041 pW/ Hz

Table 3.3.1-4.

[Index-Matching and Sealant Selection] - As stated in the optomechanical consideration sub-section of the optical sensor research, the introduction of an optical adhesive sealant film to the surface of a sensor can provide durability and performance enhancements to the device. This additional design becomes more relevant when taking into consideration the planned introduction of optical barriers that will impose a gap between the top of the structure and the optical components, giving way to a Fresnel loss associated with the component-to-air and air-to-skin interfaces.

In figure 3.3.1-9, the Fresnel losses for the absence and presence of an index matched sealant layer are explored. It can be seen that in case (A) experiences a loss of about 5.716% for incident light parallel to the normal, while case (B) experiences virtually less than 0.01% loss. It is worth noting that while a 94% transmission for non-sealant configuration might seem adequate, it does not take into account the factor of incident angle. Not all light rays transmitted through the interfaces will be parallel, thus reflection losses will substantially increase for non-matched mediums as refraction index plays a bigger role.

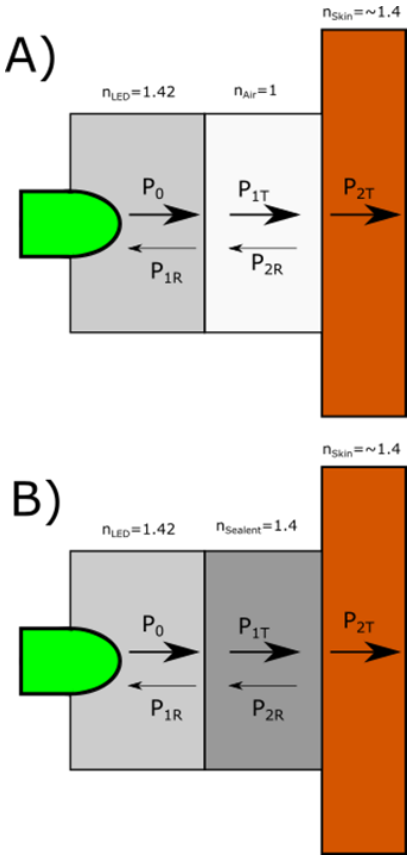

Case A

Incident reflection loss at interface 1

$$R = \left|\frac{n_{LED} - n_{Air}}{n_{LED} + n_{Air}}\right|^2 = \left|\frac{1.42 - 1}{1.42 + 1}\right|^2 = 0.030$$

$$P_0 - P_{1R} = (1 - 0.03)P_0 = P_{1T} = 0.97P_0$$

Incident reflection loss at interface 2

$$R = \left|\frac{n_{Air} - n_{Skin}}{n_{Air} + n_{Skin}}\right|^2 = \left|\frac{1 - 1.4}{1 + 1.4}\right|^2 = 0.028$$

$$P_{1T} - P_{2R} = (1 - 0.028)P_{1T} = P_{2T} = 0.972P_{1T}$$
$$= 0.972(0.97)P_{1T} = 0.94284P_0$$

Case B

Incident reflection loss at interface 1

$$R = \left|\frac{n_{LED} - n_{Sealent}}{n_{LED} + n_{Sealent}}\right|^2 = \left|\frac{1.42 - 1.4}{1.42 + 1.4}\right|^2 = 5.03 \times 10^{-5}$$

Reflection Loss at interface 2

$$R = \left|\frac{n_{Air} - n_{Skin}}{n_{Air} + n_{Skin}}\right|^2 = \left|\frac{1.4 - 1.4}{1.4 + 1.4}\right|^2 = 0$$

$$P_0 - P_{1R} = (1 - 5.03 \times 10^{-5})P_0 = P_{1T} = 0.9999P_0$$

$$P_{1T} - P_{2R} = (1 - 0)P_{1T} = P_{2T} = P_{1T} = 0.9999P_0$$

Figure 3.3.1-9.

The components selected have a packing composed of clear silicone, while the planned material to be used for the mechanical design of the device is a plastic filament, therefore it is necessary that the adhesive used provides good to excellent adhesion for glass-to-plastic bonding. Another important parameter to pay attention to is that for proper refractive index matching, the adhesive must have a refractive index of about 1.40.

Further consideration was made to the methods for curing silicone-based adhesives sealants. Adhesive curing is a process in which by some catalyst, the adhesive converts from a viscous liquid in a crystalized solid, thus providing mechanical support and dielectric optical properties. Methods for curing are highly dependent on the adhesive's chemical properties and are specified by the manufacturers. Temperature-based curing requires that an adhesive be placed in a device, such as a wind tunnel, that uses air convection to raise the temperature of the adhesive to initiate curing. For this method curing times can take anywhere from 1-4 hours. Room temperature curing adhesives do exist but can at times require timeframes of 24 hours to a few days. A popular method of curing that manufacturers have proposed for optic adhesives is that of UV curing. UV curing requires that the adhesive be exposed to UV light for a timeframe of about 20 minutes for two-step curing processes.

After researching for possible options of optical adhesives, we found that the majority of our options were limited to UV cured options. The first option that we considered was a NOA 84 by Norland Products. This adhesive works best for plastics like polycarbonate and glass, which is ideal for our case. The refractive index that this adhesive provides is stated to be about 1.46 at an unspecified wavelength. For curing we would need to utilize an UV or Blue-violet light source to induce photopolymerization. The second option considered is the Viltralit 1527 by Panacol. This option is designed for optoelectronics and must be cured at UV wavelengths for only a few seconds. The refractive index of the adhesive is 1.497 at an unspecified wavelength. A comparison similar to that of figure # is done in figure 3.3.1-10 to evaluate the impact of Fresnel loss.

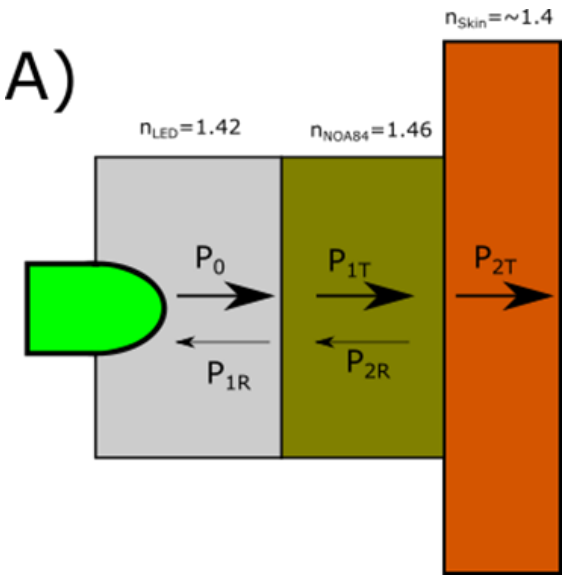

Case A

Incident reflection loss at interface 1

$$R = \left|\frac{n_{LED} - n_{NOA84}}{n_{LED} + n_{NOA84}}\right|^2 = \left|\frac{1.42 - 1.46}{1.42 + 1.46}\right|^2 = 2 \times 10^{-4}$$

$$P_0 - P_{1R} = (1 - 2 \times 10^{-4})P_0 = P_{1T} = 0.9998P_0$$

Incident reflection loss at interface 2

$$R = \left|\frac{n_{NOA84} - n_{Skin}}{n_{NOA84} + n_{Skin}}\right|^2 = \left|\frac{1.46 - 1.4}{1.46 + 1.4}\right|^2 = 4.4 \times 10^{-4}$$

$$P_{1T} - P_{2R} = (1 - 4.4 \times 10^{-4})P_{1T} = 0.9995P_{1T} = (0.9995)(0.9998)P_0 \approx 0.9994P_0$$

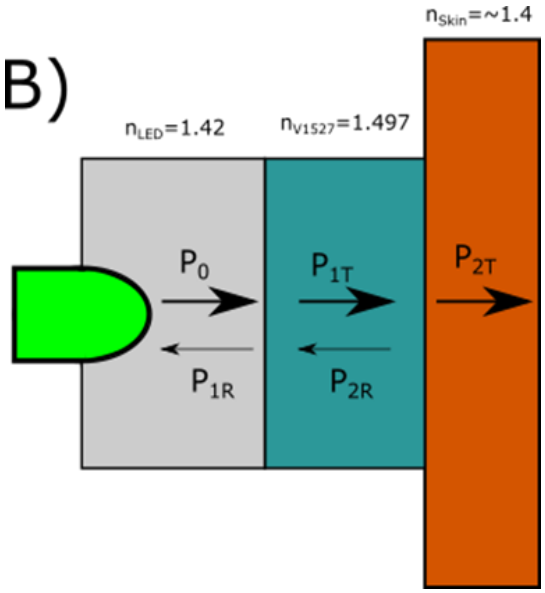

Case B

Incident reflection loss at interface 1

$$R = \left|\frac{n_{LED} - n_{V1527}}{n_{LED} + n_{V1727}}\right|^2 = \left|\frac{1.42 - 1.497}{1.42 + 1.497}\right|^2 = 6.97 \times 10^{-4}$$

$$P_0 - P_{1R} = (1 - 6.97 \times 10^{-4})P_0 = P_{1T} = 0.9993P_0$$

Reflection Loss at interface 2

$$R = \left|\frac{n_{V1527} - n_{Skin}}{n_{V1727} + n_{Skin}}\right|^2 = \left|\frac{1.497 - 1.4}{1.497 + 1.4}\right|^2 = 0.00112$$

$$P_{1T} - P_{2R} = (1 - 0.00112)P_{1T} = 0.9989P_{1T}$$

$$(0.9989)(0.9993)P_0 \approx 0.9982P_0$$

Figure 3.3.1-10.

It can be observed in figure calculations of figure #+1 that the NOA 84 option offers better transmission for index matching. In addition to this, the ability to cure with blue-violet light makes this option more feasible which is why we have decided to go with this option.

3.3.2 Microcontroller

Microcontrollers are the backbone of many consumer electronics. At their core, they house a CPU, memory, and programmable pins to interconnect several peripherals, whether they be input or output. Microcontrollers have revolutionized the way in which we can take information from a device, process it, and output data in a cost-effective way without a lot of investment or need of dedicated hardware. For our wearable PPG biometric tracking device, we need a microcontroller that is light-weight, portable, low power, and could interface with multiple devices. The microcontroller would primarily transmit data from optical sensors and use this in conjunction with data from an accelerometer and temperature sensing module to analyze whether the data should be discarded in the first place or not, and if it is of use, interpret it and package it to be sent over Bluetooth to a personal device.

The most important factors to consider when choosing a microcontroller would be that it fit the connectivity requirements, then narrow it down to the microcontroller with the smallest form factor given the performance standard is met. The wearable Biometric capturing device will require a large amount of simultaneous analog to digital conversion so that the data may be interpreted in a digital format. To meet the project's needs, there are four products under consideration that will be used for testing and ultimately have their components embedded in the final PCB of our wearable device: Raspberry Pi Pico, STM3210, Arduino Nano 33 BLE, and the TI MSP430FR6989.

Raspberry Pi Pico

The Raspberry Pi Pico hosts an ARM processor, housed in the RP2040 microcontroller, which is a dual core that can operate up to 133 MHz, has 264kB of SRAM and 30 GPIO pins. This microcontroller has the capability to create two UART connections, along with two SPI channels, and two I2C channels. The microcontroller has a major drawback in the form of needing to add flash storage and does not have any built-in storage for programs. The Raspberry Pi Pico features a four channel ADC that outputs 12-bit values, which may be helpful in converting the analog signal received by the photodiode.

STM3210

The STM family of boards are strong contenders for this project because of how robust their microcontrollers are. The STM3210 in particular hosts a very powerful ARM Cortex-M3 microcontroller, the STM32F103ZGT6. This microcontroller is capable of two I2C connections simultaneously, three

concurrent SPI connections, and USART; all features which could help the influx of information from the 4 photodiodes constantly capturing data and after processing it, transmitting it through Bluetooth. The microcontroller contains 96KB SRAM and 1MB Flash memory which are invaluable because having more memory means the device could store more samples for a more thorough analysis before transmitting.

MSP430FR6989

The MSP430 family of microcontroller evaluation boards are well known because of their use in educational endeavors. The processor is made of a 16-bit architecture and runs at 16MHz, making it a weaker option compared to the other options computationally. It makes up for the lack of comparative processing power by being an affordable alternative and easier to obtain, as well as its ability to interface with multiple devices using I2C. As seen in the figure above, the MSP board has the advantage of housing a display which can be used for testing purposes.

Arduino Nano 33 BLE

The Arduino platform prides itself with being one of the most accessible ones with a vast array of peripherals and components being used in open-source projects to show compatibility. The Arduino Nano 33 BLE (figure 3.3.2-1) offers the unique advantage of having a microcontroller already equipped with a Bluetooth antenna and is configured to transmit in a variety of Bluetooth modes. In addition to its innate ability to transmit through Bluetooth, the microcontroller has 1MB flash memory, and 256kB RAM paired with a 32-bit processor that can clock up to 64MHz. The processing capabilities of this microcontroller make it a lucrative choice, especially when paired with the ability to interface with up to four SPI devices and two I2C devices.

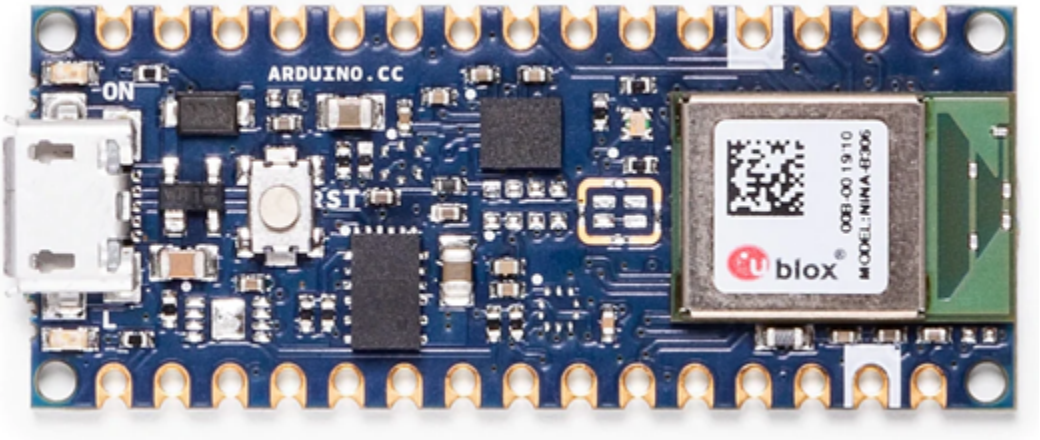

Figure 3.3.2-1.

3.3.3 Power Delivery

When contemplating a power delivery system for our wearable device, there were three popular options, utilizing USB power, a wall AC to DC adapter, or a battery powered solution. USB power is a possible solution when used in combination with a battery, however it has a significant impact on mobility. A wall AC to DC adapter is practically discounted as a power delivery system unless the project were to shift in a less wearable direction, and instead would read biometrics as a fixed location device. With portability at a premium, a purely battery powered solution is the most appealing one, as it would allow our device to be used on the go, after a run, or session at the gym.

For our wearable device to be portable, we need to implement a power delivery system that is battery based. Going the battery route affords us the ability to move the device at our discretion but has the major drawback of introducing a battery life constraint which impacts the amount of power we want our system to draw. The most common consumer batteries range in sizes from the size of a coin to the ubiquitous household batteries -AAA to D - with different capacities stated in milliamp hours (mAh) and are composed of different chemical compounds.

Battery types

Batteries have evolved as a technology to a point where we are able to power a laptop, cell phone, smoke alarm, and everything in between. Batteries becoming ubiquitous in electronics has resulted in different modalities of power delivery, with there being two overarching classifications for batteries: primary and secondary batteries.

Primary batteries are the traditional type of batteries that are discardable. They are produced in several chemistries offering different qualities, but all share the same fate of being designed with a capacity, usually rated in milliamp hours(mAh), and once the battery runs out of charge it must be replaced. Due to the wasteful nature of primary batteries, they are typically used in devices that do not consume a lot of power and are powered sporadically. Television remotes are a popular example of a device in which primary batteries are ideal, as they scarcely use power when idling, and still do not consume a lot when operating sending IR signals.

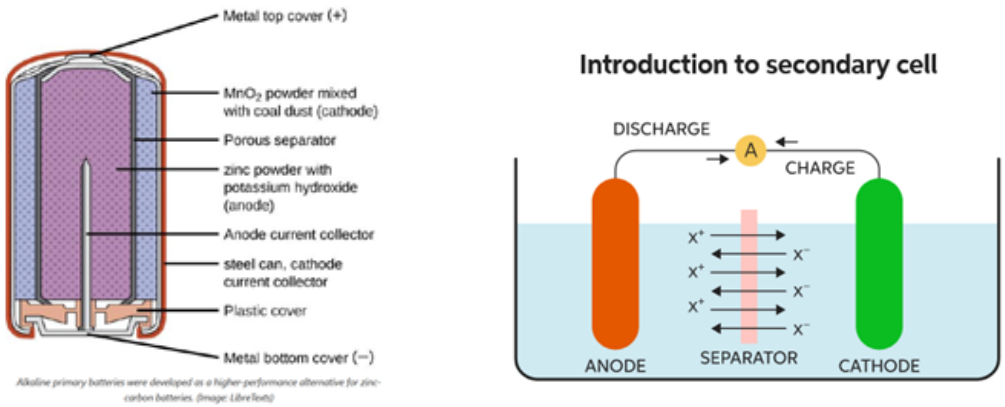

Figure 3.3.3-1.

Secondary batteries are batteries that can be recharged (Fig 3.3.3-1), and work on the principle that a voltage bias being applied acts as a catalyst for the chemical reaction that would produce a charge to be reversed and store potential energy. In today's day and age, secondary batteries have taken the world by storm, with the advent of smartphones and laptops, batteries that are small, high capacity, and rechargeable are at a premium. Secondary batteries are a hybrid solution that offers some of the most desirable traits of both primary batteries and wall plugged AC adapters. Secondary batteries present the portability of primary batteries, while not harboring the inconvenience of having to constantly switch out batteries in a moderate or high-power use environment. The convenience combined with their high energy density makes rechargeable batteries a quickly growing market, with research concerning increasing their capabilities being heavily funded, since there may be another battery revolution on the horizon as cars switch to being powered by electric motors that require very powerful battery cells.

Battery Chemistries

Primary battery chemistries:

Chemistry	Cell Voltage	Energy Density (MJ/kg)	Elaboration
Zinc–carbon	1.5	0.13	Inexpensive.
Zinc chloride	1.5		Also known as "heavy duty", inexpensive.
alkaline (zinc–manganese dioxide)	1.5	0.4-0.59	Moderate energy density. Good for high and low drain uses.
oxy nickel hydroxide (zinc-manganese dioxide/oxy nickel hydroxide)	1.7		Moderate energy density. Good for high drain uses.
Lithium (lithium–copper oxide) Li–CuO	1.7		No longer manufactured. Replaced by silver oxide (IEC-type "SR") batteries.
Lithium (lithium–iron disulfide) LiFeS2	1.5		Expensive. Used in 'plus' or 'extra' batteries.
Lithium (lithium–manganese dioxide) LiMnO2	3.0	0.83 – 1.01	Expensive. Only used in high-drain devices or for long shelf life due to very low rate of self discharge. 'Lithium' alone usually refers to this type of chemistry.
Mercury oxide	1.35		High drain and constant voltage. Banned in most countries because of health concerns.
Zinc–air	1.35 – 1.65	1.59[1]	Mostly used in hearing aids.
Silver oxide (silver-zinc)	1.55	0.47	Very expensive. Only used commercially in 'button' cells.

Summary of common primary battery chemistries. (Image: Epec, LLC)

Figure 3.3.3-2.

The table(3.3.3-2) above mentions the main battery chemistries that are used in industry applications with primary batteries and the tradeoffs. Most primary battery cells consistently supply within a range of 1.35V - 1.7 V, with the exception of LiMnO2 battery cells which operate at a substantially higher 3V(Epectec). The table below (3.3.3-3) highlights the most relevant secondary battery chemistries and gives a brief overview of the characteristics we can expect from a secondary battery regardless of the size they come in. Secondary batteries commonly have a higher nominal voltage output because most are lithium based, translating into a larger range of voltages to select from 1.2V - 3.7V.

Secondary battery chemistries:

Chemistry	Cell Voltage	Energy Density (MJ/kg)	Comments
NiCd	1.2	>0.14	Inexpensive. High/low drain, moderate energy density. Can withstand very high discharge rates with virtually no loss of capacity. Moderate rate of self discharge. Reputed to suffer from memory effect (which is alleged to cause early failure). Environmental hazard due to Cadmium - use now virtually prohibited in Europe.
Lead Acid	2.2	>0.14	Moderately expensive. Moderate energy density. Moderate rate of self discharge. Higher discharge rates result in considerable loss of capacity. Does not suffer from memory effect. Environmental hazard due to Lead. Common use - Automobile batteries
NiMH	1.2	>0.36	Cheap. Not usable in higher drain devices. Traditional chemistry has high energy density, but also a high rate of self-discharge. Newer chemistry has low self-discharge rate, but also a ~25% lower energy density. Very heavy. Used in some cars.
Lithium ion	3.6	>0.46	Very expensive. Very high energy density. Not usually available in "common" battery sizes (but see RCR-V3 for a counter-example). Very common in laptop computers, moderate to high-end digital cameras and camcorders, and cellphones. Very low rate of self discharge. Volatile: Chance of explosion if short circuited, allowed to overheat, or not manufactured with rigorous quality standards.
Lithium Cobalt Oxide ($LiCoO_2$)	3.6	>0.72	High specific energy. Relatively short life span, Low thermal stability and limited load capabilities (specific power). Should not be charged and discharged at a current higher than its C-rating
Lithium Iron Phosphate ($LiFePO_4$)	3.3	>0.32	Good electrochemical performance with low resistance. High discharging current. Cold temperature reduces performance and elevated storage temperature shortens the service life. Limited "C-rate" of around 1C, which means they take a long time to charge. Excellent safety and long life span. Moderate specific energy and elevated self-discharge.
Lithium Nickel Manganese Cobalt Oxide ($LiNiMnCoO_2$)	3.7	>0.54	C-rate" of this chemistry can range from 1-5C. Higher energy density with lower cost, long cycle life. Can have either a high specific energy or high specific power, they cannot, however, have both properties. Very low self-heating rate.
Lithium Manganese Oxide ($LiMn_2O_4$)	3.8	>0.36	High thermal stability and enhanced safety, but the cycle and calendar life are limited. Low internal cell resistance enables fast charging and high-current discharging. Can be discharged at currents of 20–30A with moderate heat buildup.
Lithium Titanate (Li_2TiO_3)	2.4	>0.23	Expensive. Excels in safety, low-temperature performance. Long cycle life: > 3000-7000 cycles. Can be fast charged and delivers a high discharge current of 10C. Cycle count is said to be higher than that of a regular Li-ion. Thermal stability under high temperature is also better than other Li-ion systems.

Figure 3.3.3-3.

Battery Sizes

AA Batteries

AA batteries are one of the most common battery sizes in household electronics. They sit at a middle point in terms of trading off size for power capacity and are easy to acquire, as they are offered in many grocery and convenience stores. AA batteries are the higher power solution to our device if performance is hampered by a lack of energy capacity or if our device draws too much current at a given moment while transmitting and driving LEDs to brown out a smaller battery.

Chemistry	Common Name	Rechargeable	Typical Capacity (mAh)	Voltage (V)
Zinc Carbon	R6, 15D	**No**	600 - 1600	1.5
Alkaline	LR6, 15A	**No** (Mostly No)	1800 - 2700	1.5
Li-FeS_2	FR6, 15LF	**No**	2700 - 3300	1.5 (1.8 max)
Li-ion	14500	Yes	600 - 2000+	3.6 - 3.7
$LiFePO_4$	IFR14500	Yes	500-750	3.2
Li-$SOCl_2$	(14505)	**No**	2400-2700	3.5-3.6
Li-MnO_2	CR AA	**No**	~2000	3.0
Lithium	-	Yes	1000-2000+	1.5
NiCd	KR6, 1.2K2	Yes	600 - 1000	1.2
NiMH	HR6, 1.2H2	Yes	700 - 2800	1.2
NiOOH	-	**No**	2200 - 2700	1.5 (1.7 max)
NiZn	ZR6	Yes	1500 - 1800	1.6 - 1.65

Figure 3.3.3-4.

Source: batteryequivalents.com

Coin cell batteries are the form of highest interest because of their small footprint. The main chemistries when considering a coin cell battery are Alkaline, Silver-Oxide, Zinc-Air, and Mercury-Oxide. Alkaline batteries of this size tend to have a nominal voltage of 1.5V and a capacity of about 120 mAh (Fig 3.3.3-4). This chemistry happens to be the most affordable one typically, at the cost of the voltage depreciating over the life cycle of the battery. Silver-Oxide coin batteries have a slightly higher nominal voltage of 1.55V and keep a more consistent voltage across their life cycle, which is bigger to begin with, coming in at approximately 150-200 mAh depending on the manufacturer. The drawback of a silver-oxide battery is the higher monetary cost. Zinc-Air batteries range in nominal voltage from 1.4-1.45 V and have a much higher capacity at 600-700 mAh but are harder to implement in a device due to the nature of how they consume ambient oxygen resulting in environmental factors such as humidity and temperature adversely affecting them to a higher degree than other batteries. Mercury-Oxide batteries have a nominal voltage of 1.35V and a higher capacity at 180-200 mAh than the first two chemistries. They used to be a lot

more commonplace, however due to their potentially toxic nature, they will more than likely not be used in this project.

Finally, we have Lithium-Ion Polymer batteries, which have been drastically rising in popularity as high-powered electronics have been trending towards downsizing, and battery needs are nowadays better met via rechargeable batteries, since smartphones have similar batteries, practically most consumers will have a way to power Lithium-Ion Polymer batteries, albeit with some conversion circuitry being necessary sometimes. For our project we have chosen a Lithium-Ion Polymer battery because although coin batteries fit the physical profile we are after, they tend to not do well under our intended purposes. Coin batteries are primarily made to have extremely low current drawn constantly, or for several milliamps very sparingly. Our device would use over 100 mA current for several seconds at a time with some respite every couple of seconds. This power use pattern better aligns with a Lithium-Ion Polymer battery, which is designed to be used in high drain applications and is perfectly suitable for delivering hundreds of milliamps at a time. Lithium-Ion Polymer batteries come in small packages nowadays, occupying just under 500 mm^2 which is at about the maximum size we would like our battery to be. Another important consideration when choosing this battery is the 3.7V nominal voltage it can output. This voltage level allows it to be close to the main voltage level that will be used in the circuit, 3.3, which means the voltage level conversions will be more power efficient. Being able to use just one battery in our design is a significant advantage, as designing a power delivery system with multiple batteries in series to obtain a higher voltage, or multiple batteries in parallel to obtain more throughput current, present issues in the form of unoptimized battery spacing, and will heavily tax our size constraints.

The specific battery we have chosen is the Lithium-Ion Polymer 500 mAh from PKCELL. It has a nominal voltage of 3.7V and an outstanding energy density providing 500mAh in a 29mm x 36mm x 4.75mm form factor. The Wearable Optical Biometric Tracking System will never exceed one Amp in current draw, and is unlikely to ever get close, a moderate estimate of current consumption places it at under 200 mA at peak load, suggesting the device is likely to have over two hours of battery life if heavily used with the LEDs pulsing at high currents.

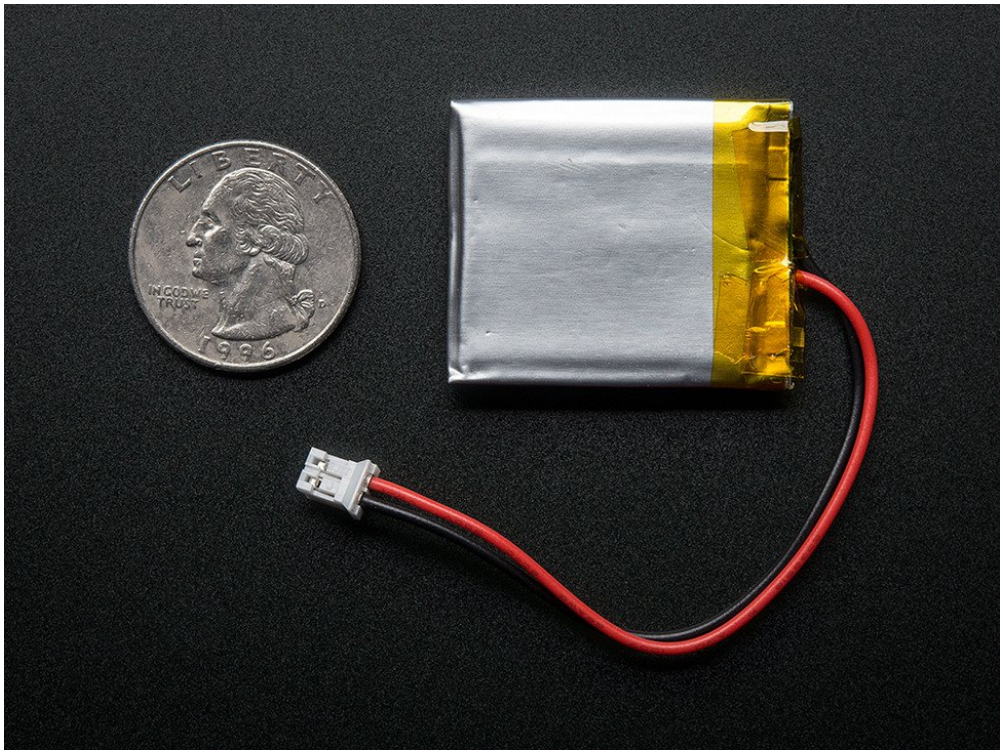

Figure 3.3.3-5.

Lithium-Ion batteries are usually rated for how much current they can have flowing in or out in terms of their total battery capacity when fully charged. The battery pictured above (3.3.3-5) is rated for continuous discharge of 0.2C, which would in this battery be 100mAh, it can however sustain significantly higher discharge rates when it is intermittent. To charge the battery can be supplied between 100mA to 500 mA in a time frame of between one hour and five hours. As seen in the table below, this particular battery fluctuates in voltage across its life cycle. 3.7V is an average of the voltage output by the battery, with the real output voltage being in a range of 4.2V when the cell is fully charged, to approximately 3.0V when it has been nearly entirely discharged (Fig 3.3.3-6). This leads to the issue of having to regulate the output voltage, a problem just about any battery powered system would face. The variance in voltage calls for additional circuitry that will keep the voltage level constant so that all the components in the circuit can adequately measure logic levels and power devices. This can be done in many forms, with that said the three main types of voltage regulators we will be considering are a Linear Dropout regulator, a Buck regulator, and a Boost regulator.

No	Item	Rated performance	Remark
1	Capacity	Nominal 500mAh Minimum 450mAh	Standard discharge after standard charge
2	Nominal voltage	3.7V	Mean operation voltage during standard discharge after standard charge
3	Voltage at end of discharge	3.0V	Discharge cut-off voltage
4	Charging voltage	4.2V	
5	Standard charge	Constant current $0.2C_5A$ Constant voltage 4.2V Cut-off current $0.01C_5A$	
6	Quick charge	Constant current $1C_5A$ Constant voltage 4.2V Cut-off current $0.01C_5A$	
7	Standard discharge	Constant current 0.2 C_5A End voltage 3.0V	
8	Maximum continuous discharge current	1 C_5A	
9	Operation temperature range	Charge: 0~45℃ Discharge:-20~60℃	60±25%R.H
10	Cycle life	>500cycles	Charging/discharging in the below condition: Charge: standard charge Discharge:$0.2C_5A$ to 3.0V Rest time between charge/discharge:30min Until the discharge capacity <60% of NC
11	Storage temperature	During 1 month: -5 ~ 35℃ During 6 months: -20 ~ 45℃	60±25%R.H

Figure 3.3.3-6.

DC-DC Conversion

With an input voltage of 3.0-4.2V, the battery will need to be regulated to the different voltage levels needed for the system. The power system needs to be able to supply the 3V3 logic level for varying components, which means we need to regulate the voltage from above and below the target voltage. The voltage will need to be dynamically dropped to 3v3 or be boosted to 3V3 when the battery is near the end of its charge cycle. Three of the most popular types of regulators are Buck, Boost, and Low Drop Out Converters. Buck and Boost regulators are types of switching converters which use several inductors and or capacitors as memory elements to store charge and release it periodically to counter variances in voltage. Low Drop Out regulators require less components and produce less signal noise but present a huge drawback in the form of being inefficient in transmitting power.

A Buck converter is a type of switching converter that uses a combination of a switch, diode, inductors, and capacitors to step-down voltage. Buck converters present the best power efficiency when converting a DC voltage to a lower one. Their performance with respect to efficiency and versatility makes them a strong

contender for use in this device. These switching converters tend to create noise in a circuit, which is undesirable, but through the use of bypass capacitors they will be mitigated.

A Boost converter as the name implies, boosts a voltage level to a higher one. Using the same parts that constitute a Buck converter, but in a different arrangement, the Boost converter can supplement a voltage source and in turn output more voltage, therefore boosting the total voltage level. Their limitation is not being able to drive high currents at the boosted voltage levels, due to the nature of how they function, not supplying extra power to the circuit.

Low Drop Out regulators are a type of linear voltage regulator. They offer a simpler device layout because of the reduced number of components. A Low Drop Out regulator will reduce the voltage by combining a field effect transistor with an amplifier that feeds it the voltage difference and uses resistances to lower the voltage by dissipating heat. Low Drop Out regulators tend to work very well when the voltage output will be very close to the voltage input, but as soon as the voltage difference is sizable, the power efficiency plummets, and the heat generated vastly increases.

The final system utilizes a hybrid converting system, a Buck-Boost converter will be utilized for the necessary 3V3 voltage, and a Buck converter alone will be used to convert the input from the battery to a constant 1V8. A Low Drop Out regulator was chosen against, because at the given voltage levels the power efficiency drop was not worth it.

3.3.4 Biosensing AFE

For our device, we planned to implement a total of six LEDs and two photodiodes divided into two separate sensing modules each composed of three LEDs of differing wavelengths and a photodiode. With each sensing unit configured in a square arrangement we were able to achieve symmetrical light sensing. The implementation of two photodiodes receiving input from a total of six LEDs in a round robin fashion may be beyond the capabilities of a low-profile microcontroller on its own. Compact Micro-controllers on their own do not feature very high resolution analog to digital conversion, and are limited in their ability to sample from four different photo-diodes accurately. To facilitate the integration of all the LEDs and photodiodes we investigated employing Analog Front Ends to manage the whole sensing units on their own and deliver the conditioned digital signal to the Microcontroller.

An Analog-Front-End in this context would be the driver for three LEDs of different wavelengths and receive the corresponding current signal from a photodiode. When the photodiode captures light and translates it into a current signal, the current signal is a composite of three signals: an AC component that correlates to changes in blood volume, a DC component that is generated by the light reflected from the body's time invariant systems, and ambient light. The current signal from the photodiode is then converted to a voltage level through the means of a transimpedance amplifier. The signal is then conditioned through the use of a digital-to-analog converter which attenuates the signal from the transimpedance amplifier according to the level of ambient light, with the aim of amplifying a voltage signal with less interference. Once the voltage has been amplified, capacitors store the LED reflected light value and ambient light values separately, where they are then sequentially converted to a digital signal. The resulting output from the specialized Analog-Front-Ends we are researching is composite light signal, ambient light, and the isolated voltage signal which is composite signal minus the ambient light.

Analog-Front-Ends designed to be used with optical imaging for biometric purposes are a relatively new technology with major innovations taking place. When researching the different AFE options, newer high-performance devices which are capable of parallel processing different sensor inputs faster and allow for the interconnection of more devices do not publish their instrumentation data or offer data sheets beyond simple feature lists. The information for the newer biosensing Analog-Front-Ends were under Non-Disclosure Agreements. The group has tried to request the Non-Disclosure Agreement for specifically the TI AFE4900, but upon contacting TI about the request we were informed that none of the devices requiring a Non-Disclosure Agreement were being supported in academic endeavors. This has led us to consider two Analog-Front-Ends which the Product Marketing Engineer for Medical Imaging at TI recommended we use for academic purposes. The TI AFE 4403 and TI AFE4404 are the two biosensing Analog-Front-Ends recommended. In addition to the TI offerings, we will be considering the ADPD4100 from Analog Devices as an alternative that can be used to drive more than one of the sensing units with different LEDs and a photodiode at a time.

The AFE4403 is a 3.07 mm x 3.07mm x 0.5mm Analog-Front-End which supports up to three LEDs being driven sequentially in combination with one photodiode for receiving input. It offers an 8-bit current resolution programmable up to 100 mA to drive the LEDs with, allowing for fine tuning of the level of light being given off. Its power consumption is 30 microamps not including LED current and can poll at frequencies ranging from ~62 to 2000 samples per

second and communicate with a microcontroller using SPI. This Analog-Front-End also has the ability to detect faults with the LEDs or Photodiode and can signal when it finds a short or open circuit at either of the parts, providing a great diagnostic tool for an amateur project such as this.

TI's second Biosensing Analog-Front-End offering being considered is the AFE4404 which is a smaller module intended to aid in the creation of wearable biosensing devices. The full package measures in at 2.60mm x 1.60 mm x 0.5mm (Fig 3.3.4-1). The AFE4404 allows for a 6-bit current resolution when programming LEDs and a maximum of 50 mA. Three LEDs and a single Photodiode can be interfaced using this device, with it consuming an average current of 200 microamps when capturing a PPG signal. This AFE is configurable for between 10 to 1000 samples per second and transmits to a microcontroller through an I2C interface.

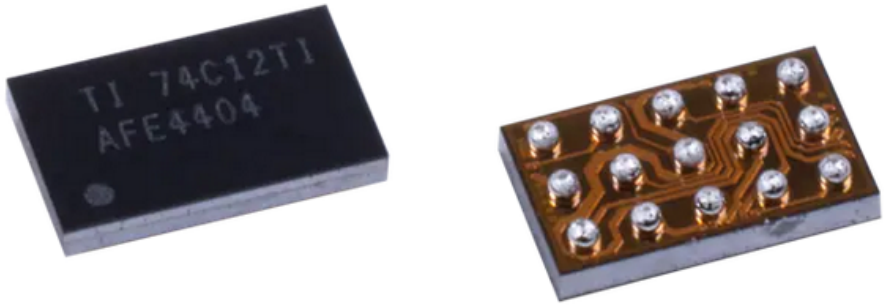

Figure 3.3.4-1.

A more robust option is a newer Analog-Front-End released in December 2020 by Analog Devices, the ADPD4100. This Analog-Front-End is 3.11 mm x 2.14 mm x 0.4 mm (Fig 3.3.4-2) and has the unique capability of driving eight LEDs with support for four LEDs being driven at the same time. In addition to capacity for a total of eight LEDs this AFE has dual channel processing, allowing it to process input from two different photodiodes at a time. The LED drivers have a current resolution of 7-bits with a range of 1.5 mA to 200 mA, with a max of 400mA of current allowed at any given time to drive LEDs.

Figure 3.3.4-2.

The two TI AFE options are very similar as far as features go, with the AFE4403 being the slightly bigger device, albeit housing sampling and LED driving capabilities at a higher frequency and current respectively. With one of the goals of this project being to maximize biometric reading accuracy, while being size conscious, the TI AFE4404 offers almost the same level of precision in capturing data, all in a package that is almost half the area. The TI AFE4403 would occupy an area on the PCB of approximately 9 square millimeters, and the TI AFE4404 would occupy an area of approximately 4.15 square millimeters. At half the area, taking into consideration the necessity for multiple AFEs due to the nature of having a large array of LEDs and photodiodes, the space that would be saved by choosing the TI AFE 4404 would be invaluable. Ultimately, we chose to go with the AFE4404 because of its smaller size, and the cost of its development board as well as its availability.

3.3.5 Thermal Sensor Module

The human body, through healthy thermoregulation, typically maintains its internal core temperature within the ranges of 36.5-37. While the internal core temperature provides direct insight into the health of an individual with regards to possible ailments, it often requires invasive methods for measurement. Skin temperature can be used to estimate the internal temperature of the human body when considering the skin as an outer layer, thus can often be measured within the lower bounds of 33-34. Using Wein's law one could estimate the average radiation from thermal emission of the human body to emit wavelengths around the near infrared range of 930 to 970 nm. Given this range, we initially planned on sampling skin temperature via the photodiode given that responsivity provided by the broadband response often peaked around these wavelengths. This

method proved to be possible with our planned sampling architecture but would severely limit our ability to use a selection of AFEs. The reason for this limitation arises from the ambient sampling that the AFE collects to eliminate ambient illumination, which would consequently register any thermal emission as ambient. Due to this reason, we found it more practical to implement a thermal sensor module independent of the optical module, given that most thermal sensors are sold with on-device ICs.

For picking a thermal sensor we were faced with two possible methods of implementation: contact or non-contact. From a generalized perspective, contact thermal sensors measure temperature by measuring their own temperature as thermal equilibrium is reached between them and the object of measurement. Non-contact thermal sensors measure temperature through the method we previously proposed where thermal radiation was used.

The two thermal sensors we found in stock for this module each fell into one of these two categories. The MAX30208 by Maxim Integrated is a contact thermal sensor that is designed for wearable fitness devices as well as medical devices. The MLX90632 by Melexis is a non-contact sensor that is designed for multiple temperature monitoring applications ranging from healthcare, industrial temperature control, and livestock monitoring. The benefits of the first option is the high level of accuracy of 0.1 as well as a low power consumption design. The downsides to this option are the requirement of contact to the skin directly. This would require additional consideration towards the mechanical design of the full device such that it can have contact with the skin and be connected to the microprocessor. The benefits of the second option are that the thermal sensor can be placed in the same platform as the optical sensor, therefore facilitating mechanical design and helping us meet our dimension’s constraint. Another benefit of the device is although it has less accuracy than the contact option, it offers an accuracy of 0.2 which is still considered rather well for this application. The main downside to the noncontact option is the price of the device being lansalmost 5 times the price of the non-contact option. Given that our group plans to use optical adhesives, the implementation of a contact thermal sensor would take additional mechanical considerations, which is not the strong suit of any member, therefore we prefer using the noncontact option, even though it is considerably more expensive. . For this reason we chose to use the MLX90632 as our temperature sensor.

3.3.6 Wireless Communication Modules

The intention of this system, as is common in many of the commercial competitors and other example projects cited above, is to utilize a constructed device to do the majority of the sensing. Once this is completed the system should ideally relay this information back to another device, presumably a mobile phone or similar platform. This system intends on utilizing the extra compute power provided by the additional platform. The cost of this decision is that data communicated will require a compatible medium for transmitting the data from the sensing device. Most mobile phones have few wired interfaces but often support both wifi and some revision of Bluetooth.

Although creating a device to communicate over wifi would be possible, incorporating a complete TCPIP network stack on the constructed sensing device would take up additional processing while making limited use of the features provided by this fully developed network protocol. Bluetooth Low Energy seems to be made explicitly for this kind of device, removing the need to try to connect via wifi. Given the advantages of the standard's capability to interface with peripheral devices and its lightweight ad hoc networking capability this is the obvious choice for wireless connectivity for our sensing device. This section aims to compare and contrast available Bluetooth Low Energy modules.

Due to the large range of choices available for Bluetooth Low Energy wireless communication and the current market conditions this section is still under revision. At this time the intention is to use the Ublocks NINA-B306 depicted in the figure 3.3.6-1 below. This image was taken from a physical device, Arduino Nano 33 BLE which is open source and may end up being the exact module used if part shortages require desoldering of the Bluetooth.

Figure 3.3.6-1.

This module is available on an integrated circuit that was available to use for testing such as the Arduino Nano 33 BLE. Although the module can be difficult to find individually, using the open source Arduino platform gives the ability to model the PCB after the embedded system, simplifying device programming. Further if the module becomes not available while this system is being assembled the Nanos can be desoldered to supplement availability of parts. The entire Arduino Nano's price is only a small increase over the cost of this Bluetooth module.

3.4 High-Level Architectures and Diagram

The planned system will incorporate the function of a designed device that uses LEDs and sensors to gather biometric data. It will then analyze the information gathered and use a communication protocol to push the results to another device for display and storage. The various components will be completed by each of the members of the team. Each member of the team will be responsible for the completion of at least one of these components from an administrative perspective but any or all of the team may end up working on any given component. Responsibility for each is labeled in the figure below (Figure 3.4-1).

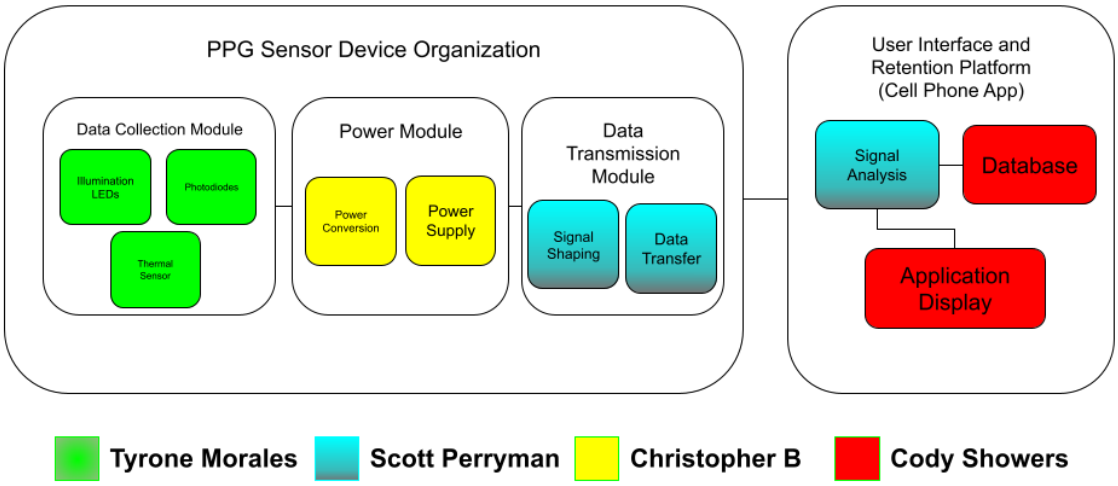

Figure 3.4-1. High Level Architecture diagram

3.5 Parts Selection Summary

This chapter will be used to discuss our final decision on parts and their implications on our design. The currently selected components are listed below in table 3.5-1. As more components that fit the criteria are found in stock, this table will be updated.

Component Name	Sub-system used
SFH 2200 - OSRAM	Sensor (Final)
SFH 7016 – OSRAM	Sensor (Final)
LED525L - Thorlabs	Sensor (Demo)
BPX 61 – OSRAM	Sensor (Demo)
AFE4404	Sensor (Final)/Power/Preprocessing
MLX90632	Sensor
Arduino Nano 33 BLE	Microprocessor, Bluetooth, IMU
Lithium-Ion Polymer 500 mAh	Power System
MCP73831	Power System

Table 3.5-1.

4.0 Related Standards and Realistic Design Constraints

The purpose of this chapter will be to review relevant and related standards as well as the constraints which will influence this design and its intended functionality.

4.1 Standards and Their Relevant Impact

Standards allow systems to be designed and created within an existing ecosystem and prevents the need to design every element from scratch. The purpose of this chapter will be to review some of these standards which have made their way into this design and their relative impact.

4.1.1 Bluetooth

Given the complexity and interoperability of Bluetooth, maintaining its use in modern applications requires efforts from several groups in defining and adapting standards. Bluetooth Special Interest Group has created standard packaging schemes for establishing a basic server client relationship between two bluetooth enabled devices. Figure 4.1.1-1, courtesy of Software-dl, shows the Bluetooth Low Energy protocol stack.

This section will be focussing on a select portion of this protocol stack due to its extensive nature. As a list, the standard protocols discussed in this section are Generic Access Protocol(GAP), Generic Attribute Profile(GATT), and Attribute Protocol(ATT). These are found to be important to the discussion due to their involvement in the development process. Lastly, the Bluetooth link layer will be discussed due to its benefits to our design.

The Generic Access Protocol(GAP) is one of the main host protocols for Bluetooth and defines the device's mode with regards to connectivity. Through the use of this protocol a device can set itself in one of the following settings: Broadcast, Non-discoverable, Limited discoverable, General discoverable, Non-connectable, and Any connectable. We will be taking advantage of this to maintain user data security.

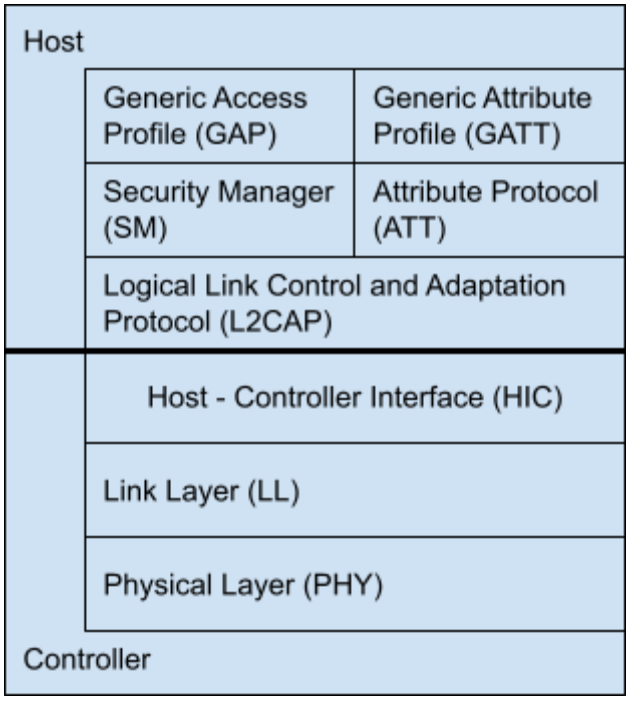

Figure 4.1.1-1.

The Attribute Protocol(ATT) is a data structure and transport protocol standard that defines a common way for bluetooth applications to communicate(Protocol Data Units) and a common way to reference information(attributes). The standard is written below:

Attributes Data Structure:

- Attribute Type(Universally Unique Identifier)
- Attribute handle(Attribute Identifier)
- Attribute Permissions(Client Permissions)
- Attribute Value

Attribute communication packet structure(PDU):

Attribute Opcode (1 Byte)	Attribute Parameters (Variable Size)	Authentication Signature (0 to 12 Bytes)

Attribute Opcode Structure:

Method{Read, Write, Broadcast} (6 bits)	Command Flag (1 bit)	Authentication Signature Flag (1 bit)

Generic Attribute Profile(GATT) builds on Attribute Protocol(ATT) to define abstract capabilities of the device. This is an interface standard that lets software developers define the attributes available on the server and services you can perform on them. A diagram of example sensor in the GATT profile is below in Figure 4.1.1-2

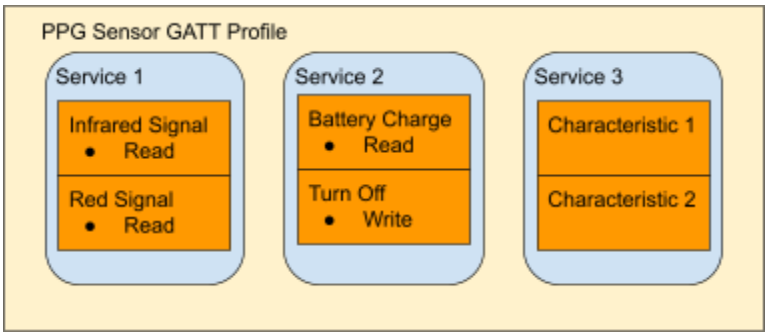

Figure 4.1.1-2.

The link layer of the protocol stack implements the communication standards between bluetooth devices. Below is the packet format that is defined. Due to the CRC being included in the link layer standard protocol, the PPG sensor is alleviated of all responsibility to implement error detection.

Preamble (1 Byte)	Access Address (4 Bytes)	Protocol Data Unit(PDU) (2-257 Bytes)	CRC (3 Bytes)

4.2 Realistic Design Constraints

Taking a design from a theoretical exercise to actually implementing is a process which adds in additional factors that can be impacted by external forces and events. In this section there will be discussion of different and often external constraints as they relate to possible consequences on the realization of this design. This section is divided into four sections: economics and time contractions; Environmental, social, and political constraints; ethical, health, and safety constraints; as well as manufacturability and sustainability constraints.

4.2.1 Economic and Time constraints

Time constraints that were present on this project limited some of the capabilities that are planned to be implemented. Bluetooth wireless communication is a notoriously compromisable channel and definitely is at risk of exposing user data. Considering the nature of the device, privacy is something that should be taken very seriously. Some of the plans to combat this was to encrypt all data that would be sent through the wireless medium. To accomplish this realistically would require encryption and decryption on both sides of the communication channel.

Since members of the group have other obligations and are not full time employees of a company tasked with creating a product, we are inherently constrained by the amount of time we are able to dedicate to this project. Having to work or go to school five days a week while not receiving compensation significantly hampers our ability to create a device competitive with professional consumer products.

Economic constraints are in no shortage at the time of this project. Global inflation and other external factors such as the rise of gas prices have exacerbated the financial issues we may face in the completion of this project. As a result of the aforementioned problems, the prices of components, as well as shipping have gone up.

4.2.2 Environmental, Social, and Political constraints

Developing a product amidst a global pandemic radically changes the modalities in which collaboration is allowed. Shifts in the political or social climate could result in an inability to meet in a public space including but not limited to labs at the university. In the current climate it appears that barring university implemented protocols, there will be no legal hurdles to overcome when meeting for this project implementation. At the time near the end of the Spring 2022 semester the US and Florida specifically lifted many of its pandemic restrictions on gathering and movement in public. However this is not the case globally and could change if there is a resurgence of sickness in this region.

Post first pandemic wave has had an impact on delivery of goods including but not limited to semiconductor components locally. Among affected industries of labor shortages, trucking is one that has made considerable news in the first quarters of this year. Even when supply chains are otherwise no longer affected by pandemic issues, trucking has seen retention issues due to the distance traveled, and number of people interacted with. It is also worth noting that US truckers carrying freight were detained in Canada if they could not prove appropriate vaccination status. Illness risk and political climates surrounding it has resulted in protests, renegotiations, delays in service, and even some leaving the industry altogether. These factors have impacted the industry and resultantly domestic distribution networks and supply chains.

Internationally supply chains have also had an impact. Upticks of illness, in particular Omicron variant Covid cases in China, have resulted in a change in Chinese policy. Their “Zero-covid” strategy has resulted in large scale lockdowns in the region. This includes major ports such as the port in Shanghai. This is not only one of the largest and busiest ports in the world, but also one of China’s most critical manufacturing ports. Even if exports could continue at pre pandemic rates, the lockdown has affected manufacturing in two major ways. In affected regions either workers are being forced into home lockdowns where they cannot leave the complexes in which they live to travel to work, or they are being forced to stay in the place that they work. Not all of these facilities are properly equipped with facilities required and some cannot receive required materials for the manufacturing. This can only serve to further complicate supply issues, if not directly on chips in this implementation plan then indirectly when affected chips are not otherwise available.

Especially in the local environment it is not expected that restrictions would get anywhere near China’s restrictions local to the university. However, it is always possible increased restrictions would be put into place if there is another wave of the illness. This will have to be in contingency plans for availability of resources for anything that is reliant on the university, whether it be access to lab equipment or even just the group meeting for design discussion or implementation.

4.2.3 Ethical, Health, and Safety constraints

Developing a consumer system which informs users on potential health issues comes with various ethical, health, and safety concerns which will be addressed by or should impact the design. The system as it is outlined will also be storing data relevant to consumer health and is considered quite private and need to be made secure. Any information provided to the user should be as accurate as feasibly possible, but an electronic device is no substitute for medical advice from a trained practitioner.

As mentioned in the section related to time constraints there is an inherent risk in transferring the data wirelessly. When related to Bluetooth when the device is broadcasting data, it will be open in the air. However with our intended system any security limitations of the medium will be mitigated somewhat naturally as the data exposed to wireless transfer will be uninterpreted or processed. It will also not contain any metadata which should indicate the identity of the user but caution will still need to be taken as this data can be interpreted to gain confidential or sensitive data about the user. Further use of the Bluetooth Low Energy protocols will make this communicated data available to all applications with Bluetooth permissions on the Android platform due to how the operating system deals with this form of communication. Time permitting this designed system may have room for application level security or obfuscation which can help further safeguard user data in this situation.

Since the system will be dealing with private data, data security in the database structure is also a top priority. Requiring user login and handling the security through a standard SQL implementation should limit unauthorized exposure. This has led the design to require a separate username and password specifically for this implementation to access this data. This should prevent reasonable attempts at unauthorized access because it will be also stored locally on the user's mobile device, however advice that sharing the device may help permit unauthorized access should be considered in the design.

Beyond potential failures in interpreting or measuring biometrics since the purpose of the device is to inform users on health issues appropriate warnings will be required. This system is not meant to be a replacement for a medical professional, rather a tool to help inform the relevant professionals and help educate users. However because this system will present medical standards it is important that they are outlined as typical but not necessarily representative. It must be noted before and wherever this information is provided that consulting with medical professionals is advised whether within or outside of recommended ranges.

4.2.4 Manufacturability and Sustainability constraints

The development of this project happened to be during a relatively volatile period in supply chain history. Many of the parts and modules that were considered for this project were not available and have extended the intended period of development. The world is going through a large semiconductor shortage and a solution is not in sight. Figure 4.2.4-1 is a graph of semiconductor component construction from recent history.

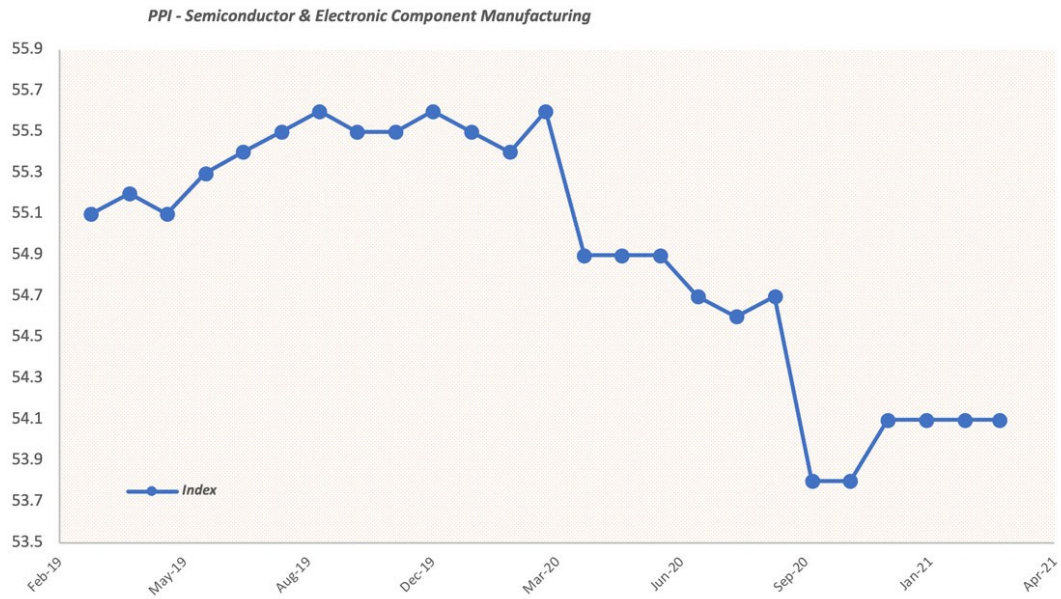

Figure 4.2.4-1. (Taken from GEP, et al).

Due to COVID-19, semiconductor production has significantly decreased despite a steady increase in demand. This has had a serious effect on part selection. Almost every optimal part is out of stock and will not be back in stock before the due date of this project if it will be in the calendar year. Semiconductor manufacturing is plotted across time in the image below.

5.0 Project Hardware and Software Design Details

In the following sections we will be going into detail about the inner workings of each sub-system, providing diagrams and schematics to provide a high-level overview of how our systems will operate, and then go into a more exhaustive analysis of how they will be sending data, as well as how each system will be powered. The main subsystems of the project are divided into optical sensing, communications, software design, signal processing, and power delivery. We will be exploring how the optical sensing system connects 6 LEDs and two photodiodes, the data path for information received from the optical sensing, and the physical arrangement of LEDs and photodiodes. When discussing the communication subsystem, we will be homing in on how it is the project will communicate through Bluetooth. The software design subsystem describes the user experience when using the device and how an LED indication system will be integrated that interacts with the mobile application to provide feedback on what the device is doing. The Signal Processing subsystem will divulge the methods of extracting and analyzing the data received from the optical sensing system which entails the use of various filters and optimization algorithms. The power system section will provide insight as to how each system's power needs will be met, as well as how the different necessary voltage levels will be established.

5.1 Initial Design Architectures and Related Diagrams

This section is going to cover some high level diagrams of the main systems in this project. The data transmission and processing diagram shown in Figure 5.1-1 represents the flow of information from the AFE to the external device. This image does not include the read packets the external device would send to the phone to maintain simplicity. The flow of arrows really represents the device's response to a read packet from an external device acting as a client on the bluetooth network. From the beginning the AFE's will be outputting a digital signal at 100 Hz. The CPU will read from the device using I2C at a rate of 100 Hz. As the CPU reads the output the, AFE it will accumulate the signal on an internal register and write it to memory every R additions, where R is the input to output frequency ratio. By downsampling we can conserve bandwidth and memory. When a client on the bluetooth network makes a read command to the device it will map the attribute handle to a memory address through the bluetooth software stack running in parallel to the CIC digital filter. Once the memory is

mapped it will return the N samples corresponding to the signal demanded by the bluetooth client.

On the bluetooth external device, the image emphasizes the distribution of information to the signal processing algorithms that we will be using on it. It also shows the output of each signal processing algorithm to each prediction algorithm.

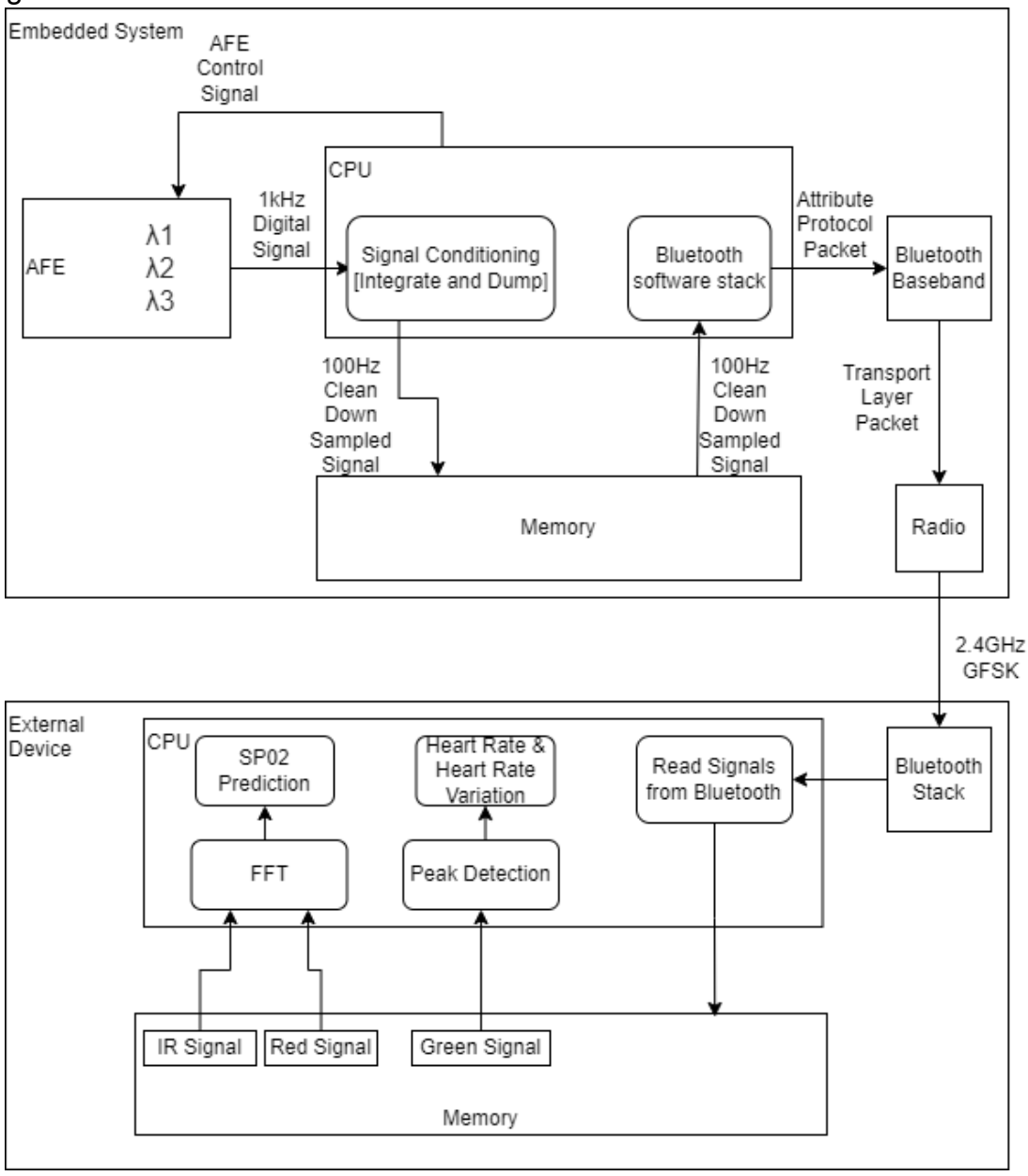

Figure 5.1-1.

5.2 Sensor Subsystem

[Overview of Design] - We plan to construct a 6 channel multiwavelength sensor module which will interface with an AFE, thermal sensor, and microprocessor to optimize signal collection. The sensor module will be composed of two sub-sensor modules arranged in a symmetric geometry as can be seen in figure 5.2-2. Each sub-sensor will consist of one Multi-Chip LED SFH 7016 and one TOPLED SFH 2200.

The configuration of the LEDs, photodiodes and AFEs can be seen in figure 5.2-1. The sub-sensors were connected to an AFE and set to provide a forward current of 50 mA for the green LED, 6.8 mA for the red LED, and 8 mA for the IR LED. The AFE's transimpedance gain was set to 500kΩ gain for the green wavelength, and a 100kΩ gain for both IR and red wavelengths. For the DC-cancellation values for offset correction of the photocurrent, the green wavelength was set to -0.93 mA, the red was set to -1.87 mA, and the IR was set -2.8 mA. The AFE's signal conditioning stage converts the photocurrent into a voltage during amplification via transimpedance amplifier, removes offsets from ambient light and other sources of noise, and then converts the analog signal into a digital one. A schematic of the LED, photodiode, and AFE integration can be seen in figure 5.2-3 where the connections to the AFE are shown.

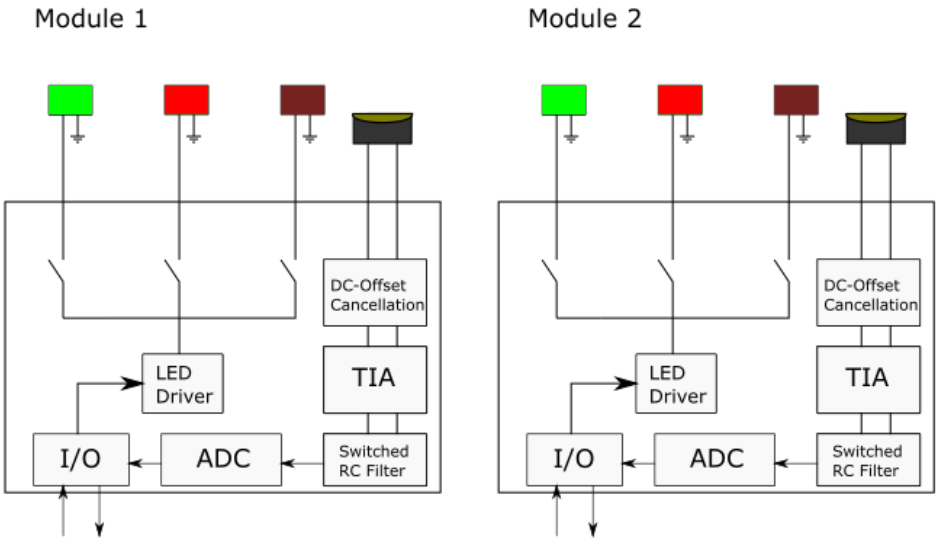

Figure 5.1-2. Sensor Diagram

The spacing of the photodiode and LEDs was initially set at 2mm due to its sufficient spacing to allow for optical barrier placement to prevent *ICT*, while still allowing for a higher level of collection efficiency than would be present at longer spacings. The space between the components ended up being closer to 2.5 mm due to issues with the manufactured sensor PCB being larger than the stated dimensions. Initially the plan of a dynamic illumination feedback system was to result in slight current increments (0.5mA) errors in PPG processing. This was scrapped due to an increasing complexity in programming and configuring the AFE signal conditioning and LED driving stages.

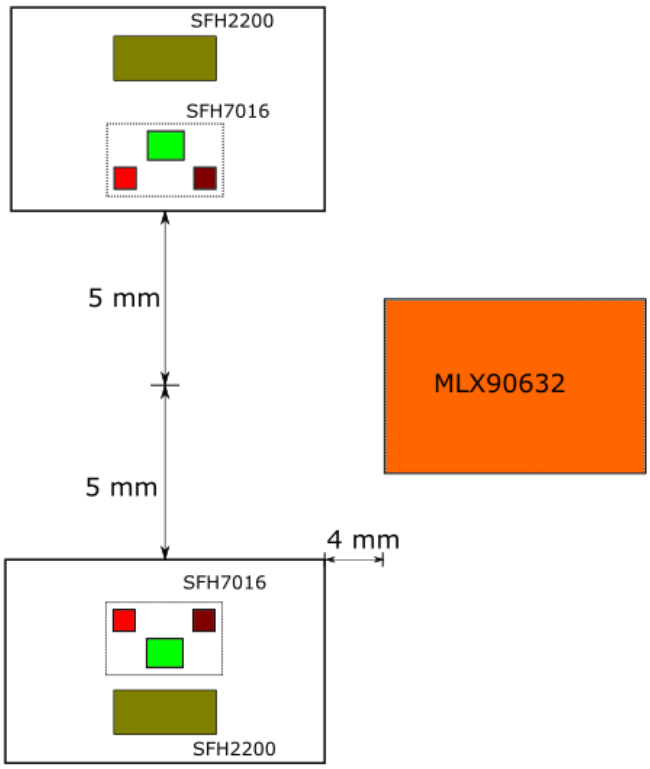

Figure 5.2-3. Optoelectronic component placement

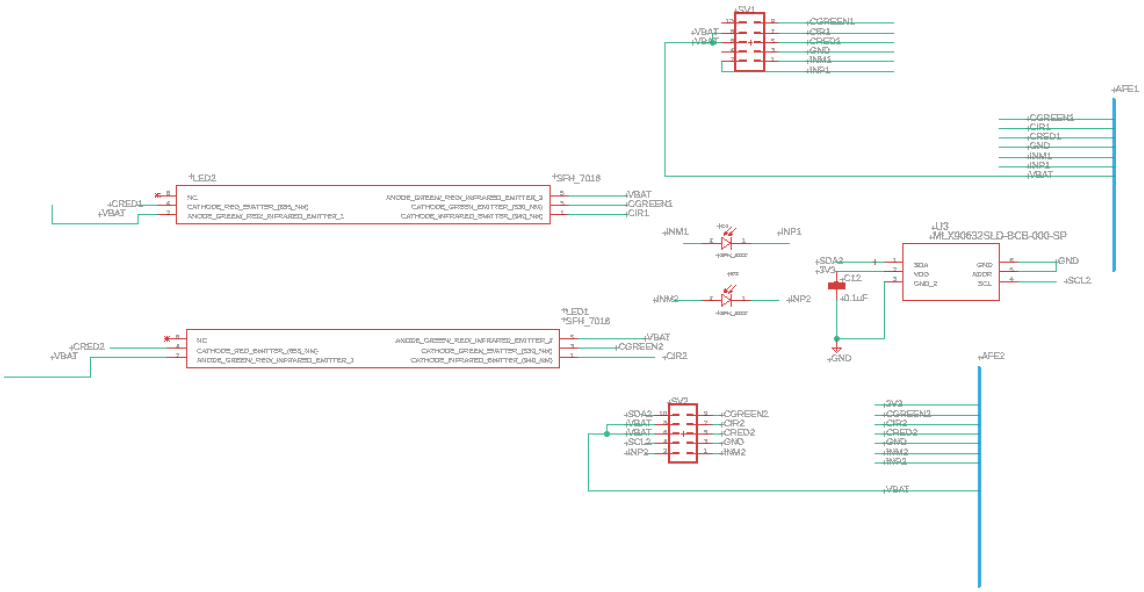

Figure 5.2-4.

5.3 Communication Subsystem

Due to computational limitations, it is most likely favorable to do feature extraction computations on an external device. To make this possible we would have to relay all of the received PPG signals without any information loss. Since we are sending the data to an external device it is required that we send control signals from the external device to the PPG sensor demanding two way communication. This section will be dedicated to the communication subsystem and its peripheral connections to clearly show this process.

Bluetooth Low Energy is a digital radio standard that operates at 2.4GHz and supports a data rate up to 1 Mbits per second. Considering that we are not worried about long range transmission this seems like a highly interoperable solution. Figure 5.3-1 is a diagram identifying how each system on the embedded system and external device relates to the bluetooth communication stack.

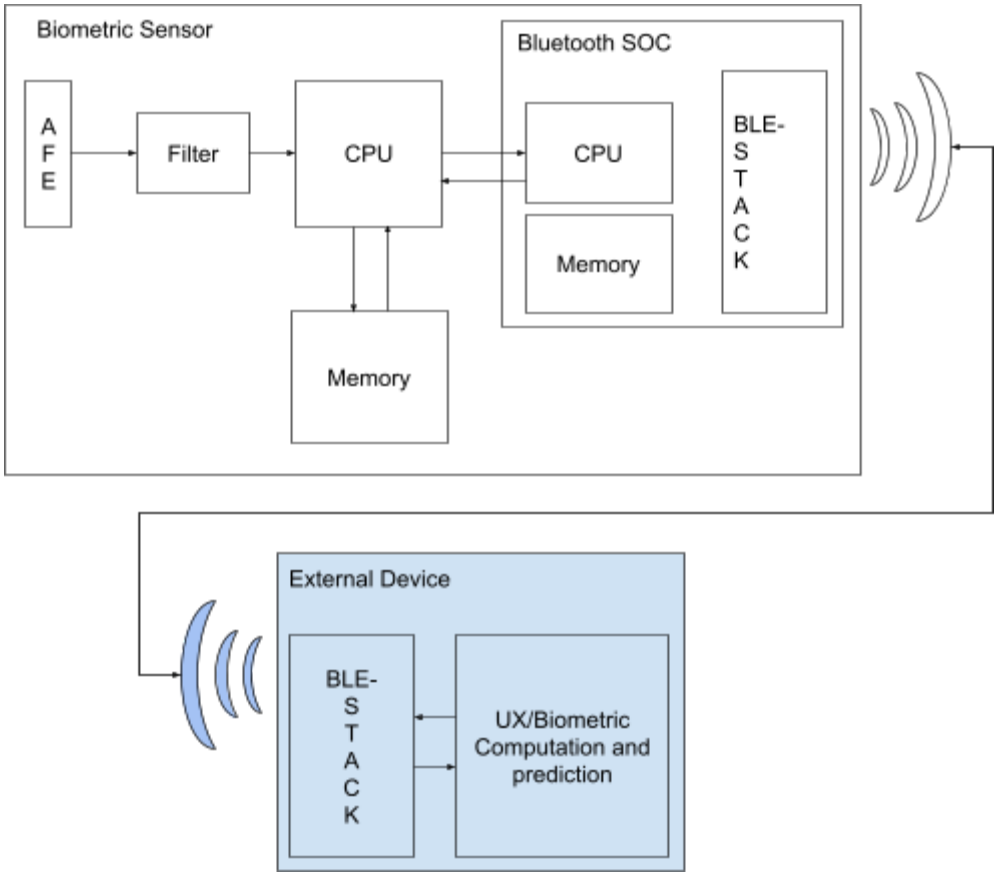

Figure 5.3-1.

5.5 Software Design

The primary elements of the software design of this system come in four key components. The device will need a control system to switch between operating modes. The device itself will do some data interpretation in order to inform some of the essential hardware components responsible for sensing and transferring sensor data. Once the data is sent the most computationally challenging component of the design will take over in the form of the signal processing. This will have its own dedicated section below so it will only have brief mention in this section. Finally there will also be a section dedicated to the display and storage of the interpreted data.

On the local device composed of the sensor array and transmission module, there will be a requirement of the system to briefly interpret the signals from some of the sensors to inform them if adjustments are required or if data needs to be reread. This system was also going to be responsible for updating the indicator LEDs on the local device, however this was not implemented. Any security or extra data integrity checking will also need to happen at this level of the software implementation on the local processor.

The corrective software running on the processor on the PCB will need to await input from the sensors in order to return feedback. Ideally when a signal comes in it should be able to review the incoming data from the inertial sensor, specifically the acceleration measurements, and ascertain if there is a significant amount of motion which may impact the readings. Further the system should also take in the information from the sensor connected to the AFE in order to determine if there is noise and adjustments need to be made to the LEDs to compensate. This will be handled by adjusting the current to the LEDs in the sensors to try to counteract this noise.

In order to inform the user of the status of the device, originally it was planned to have a series of LEDs which would have been updated. Instead the system was not implemented with this system, as it would require two way traffic with the mobile application. Instead the plan was to update the user of the status using the mobile application. The onboard processor will need to interpret the status of the sensing system, bluetooth connection, and response to sent data in order to report the system status to the indicator LEDs but to ensure accuracy the extra communication seemed to over complicate the already redundant system. Very little processing was to be involved in this section; it is mostly going to be informed by the status of individual variables defined by their respective processes and updating the LEDs accordingly.

No additional application level data checking or security was added, but it would have to be also processed on the board prior to the transmission. At this it is unexpected that this will be in scope of this design, however time allowed some basic application level security could be included. Some implementations that could have been included are an app level cyclic redundancy check to ensure the messages are sent properly, the inclusion of parity bits corresponding to message data, or some basic encryption to obfuscate sensor data being transmitted.

After data is transmitted to the application on the mobile device, its first step is the signal processing. This requires enough detail that it warranted its own section below. At this point if data is found to need to be reread, a message will be sent back to the device to indicate this. Otherwise it will continue to the data storage flow. Once the message is interpreted the results will need to be displayed to the application on the mobile device so that the user can see this feedback. From here metadata will need to be wrapped around the data in order to ensure that it is filed properly. This metadata will include the user account of the application, the time it was measured, and which biometric it corresponds with. From there it will be stored in the database keyed with this relevant data. After this point it was originally planned in the design for a confirmation message to be relayed in the form of an acknowledgment to the sensor device so that the next batch of data can be received. Instead this logic was handled inside the mobile application to simplify communication with the sensor device Figure 5.5-1

describes the flow of data to be stored from the perspective of the external device storing user information.

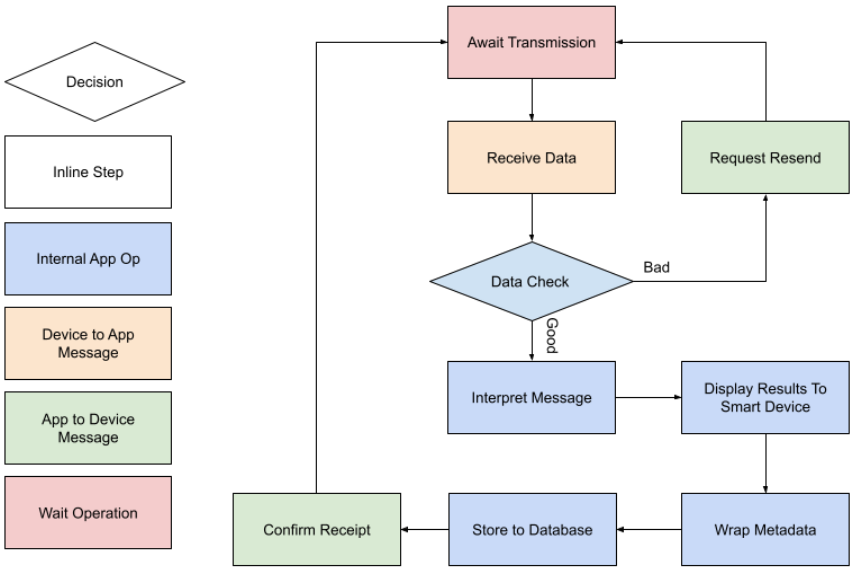

Figure 5.5-1.

5.5.1 User Interface

The user interface of the application is designed to be easy to use with very little overhead to implement. There will be two places the user should be able to receive information from the system, the wearable and the external device application. The wearable interface will not take any user input but will be able to notify the wearer of its status.

The external application will be primarily how the user interacts with the device. Below is a depiction of a sample user interface that would implement all of the capabilities that we plan to include. The figure 5.5.1-1 is a screenshot of what the interface on the app looked like during one of the tests. There are 2 main views that the user has. First is a Login screen, which allows a user to segregate data between profiles. The next is a Scan and History view, where there are buttons to cycle through between the different biometrics and a scan button used to initiate a sample cycle from the sensing device. There is also a graph showing all of the previous metrics the user has stored for this profile and a label at the top of the screen indicating a metric and the last stored value for this metric on this profile.

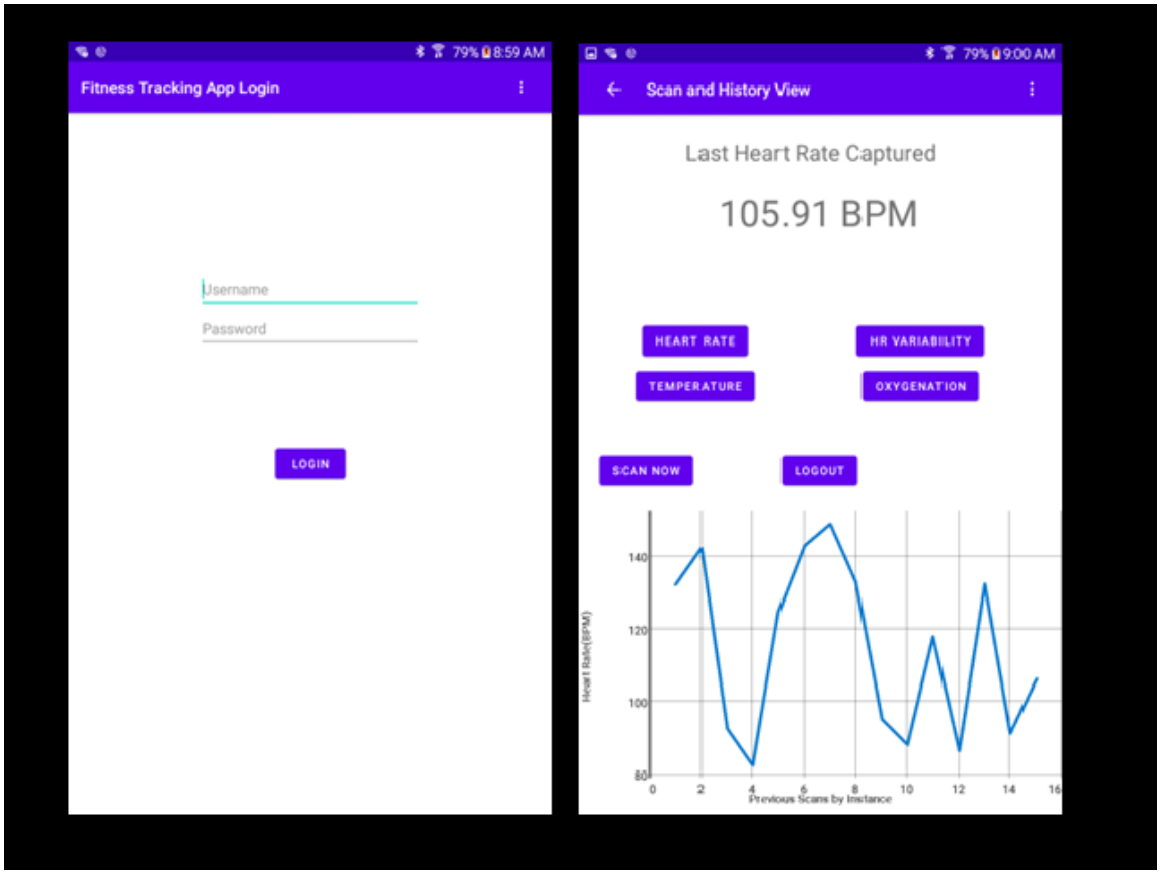

Figure 5.5.1-1.

5.5.2 Data Storage Interface

For this system to meet some of the design goals, such as having the data be available for review, it must be considered how the data is organized and stored. When trying to decide on the specific system for the data organization there are a few factors that must be considered. First the system must be reliable and predictable. Next the data to be stored must be relatively secure since it will be personal and private. Ideally the only person accessing this data will also be the one recording it. It would be possible to design a system to accomplish these goals. However, some of the most common systems for secure data storage and transactions are referred to as database management systems.

Although it would be possible to design and implement a data archival system to accomplish these goals, the frameworks are already available in preexisting database management systems. A custom-built solution may not be subject to the same security vulnerabilities that existing systems may be subject to since they may not rely on such widely used software frameworks. Despite this a custom-built solution must attempt to cover security holes without the extensive testing afforded by an already created and tested solution. This is also the problem within it comes to the features of the implementation. A custom designed system may allow for specific focus on the types of transactions

required for the implementation, possibly allowing for a more flexible or light base for storing or processing the data. Despite this being true, it may be difficult to consider all the requirements before implementation and testing. Again, an existing framework has the potential to save significant time.

If considering existing data management systems DBMS or database management systems are the most obvious choice. They have systems built in with tested features which ensure security, transactional reliability, and clearly defined limitations. These preexisting solutions afford the features this system requires with significantly less software design overhead and testing. This is particularly important in where security is involved where choosing the wrong random number generator can be the difference between a cryptographically secure message and one that is easy to decode or ensuring end to end transactional security.

Database management systems most commonly fall into one of two categories, relational and non-relational databases. Non-relational databases tend to be more free form allowing for a more flexible data set and structure. This often aids in rapid development and deployment of applications since there is less structure and planning required before the system is functional. However, this lack of structure can come at a cost. If the system is not designed to handle edge cases or an unexpected value in the database, the system can have unexpected behavior at best or critical failures at worst. Relational databases Take a greater amount of consideration to stay flexible and often take more time to develop. Failure to develop this structure carefully can result in data anomalies such as missing or duplicated data. Carelessness can also make changes from the original design nearly impossible without refactoring significant portions of the database. This is because they must be much more rigid in structure which has to be clearly defined before the data is imported into the system.

Where non-relational databases can be more difficult is directly related to their data flexibility. Coding standards are not nearly as well defined as systems which have been developed from an SQL framework. Which can complicate development, maintenance, and testing. Further, the data flexibility can also result in performance hits with complicated queries in comparison to their more structured environments. Relational databases do not have these weaknesses since they are so structured and often derived from the SQL standards. SQL systems have been tuned to have specific responses to structured and atomized queries. It is both predictable and performant so long as the queries are well planned as well. Non-relational databases also do not benefit in the same way as relational databases from data normalizations.

The biometric measurement system being developed and designed here could benefit from either of these types of database management systems. Despite this, given the benefits and downsides of each type, the available implementations, and the kinds of data that this device will need to record, a

relational database system will serve the system's requirements best. Ultimately responsiveness of queries is important for the user interface. Any delays could be perceived as inadequacies of the system, so it is important for the queries to be quick. The data will conform to a specific standard so it should be possible to structure the database system predictably. Further the scope of the metrics the system should also be predictable and easily captured within the scope of a relational database system, once the system is created long term maintenance which will modify the types of data captured should be minimized, minimizing some of the advantages of the non-relational database systems. If additional metrics need to be added, they are incorporable easily enough in the existing tables or with few additions. Also, a query to gather this data could be easily modeled after a similar request for data. Using a relational database system can ensure that the data the system collects will also meet SQL standards of security, reliability, and data integrity.

Most DBMS systems require the database to be hosted within its own separate application, however SQLite3 gives this system the option to both host the SQL database within the application but also keep many of the strengths provided by a relational database system. SQLite is supported by Android studio and is recommended for small projects that do not require collaboration and ad hoc data storage implementations that are precursors for connecting to a more standard centralized storage.

The database and storage will be contained in the device storage on the mobile device. Upon launching the application the application will attempt to connect to the data storage, if this fails a new framework will be created. Once this connection is established the user will be required to login. If a unique username is selected a new user account will be created with the password entered. If the username is not unique, the application will compare with the password already entered. If this password matches the login will complete. If this password does not match a message will indicate failure and the user will be forced to try again.

This is described in the state diagram below (Figure 5.5.2-1). In the overall application state diagram this will be referred to as the Application Login Sequence

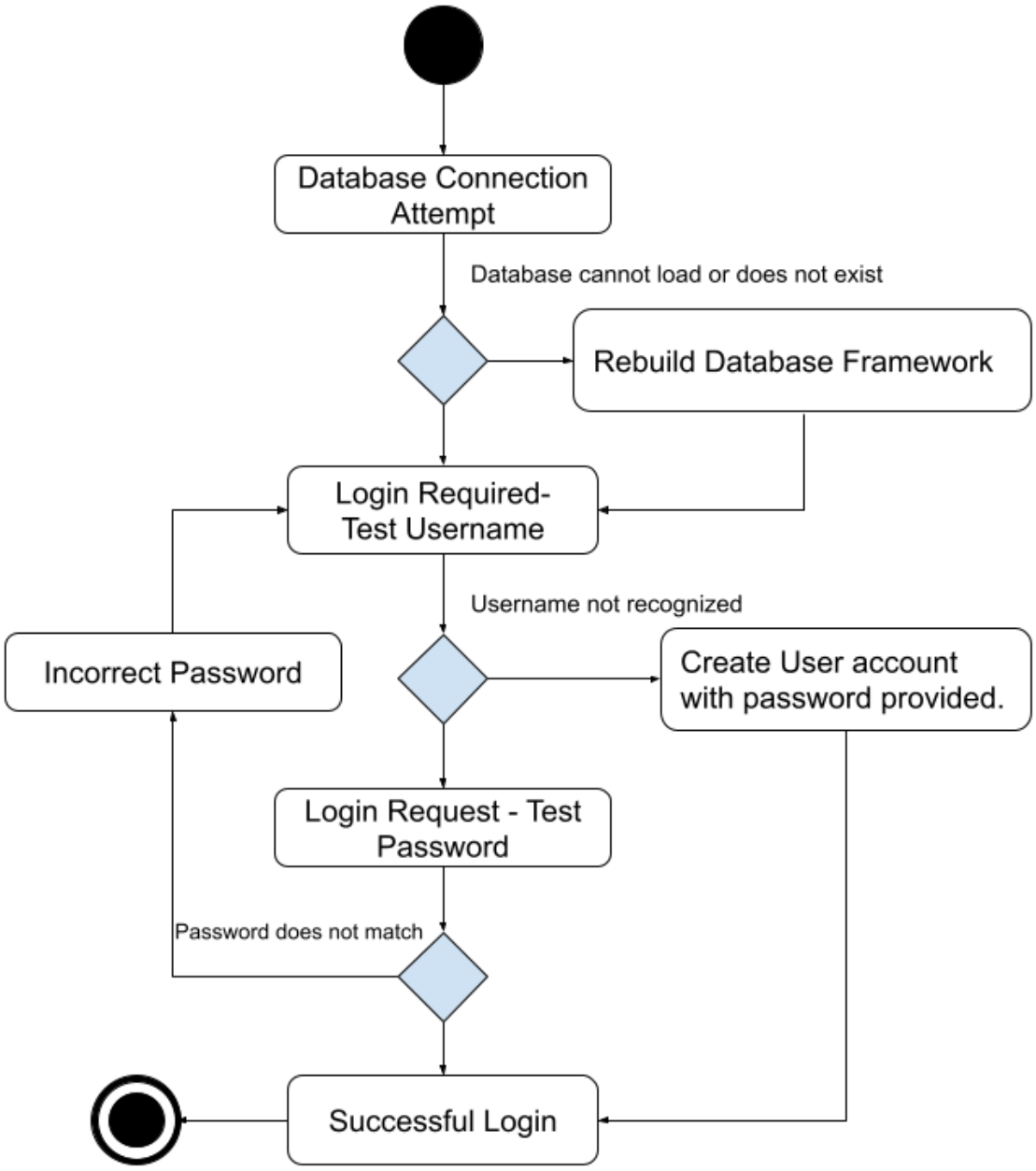

Figure 5.5.2-1.

The database table structure can have additional tables in order to add additional functionality to the overall application. However after it has been normalized it will require the following 6 tables: Users, Sensor_Function, Biometric_IDs, Recording_Sessions, Sensor_Readings_Raw, and Derived_Biometrics. A query will be used for each read or write operation to this database and each table will contain the minimum possible duplicated data while still preserving the desired functionality. This table structure is described in the image below figure 5.5.2-2 including the data types which will be required for each entry. Without including further logic to utilize all of the tables, some values were actually hardcoded, such as the sensing units and the Bluetooth class codes, however they added

such a nominal amount of space to the database it was not worth it to pull them from the final design.

Users			1
id*	username	password	
Integer	String	String	
Primary key, Inc	unique		

Sensor_Function		2
id*	blueToothClassCode	Description
Integer	Integer	String
Primary key, Inc	Unique	

Biometric_IDs			3
id*	Units	Description	
Integer	String	String	
Primary key, Inc			

Recording_Session				4
id*	UserID	Start_time	End_time	
Integer	Integer	Date_time	Date_time	
Primary key, Inc	Foreign key (1)			

Sensor_Readings_Raw					5
id*	UserID	Sensor_ID	TimeStamp	Reading	
Integer	Integer	Integer	Date_time	Floating Point Value	
Primary key, Inc	Foreign key (1)	Foreign key (2)			

Derived_Biometrics					6
id*	UserID	Biometric_ID	SessionID	Value	
Integer	Integer	Integer	Integer	Floating Point Value	
Primary key	Foreign Key (1)	Foreign Key (3)	Foreign Key (4)		

Figure 5.5.2-2.

If space became an issue maintaining this data, Raw Sensor readings were only required before the Biometrics were derived. If space is an issue this data could be cleared for cleanup. At the time of this document the only use data in this table served was to provide samples for testing. Since it was a nominal amount of use it was not worth updating especially because it could be used to facilitate expanded functionality later.

5.5.3 Wireless Communication Interface

For the wireless connection from the mobile phone to the sensor device it has been decided that Bluetooth Low Energy (BLE) would be our medium of choice. The connection will be established from the phone to the sensor device. The sensor device will be set up as a server while the phone app acts as a client. In order to pair up the device Bluetooth will need to be enabled on the mobile device and a device pairing will be required. Requests will pass from the app for the sensor device to provide a fixed sample of the data from the sensor systems. This request should result in a sample from the AFEs that is provided by the photodiodes, the inertial sensor, and the temperature sensor. These will be sent over Bluetooth to be received by the application. Anytime this request is made the application will need to confirm the Bluetooth connection. This process will look something like the following state diagram. In the overall application state diagram this will be referred to as the Verify Bluetooth Connection Sequence. This connection sequence is depicted in the state diagram below (figure 5.5.3-1)

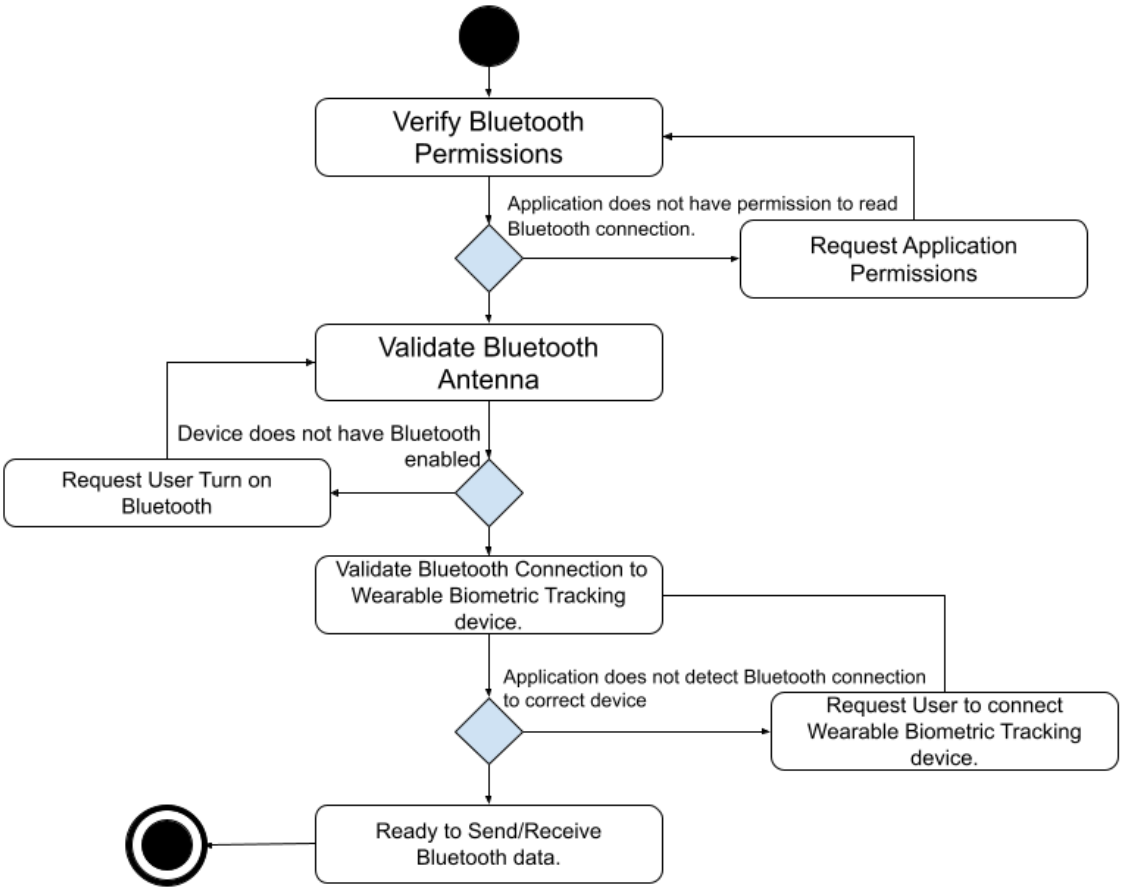

Figure 5.5.3-1.

5.5.4 Mobile Application Flow

In order to review historical biometric measurements or to take a new measurement users of this system will need to load the mobile application. A state diagram depicted below (figure 5.5.4-1) describes the complete external application logic. This application will go through its initial loading flow where it initializes required data structures and libraries before launching the Login Screen. Once the user enters a username and password it will go through the application login sequence described in the Database connection sequence in section 5.4.2. Once logged in the Main application page will launch. The user will have the choice of logging out, taking a measurement, or reviewing recorded historical measurements.

If the user chooses to log out and exit, this will end this session of the application. A user will need to relaunch the application if they wish to continue use.

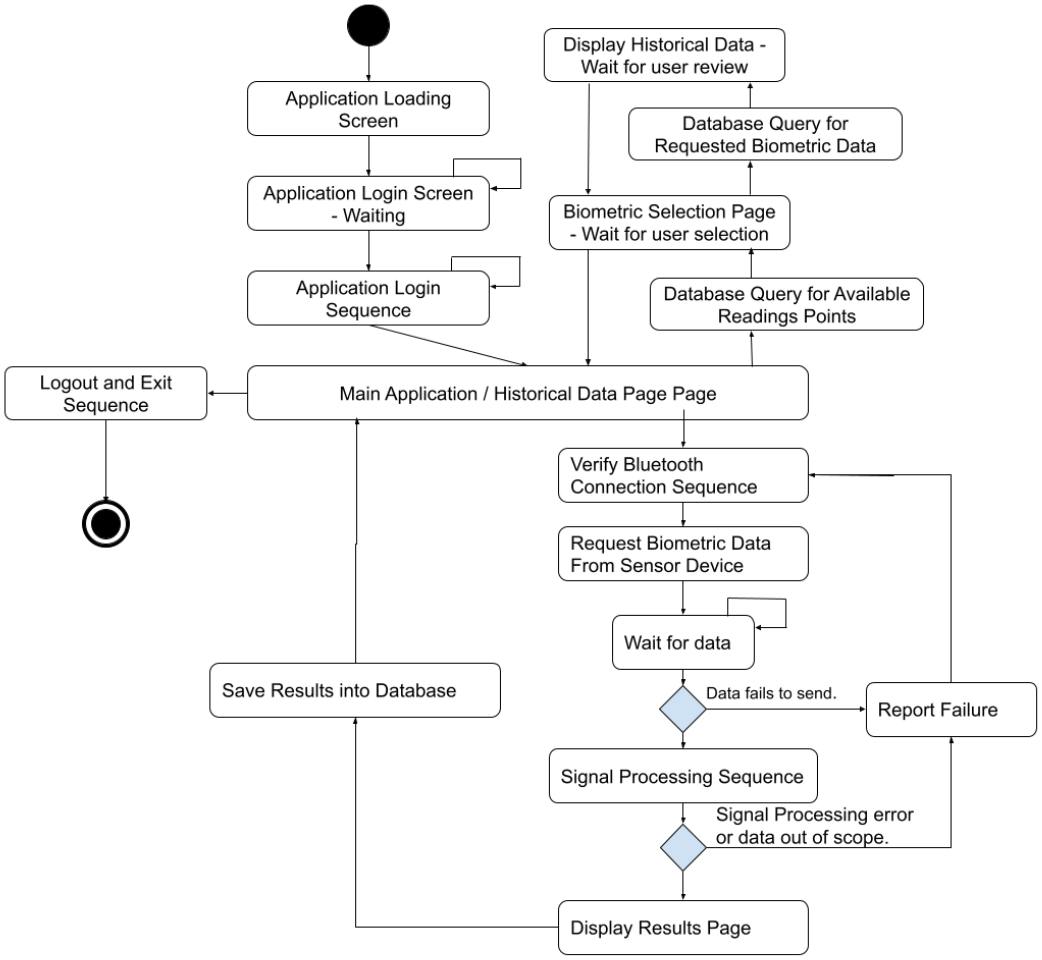

Figure 5.5.4-1.

If the user chooses to take a measurement this will initiate a verification of the Bluetooth Connection to the sensor device described in section 5.5.4-1 If successful this will result in a request for Biometric data from the Sensor device. If received the data will be processed. If the data fails to send or the data is found out of scope in the signal processing portion, it will report the error to the sensor device and begin the verification process again. If no errors occur this will bring the application to display the results of the measurements. Users will have the option of saving the results to the data storage system or discarding the results. After either is selected they will be sent back to the Take Measurement page to await a decision.

If the user chooses instead to view historical data, they will be brought to a new page. From this page the database will be queried for historical data of the user to view. Once selected this will bring the application to query the historical data for samples that are for this biometric. The user will be brought to a page for the user to select the particular biometric to review. The system will then wait for the user to complete reviewing the metric and bring it back to the previous screen.

The user should be able to back track from there back to historical data or the main application page if desired.

5.6 Signal Processing

This section will cover the main implementations of signal processing done in this project. It is a technical discussion of transforming the 3 wavelength ppg data into the intended biometric predictions. The system starts with an incoming analog current signal from the photodiode sensor array. With the use of a transimpedance amplifier, we convert the current signal to a voltage signal. The voltage signal is converted to a binary value using an ADC converter. From there, we do digital signal preprocessing to improve the signal to noise ratio to tolerable amounts. Once the signal has been brought to an approved clarity, we predict the user's biometrics using several feature extraction techniques.

5.6.1 Medium of Computation

One of the toughest decisions in the development process was deciding on which device the biometric extraction would take place. This section will be dedicated to explaining the internal discussion and reasoning that led to the final decision. There were roughly two different considerations which are listed below in a table format comparing their pros and cons(Table 5.6.1-1).

Device	Pros	Cons
Microcontroller Sampling, preprocessing, feature extraction, and biometric prediction is done on the IC.	● Reduced time between data acquisition and display. ● Increased ease of use(Maybe). ● Would be marketable to all users regardless of other technology they have excess to.	● Requires overhead of LCD display controller. ● Users have a very limited ability for storing long term data. ● Software cannot be modified after a device is released or sold.
External Device Basic initial filtering and sampling is done on Integrated Circuit. Datastream is sent wirelessly to another device(IE Mobile Phone)	● Reduces device power consumption and extends battery life. ● Easier software development. ● More resources(RAM, non-volatile memory, clock speed, internet	● Software would have to be created and maintained on several mobile platforms(IE IOS, Android, Google) ● Heavy reliance on bluetooth connection. ● Increased risk of

where feature extraction and biometric prediction is completed and shown to the user.	access) • Allows us to add or change the mobile software and users can access the updates remotely.	people stealing sensitive information. • Requires complex synchronization and data packaging protocols

Table 5.6.1-1.

5.6.2 Feature Extraction And Biometric Predictions

Our device's primary goal as a biometric sensor is to accurately and consistently map a vector of input parameters to a set of predictions. This is pretty straight forward however it's worth understanding the reasoning of why we thought this was possible. That is why this chapter is dedicated to detailing the logic driven processing algorithms our device is using. Below is an abstract yet helpful way of conceptualizing the task our device aims to complete.(figure 5.6.2-1)

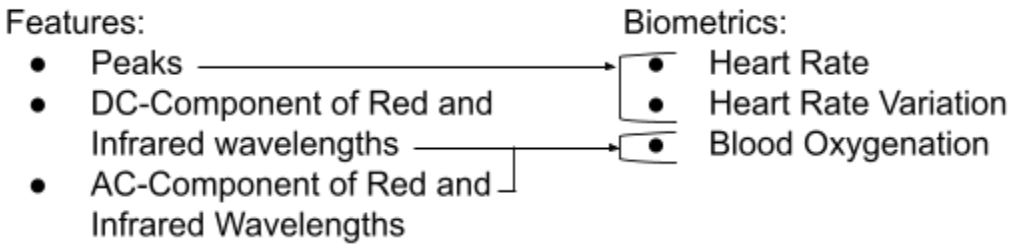

Figure 5.6.2-1.

5.6.3 Peak Detection

One of the most important features we are looking for is the signal's peaks. By taking a look at the sample PPG signal you will see there are two local maximums per heart rate period. We specify that we want to locate the highest valued maximum to maintain consistency. To achieve this, two algorithms were considered. (figures 5.6.3-1 and 5.6.3-2)

1. The derivative of the signal is equal to 0.

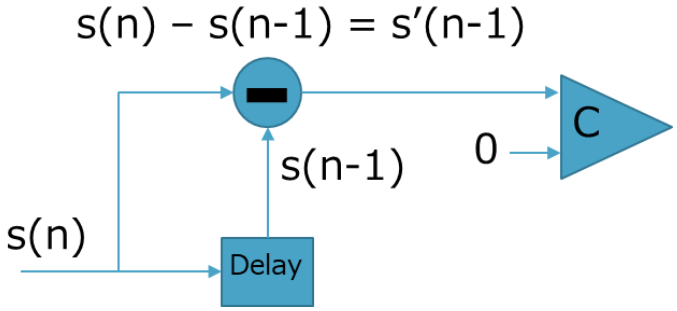

Figure 5.6.3-1.

2. Logically, if both of the temporally adjacent samples are less than, then there exists a peak. I.e. s(n-2)<s(n-1)>s(n).

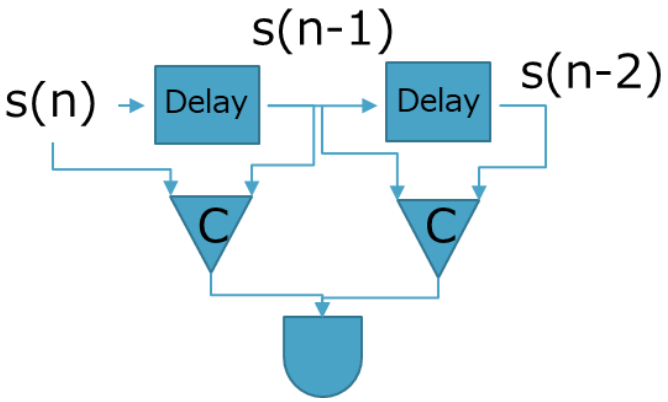

Figure 5.6.3-2.

The first algorithm(Figure 5.6.3-1) would only be possible if our sample period approached 0. Since this is not possible, use algorithm 2(Figure 5.6.3-2). Another benefit of this algorithm is that it implicitly checks for negative concavity. The image below(Figure 5.6.3-3) depicts the use of this algorithm and shows how it only detects positive peaks.

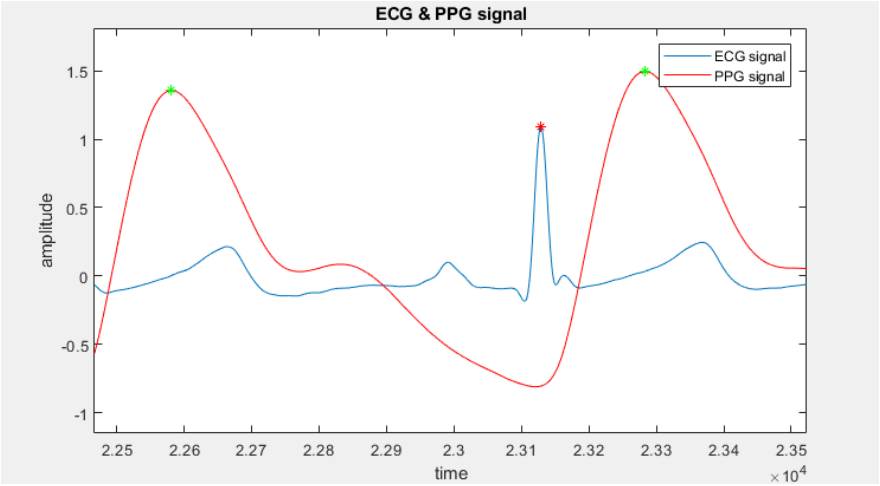

Figure 5.6.3-3. Peak detection of bio-signals

5.6.4 AC and DC Component

The DC component is the average value across the period of the signal. The dominant AC component on the other hand is just the highest magnitude non zero frequency component. By taking advantage of the fast fourier transform we can quickly identify both of these parameters. One thing to note is that the FFT can give you a better result the longer the signal you pass it. The computational complexity of the FFT is O(n) = n*Log(n) so our project strikes a balance by transforming tolerable 12.8 second chunks of recorded signal. To clarify this process, the discrete Fourier transform is defined below.

$$F\{s(n)\} = S(k) = \sum_{n=0}^{N-1} x_n e^{-j2\pi nk/N}$$

The Fourier transform maps a time domain signal to the frequency domain. The image below(Figure 5.6.4-1) is a plot of the frequency components of sample IR and Red PPG signals.

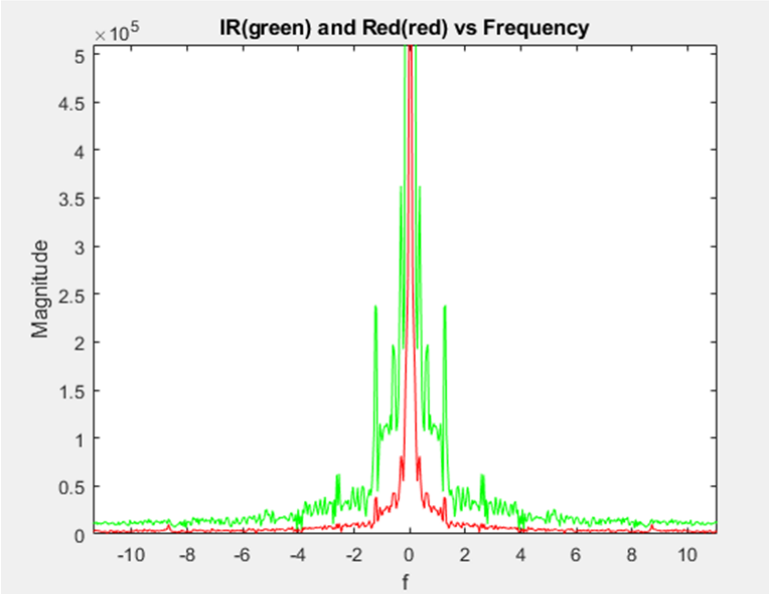

Figure 5.6.4-1.

5.6.5 Heart Rate

From the peak detection algorithm, we can identify repetition in the incoming PPG signal. This cycle has the same frequency as the heartbeat of the subject. So, the difference in the sample number multiplied by the sample period is a good approximation to the period of a heart beat cycle. A graph of a ppg example signal used to get the heart rate (figure 5.6.5-1) below.

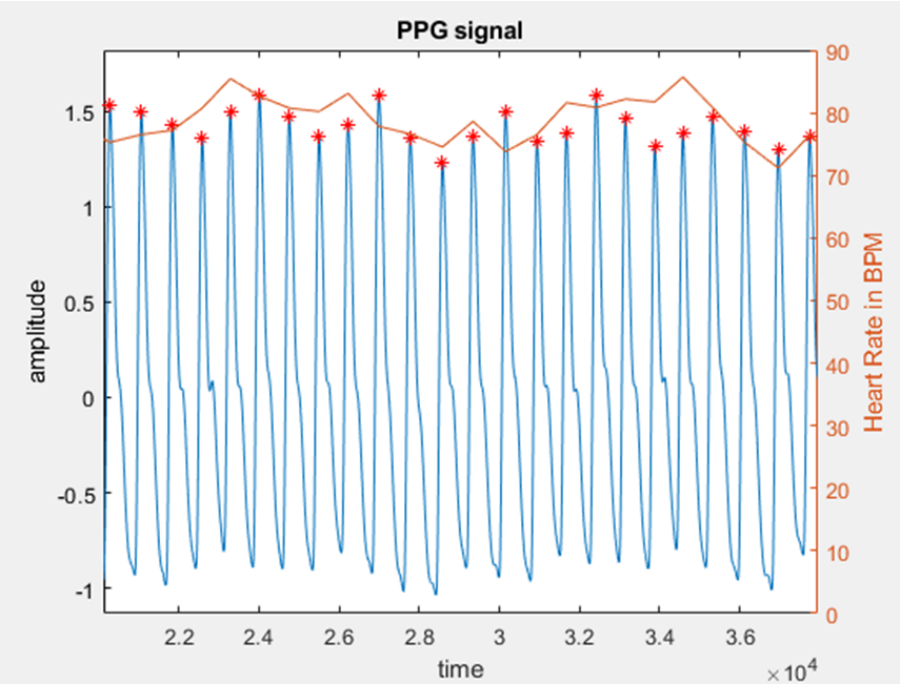

Figure 5.6.5-1.

Average Heart Rate-

By detecting multiple instantaneous heart rates in series we are able to make an estimation for the average heart rate. Figure 5.6.5-2 shows how a PPG signal estimates heart rate.

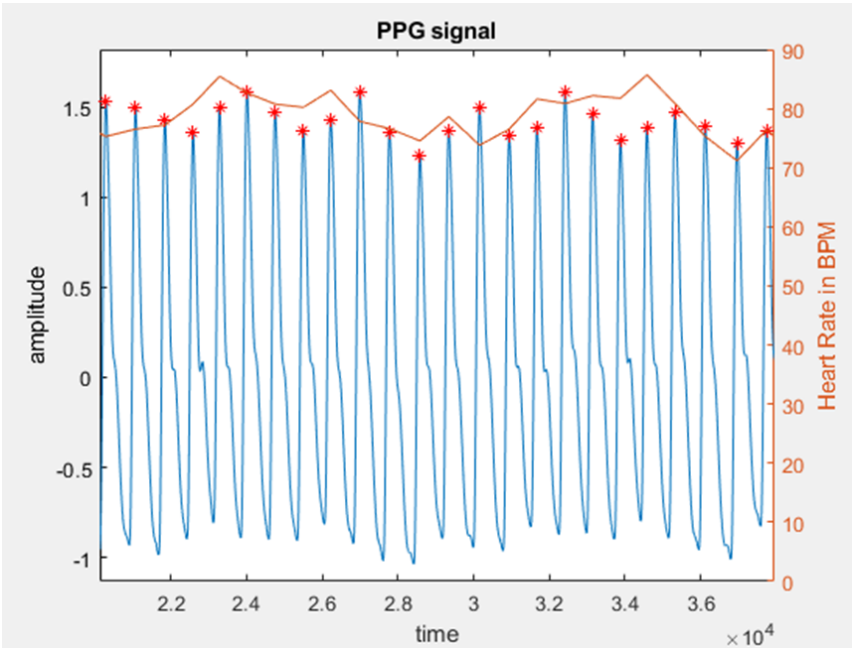

Figure 5.6.5-2.

5.6.6 Heart Rate Variation

Though there are many different ways to calculate heart rate variation, the most suited for our application would be using Root Mean Square of Successive differences. RMSSD simply requires the interval between each of the peaks we capture. This is appropriate since we already have this data to compute the average Heart Rate. Below is the formula for RMSSD as well as a plot across time using sample data. (figure 5.6.6.-1)

$$HRV = \sqrt{((T_n - T_{n-1})^2 + (T_{n-1} - T_{n-2})^2 + (T_{n-2} - T_{n-3})^2 + \ldots)/N}$$

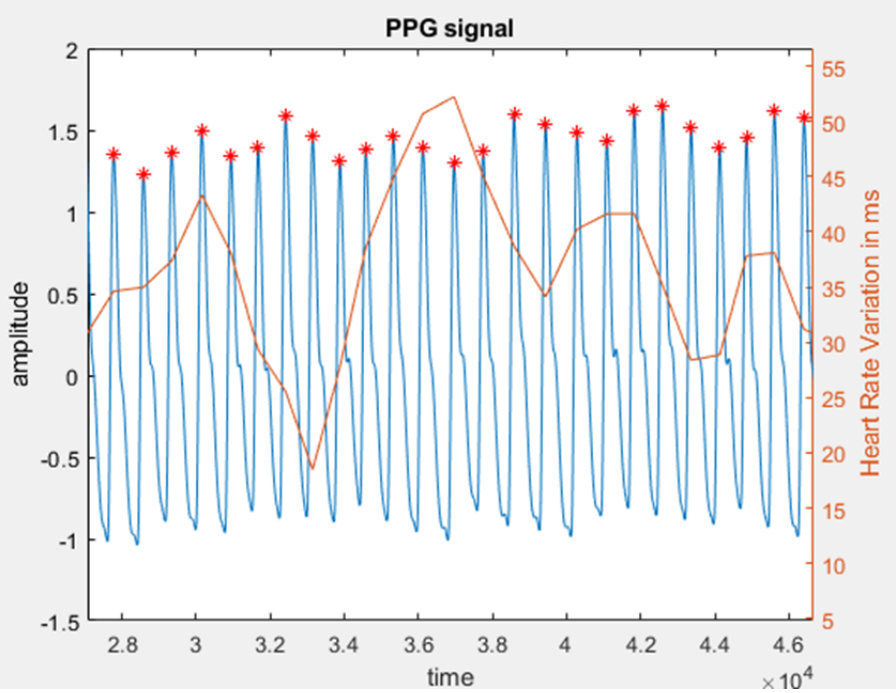

Figure 5.6.6-1.

5.6.7 Blood Oxygenation

The proper technique for predicting blood oxygenation is a debated topic. We use the simplest approach, which is a ratio of ratios. AC_red and AC_IR refers to the domininent(global maximum outside of DC component) non DC component of the signal.

$$R = (AC\_red \div DC\_red)/(AC\_IR \div DC\_IR)$$
$$SpO\_2 = C - \beta(R), \text{ where } C \text{ and } \beta \text{ are constants}$$

Though this technique is very simple it requires that the device be calibrated to find the constants. This implies that we can create a system of equations using a

trustworthy device. In this demonstration I am using typical numbers since we cannot confirm the subjects true blood oxygen content.

In the image below(Figure 5.6.7-1), you can see a sample detection of the dominant AC components of both the IR signal and the Red Signal.

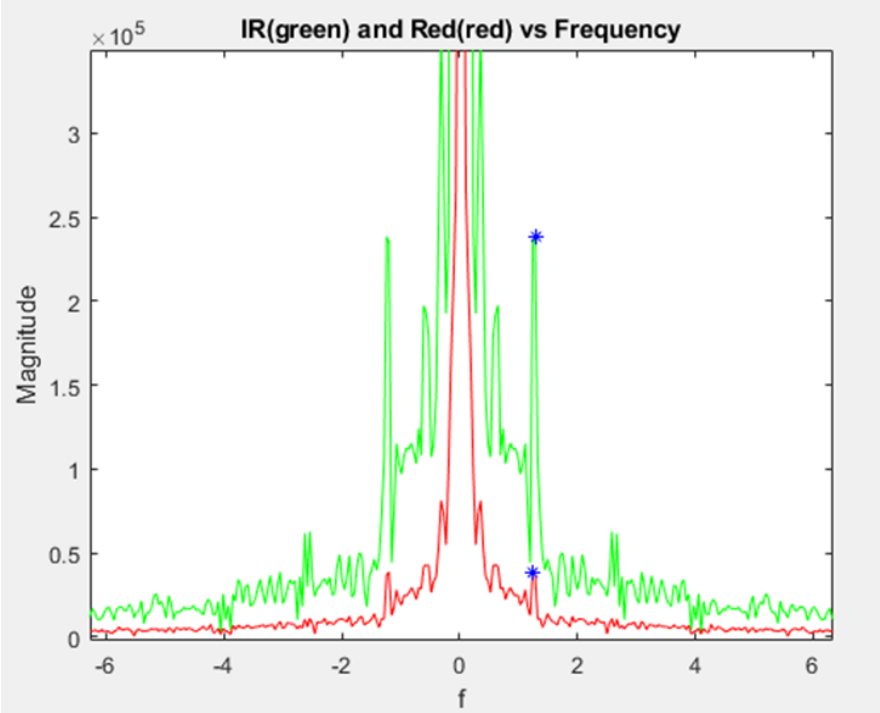

Figure 5.6.7-1.

5.6.8 Signal Conditioning

The specification for signal to noise ratio in this project is 30db. Though this does contain a decent amount of noise this specification can realistically be met. Due to the presence of this noise we can perform a test and see if we lose the ability to perform our peak detection algorithm.

To simulate this scenario we add enough additive gaussian white noise to the signal until we reach a signal to noise ratio of 30dB. In (Figure 5.6.8-1), you can see a frequency domain plot of the signal with added noise.

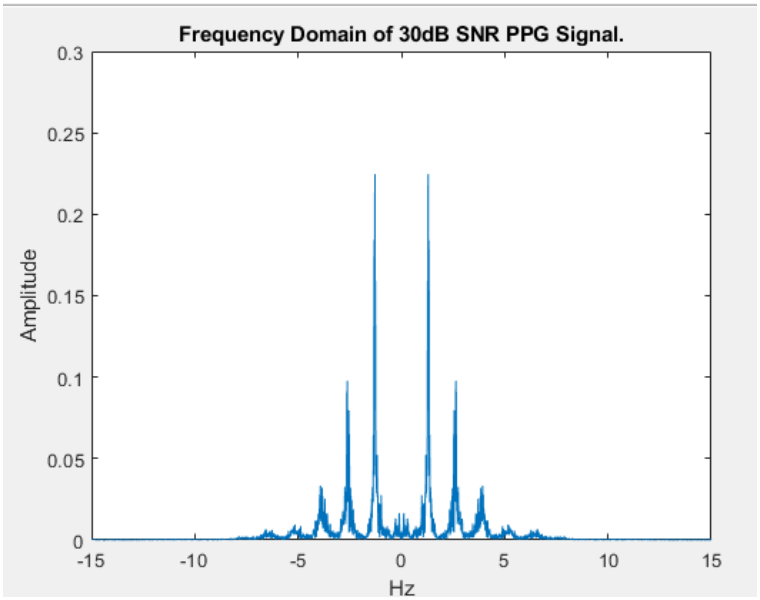

Figure 5.6.8-1.

Though it appears to be a fairly clean signal when the peak detection algorithm is applied it becomes clear it does not work. Below(Figure 5.6.8-2) you can see that many peaks are detected.

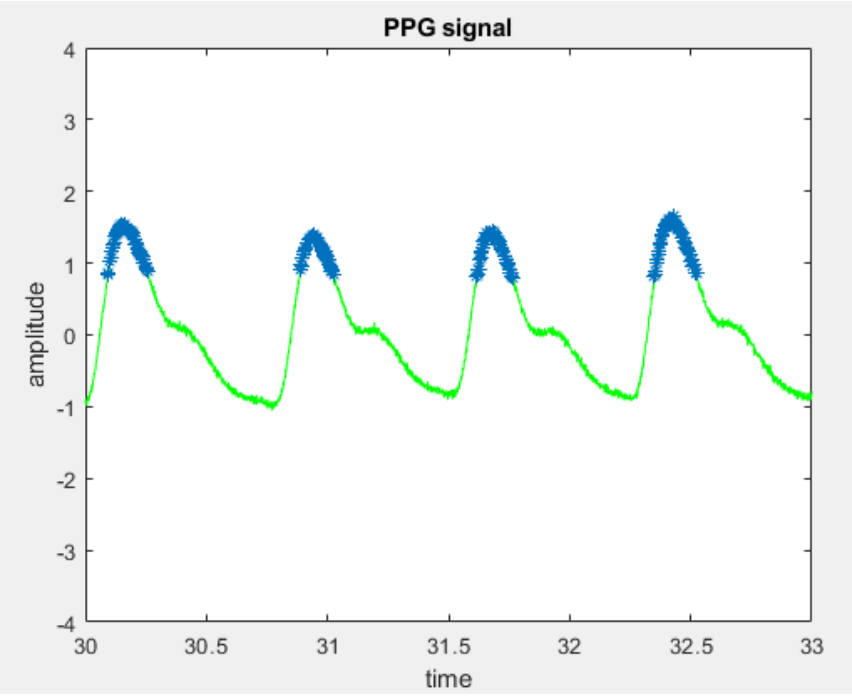

Figure 5.6.8-2.

In order to correct this we must smooth the signal using digital filtering such as an integrate and dump filter. The main reason we chose to use the integrate and dump filter is that it is low on hardware and memory usage which makes it optimal to be implemented on embedded systems. Since the plan is to ultimately

do the signal conditioning on the local device and send the conditioned signals to the phone via bluetooth, the low hardware cost of this filter fits the hardware constraints of our product.

The integrate and dump filter allows us to reduce the sampling rate as well as smooth the signal. Since an integrate and dump filter acts like a moving average, you can see how its fourier transform is a sinc function with a cut off of 100hz. Below(Figure 5.6.8-3) you can see the Fourier transform overlaid on top of the Fourier transform of the PPG signal.

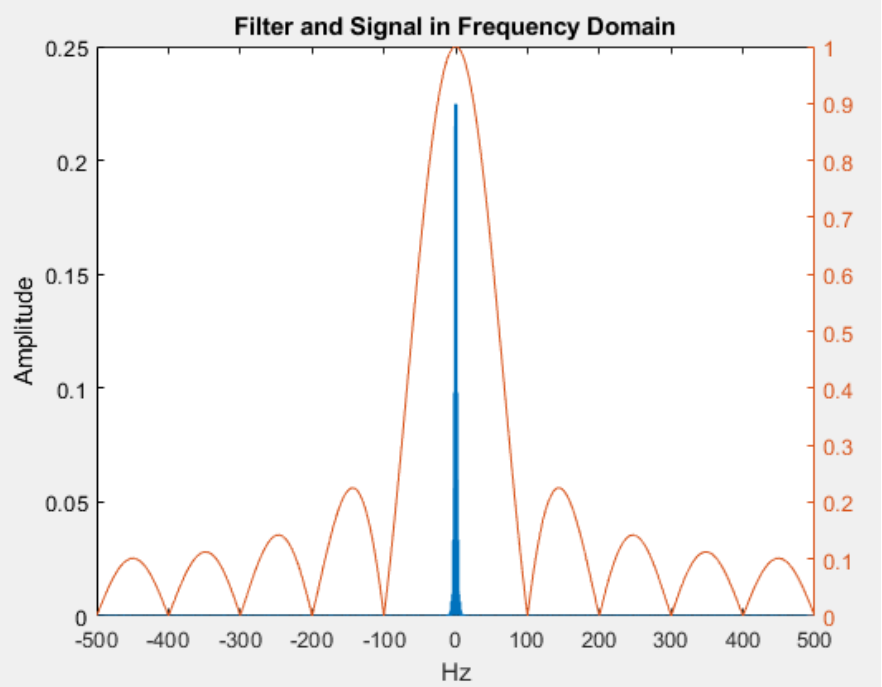

Figure 5.6.8-3.

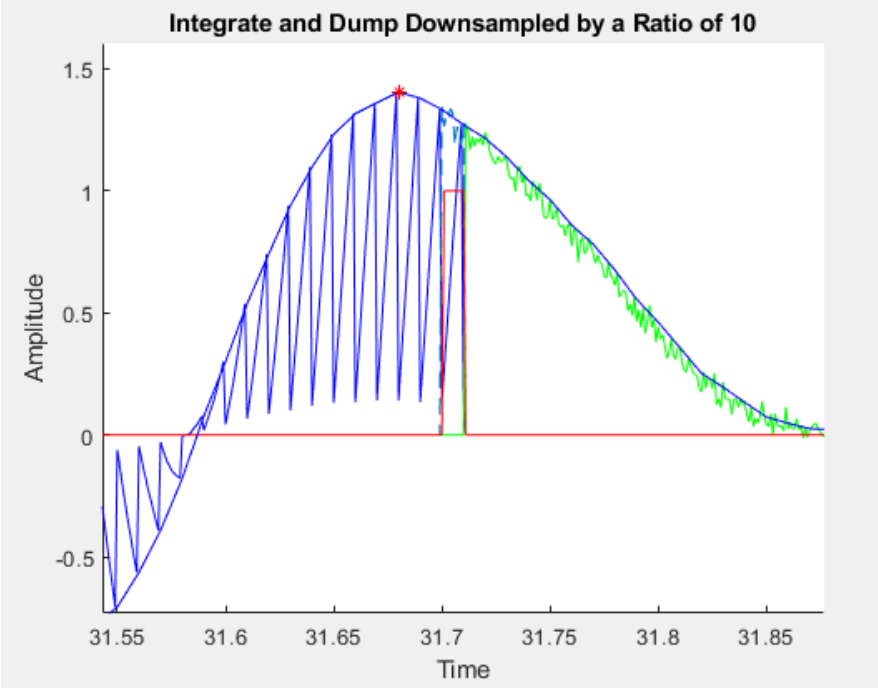

Figure 5.6.8-4.

As visible in the image above, the integrate and dump filter applies smoothing to the noisy signal returning the ability to detect a single peak in the signal. The Z transform of the moving average can be easily written as a summation.

$$H(z) = \sum_{k=0}^{k} z^{-k}$$

The image below(figure 5.6.8-5) is a realization of this.

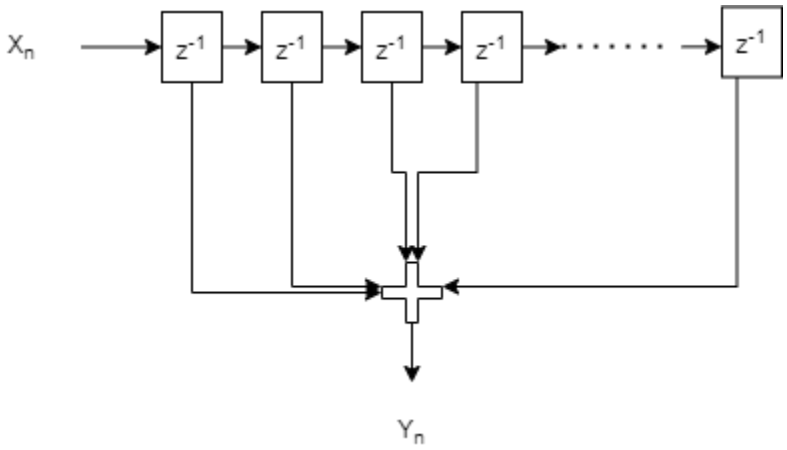

Figure 5.6.8-5.

It is worth noting that even though the moving average and the integrate and dump filters have the same time and z domain expressions even though their implementations are quite different. The integrate and dump is actually a specific variation of the CIC filter. CIC expanding to Cascaded integrator-comb filter.

This filter was designed by Eugene B. Hogenauer and allows us to use a fraction of the hardware given that we reduce the sample rate at the output. This can be shown below(Figure 5.6.8-6).

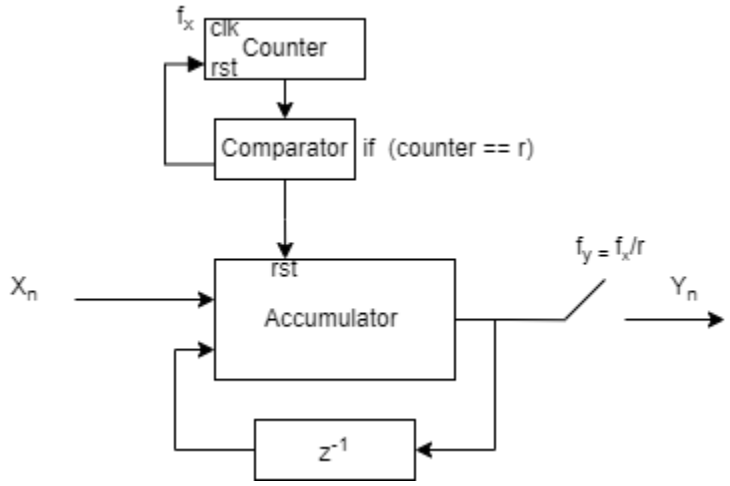

Figure 5.6.8-6.

5.7 Power System

Our wearable Optical Biometric Tracking System is battery powered to make the device portable. A battery has been integrated into the pcb design to have the entire device as compact as possible, and the use of a battery providing a DC voltage eliminates the need to convert alternating current into direct current. The device uses two different voltage levels, primarily the raw voltage from the battery which varies from 4.2V to 3.0V, and that same voltage converted to 3.3V and routed to the other components to set up a 3.3V I2C bus system and provide the necessary power to all components except the LEDs. The various voltage needs of our device creates the need for DC to DC conversion, which may be obtained in various ways, with varying levels of efficiency and complexity.

5.7.1 DC-DC Conversion

Unit	**Quantity**	**Current Consumption**	**Peak draw**
MCU	1	2 mA	10 mA
AFE	2	1 mA	2 mA

LEDs	2	2 mA	4 mA
Bluetooth	1	10 mA	28 mA
Thermal sensor	1	1.5 mA	2 mA
IMU(not used)	1	5 mA	5 mA
Total	10		46 mA

Table 5.7.1-1. Peak current draw

As seen in the table above (5.7.1-1), our system uses approximately 50 mA under worst-case scenario power consumption which entails constant sensing and bluetooth transmission . The majority of the power draw is from the LEDs, since we will need to pulse four of them at the same time to concurrently draw a current signal induced in four photodiodes from four different directions. The total of 6 LEDs must be powered by a voltage higher than 3V and as such will be powered by the 3V3 power rail that defines the logic level for the Microcontroller. To achieve the constant 3V3, this device will be employing a Buck-Boost switching converter pictured below (Fig 5.7.1-2), which could achieve a constant voltage, something crucial to our design since we are measuring analog signals in our circuit that output very small current levels, a process which would be hampered by not achieving a constant input voltage to the LEDs and the AFE which in turn would drive our photodiodes and their response. The Buck-Boost converter pictured below is able to convert power at approximately 93% when outputting our devices' expected peak current, depending on how charged the Lithium Polymer battery is, and was the intended original converter, however it was unavailable at the time of purchasing components. (Fig 5.7.1-1).

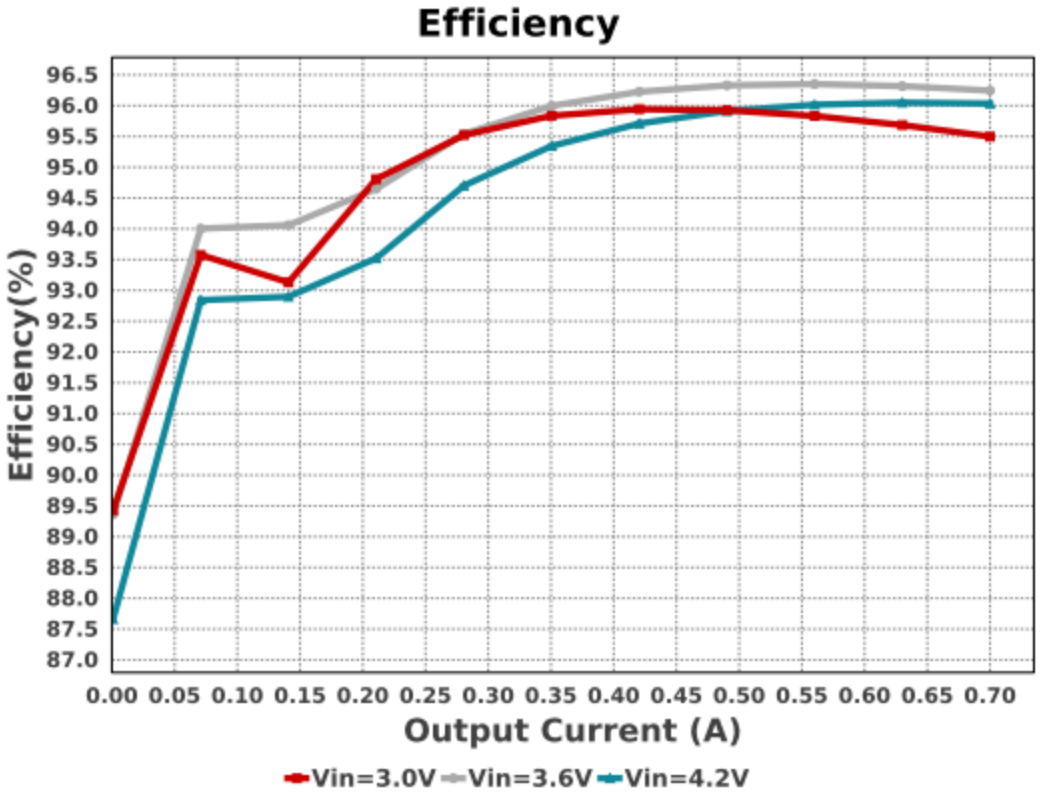

Figure 5.7.1-1. Buck-Boost efficiency per current level, Courtesy of Texas Instruments

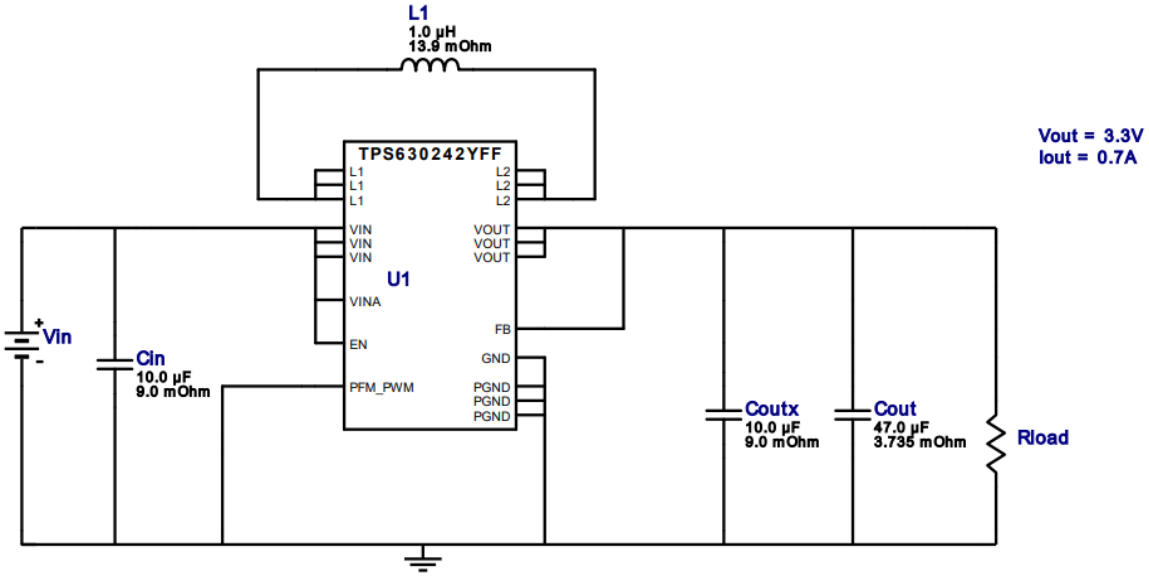

Figure 5.7.1-2. Circuit that regulates to 3V3, Courtesy of Texas Instruments

The other voltage level we needed to properly operate our device was 1V8. This lower voltage is quickly becoming popular in low power electronics and was going to be the driving force of our previous Analog Front End selection which operates with an analog core designed around 1V8. As previously stated, due to issues with sourcing the other part and its development board, we switched to another AFE and thus no longer used 1.8V in our design. As seen below in figure 5.7.1-4, a different component was ultimately used, namely the LTC 3440 Buck-Boost converter. The Buck-Boost converter is incredibly efficient when powering a very small current, in the range of 50mA to 100 mA it is in the 93% range (Fig 5.7.1-3), and when more current than that is used, it would convert at 90%+, however the efficiency of this converter is not of primary concern because of the very low power load it will be supplying compared to the battery capacity available.

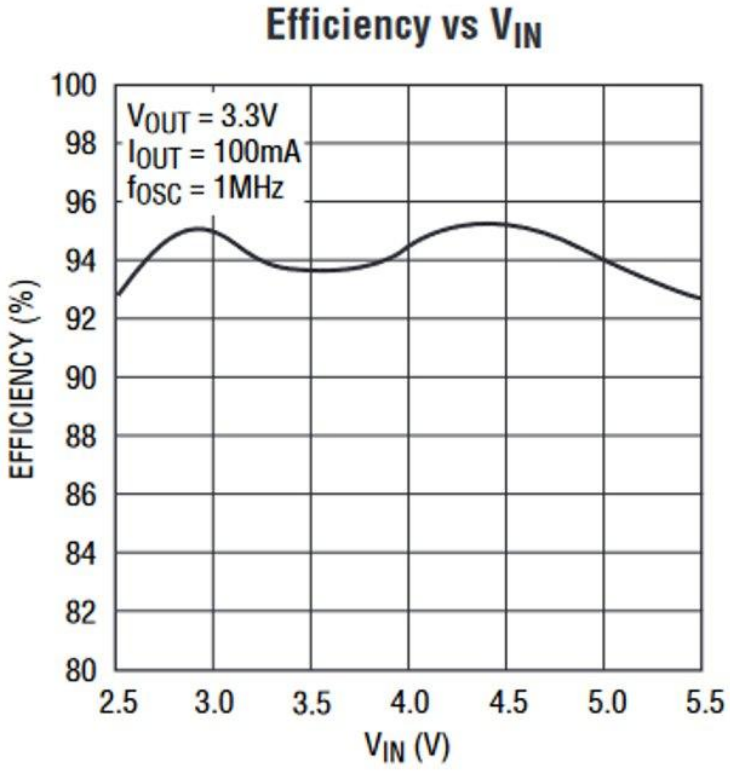

Figure 5.7.1-3. Efficiency for the buck converter per current draw, Courtesy of Texas Instruments

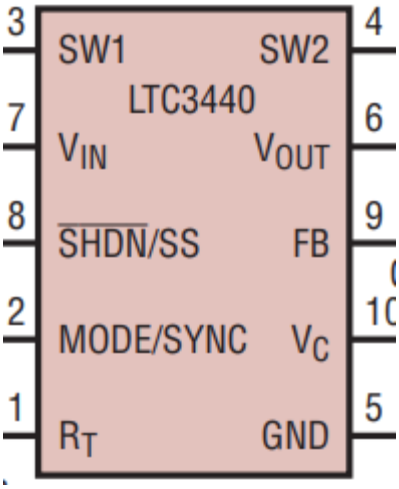

Figure 5.7.1-4. LTC3440 Symbol

The overall power delivery system can be seen below in figure 5.7.1-6, a 2-Pin JST connector will be surface mounted to the PCB, allowing the two leads from the Lithium Polymer battery to be connected to an entry point from where it will be funneled into two different subsystems, one to convert the voltage to 3V3 using the aforementioned Buck-Boost, and the other traces go to pins where they are routed into the LED modules to power them. The SMT connector pictured below (Fig 5.7.1-5) was chosen primarily for its low profile which serves our goal of minimizing the impact that our comparatively high power usage has in the form of requiring a sizable battery. The integrated circuits in the converters are required for the constant monitoring of the systems voltages, since our project is entirely battery powered, it by nature will have a significant variation in the input voltage as our battery's cell discharges and it loses driving ability.

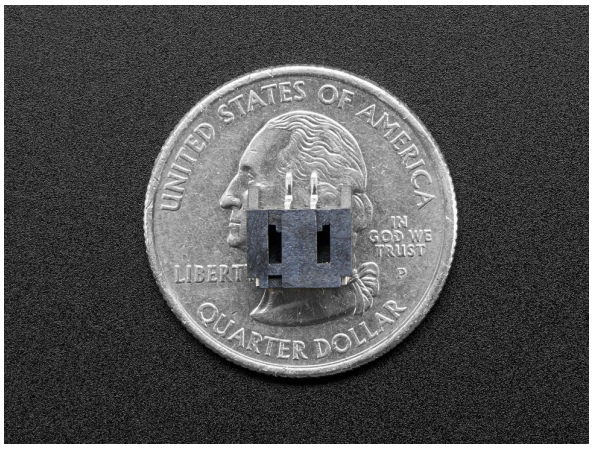

Figure 5.7.1-5. Surface mounted power connecter, Courtesy of Adafruit

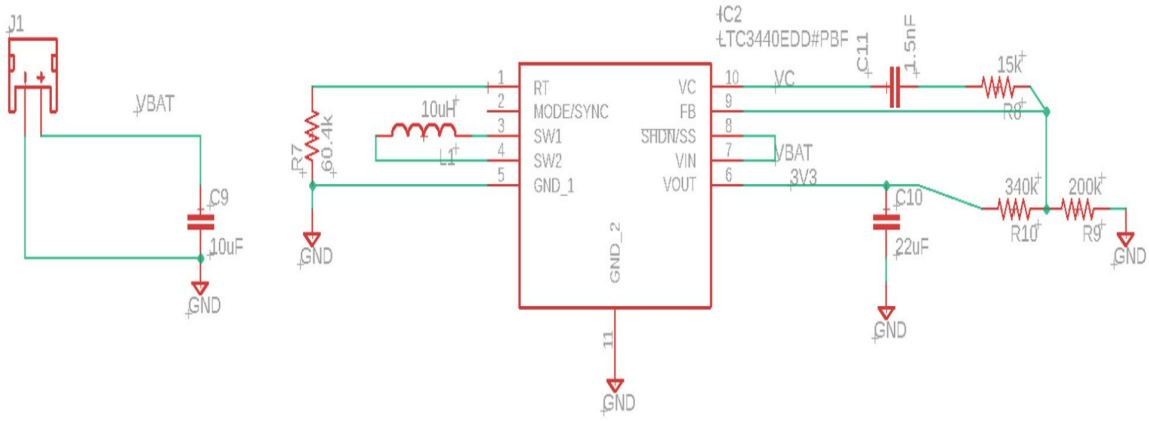

Figure 5.7.1-6. Complete voltage regulation system

Lithium-Ion Polymer batteries are liable to malfunction if they are not properly charged, and since this is a wearable device, it was crucial in our design that we accomplished two goals, safely charge the device, and to charge the device in a manner which would not inhibit the mobility of the user. For these reasons we have decided to implement a standalone charger as a companion and make the battery housing accessible, so that batteries can be switched if need be. This has the added benefit of not needing to create a larger PCB to integrate charging. The ability to charge batteries without them being connected to the wearable device offers the ability to use the device while on the go for extended periods of time, given that more than one battery is available.

When creating a charging system for the wearable device's batteries, it was decided that an interface that used technology present in nearly everyone's homes was important. To that effect, a charging system that is not physically attached to the wearable device and powered through a micro USB cable was implemented (Fig 5.8-1). The charging circuitry is capable of supplying 100 mA of constant current to charge the battery, and it is programmable up to 1 A of current by configuring the input resistance on pin 5.

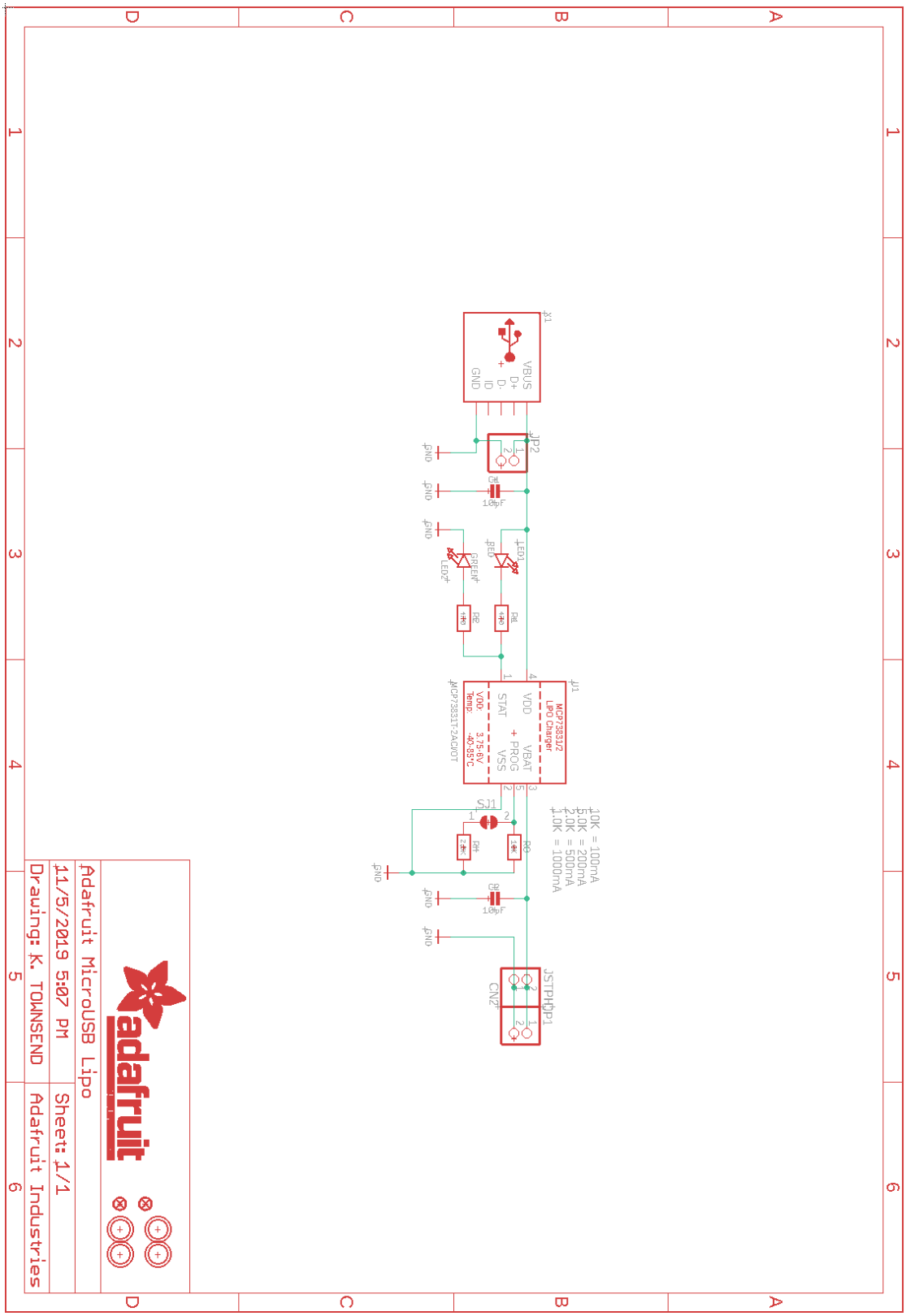

Figure 5.8-1. Recharging circuitry for the LiPo battery

5.8 Mechanical Design

For the wrist-worn device, a mechanical design must be drafted to house all the physical modules. Our group used a 3D-printer with black polycarbonate filaments as the printing material to develop and prototype mechanical designs. To begin drafting the housing design required, the sizes of the on-device modules must be considered, such that a lower bound for the overall dimensions can be established as well as the requirement of certain modules or components to be exposed in the design for intended function. The estimated dimensions of each main on-device modules and relevant components are listed in Table 5.8-1.

Module	Length (mm)	Width (mm)	Thickness (mm)	Enclosed/Exposure
Optical Sensor Module	20	20	1	Partial Exposed (Optical Components)
SFH 7016 (LEDs)	1.85	1.65	0.6	Exposed
SFH 2200 (Photodiode)	5.09	4	0.85	Exposed
AFE4404 (AFE)	2.14	3.11	0.50	Enclosed
MLX90632 (Thermal Sensor)	3.1	3.1	1	Exposed
Arduino Nano 33 BLE	45	18	4.5	Enclosed
Lithium-Ion Polymer Battery	36	16	7.8	Enclosed

Table 5.8-1.

It is worth noting that the mechanical design has an imposed constraint of not being considered ‘bulky’. We define ‘bulky’ as a thickness higher than 75% of the diameter of the average human’s wrist (~21.6 mm). To achieve a non-bulky design we have two possible options for the housing: a single rectangular-shaped housing for all components, or a C-shaped housing which joins two sections in which one houses the integrated-sensor PCB, and the other houses the MCU and battery system. Overall, the mechanical design can be divided into two sections: The outer housing structure and the sensor-barrier structure.

5.8.1 Outer Housing

Our group originally planned to design a device housing that was compact, low profile, and comfortable to wear. The initial proposed structure can be seen in figure 5.8.1-1. The housing will have an enclosed space of about 56mm length and 40mm width with a thickness of 14mm. This design was not able to be realized due to the size of the main board pcb, and later the issues that arose from integration.

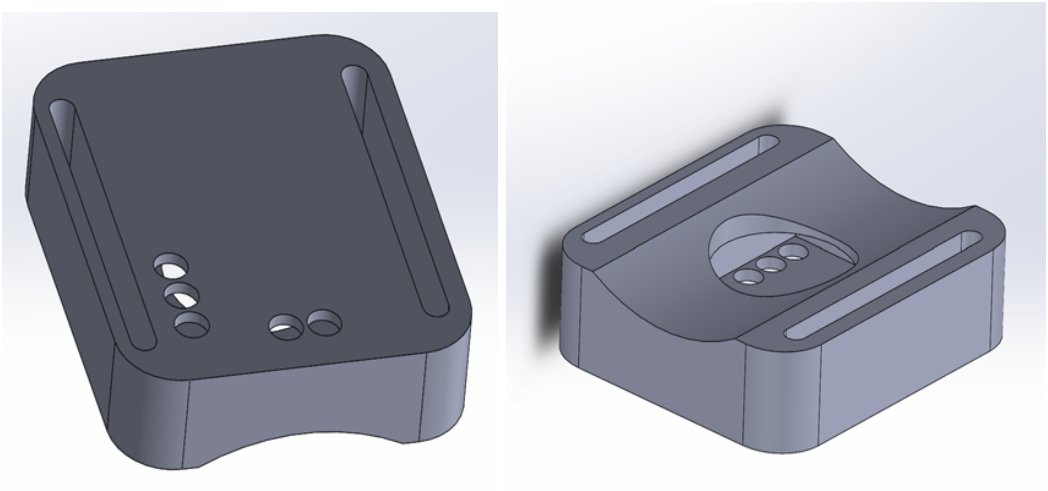

Figure 5.8.1-1.

The final housing structure that was utilized in our project was a PETG 3-D printed multi-piece casing seen in figure 5.8.1-2. This design originally had a height of 30mm prior to an extension inorder to accommodate the breakout boards for proper function. In the housing structure, six holes were included for the adjustment and use of velcro straps. Additionally a removable compartment was implemented near the roof of the device such that the battery powering the system could be replaced.

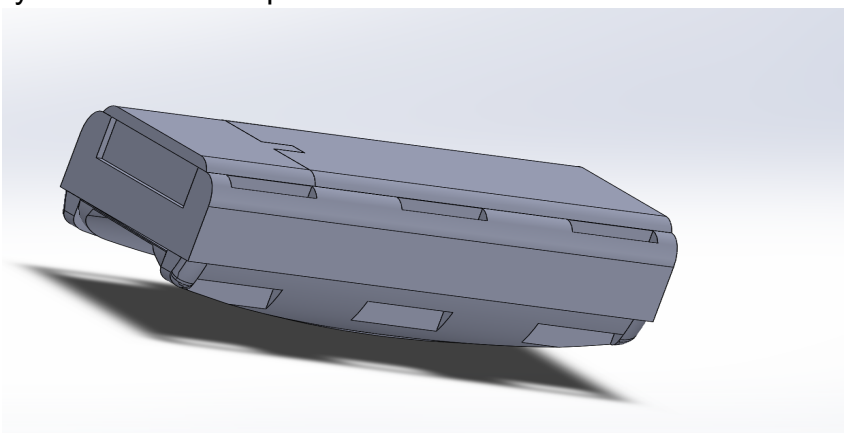

Figure 5.8.1-2.

5.8.2 Sensor Barrier Structure

To avoid illumination crosstalk (ICT), a carefully designed barrier structure must be introduced that will attach to the outer housing. The principal parameters which dictate this design are the dimensions of the LEDs, Photodiodes, Thermal sensor, and the minimum thickness of the hole provided by the outer housing.

For our design, we found that a protruding sensor structure allowed for added pressure that increased the performance. We decided on implementing a 2.7 mm barrier from the PCB and a 1.9 mm to 2.1 mm distance from the photodiode and LED, respectively. In order to incorporate the optical windows into the frame, a two-level mesa structure was utilized for the optical barrier, with the first level having a uniform thickness of 1.5 mm and a second level with a minimum thickness of 1 mm as seen in figure 5.8.2-1. It can be observed that for the photodiode opening, a support shelf was implemented for the optical window. Unfortunately, due to the printing errors, this shelf was not always printed correctly leading to removal after print if it was too small or not circular.

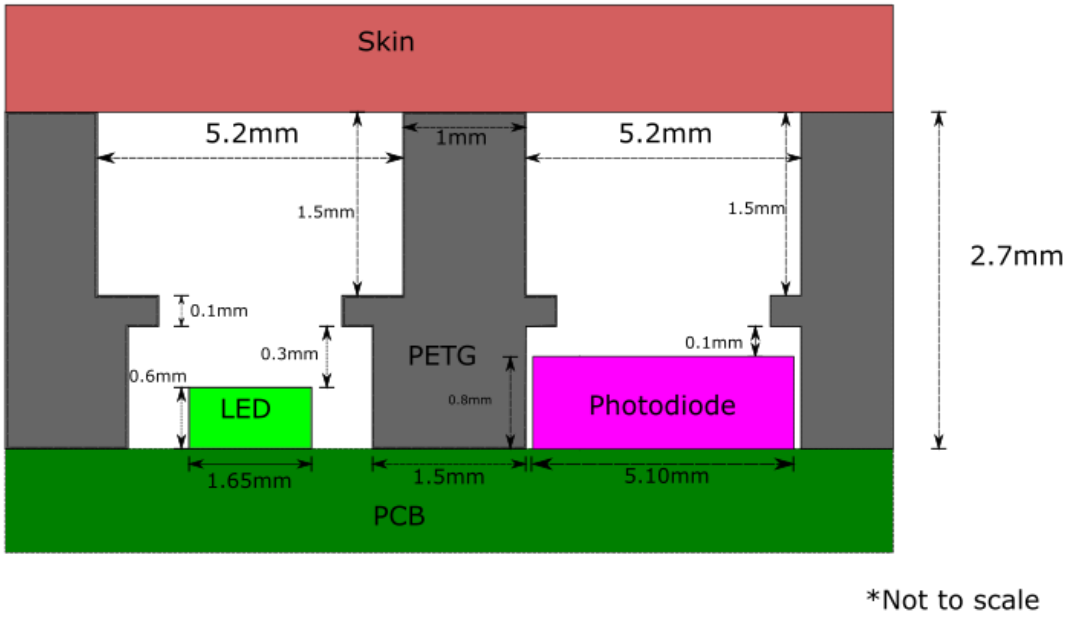

Figure 5.8.2-1

The introduction of the barrier structure with a circular exit aperture limits the output irradiance of the LED to a solid angle of about $\frac{625}{361}\pi$ steradians, as seen in figure 5.82-2. Given the forward current applied to the LEDs, and the optical

power generated from each LED, accounting for windows transmission and Fresnel losses, was 44.5 mW for green, 6.1 mW for red, 6.1 mW for IR.

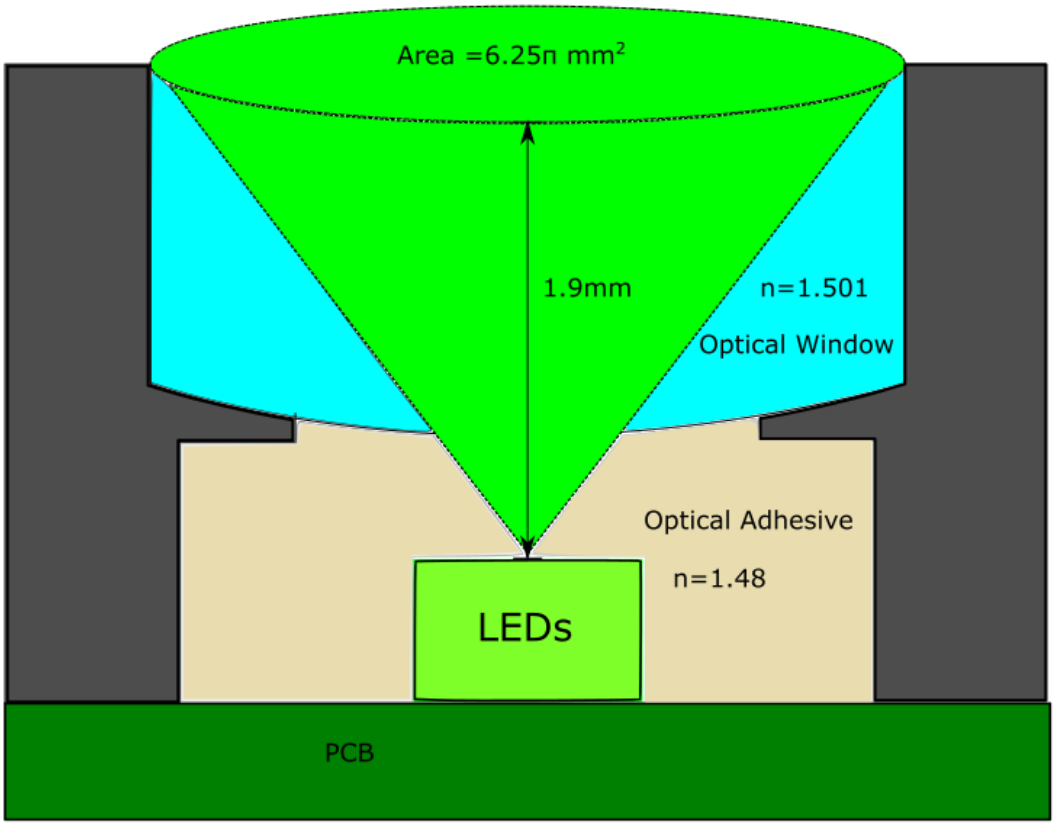

Figure 5.8.2-2.

Further consideration must be made for the thermal sensor which requires an unobstructed viewing angle of 55°. By creating a hole with a length of 4mm on each side, we can introduce 0.45mm distance between each barrier. Given the height of the thermal sensor (1mm) and the thickness of the barrier (1.3mm), the viewing angle will provide an unobstructed view as seen in figure 5.8.2-3.

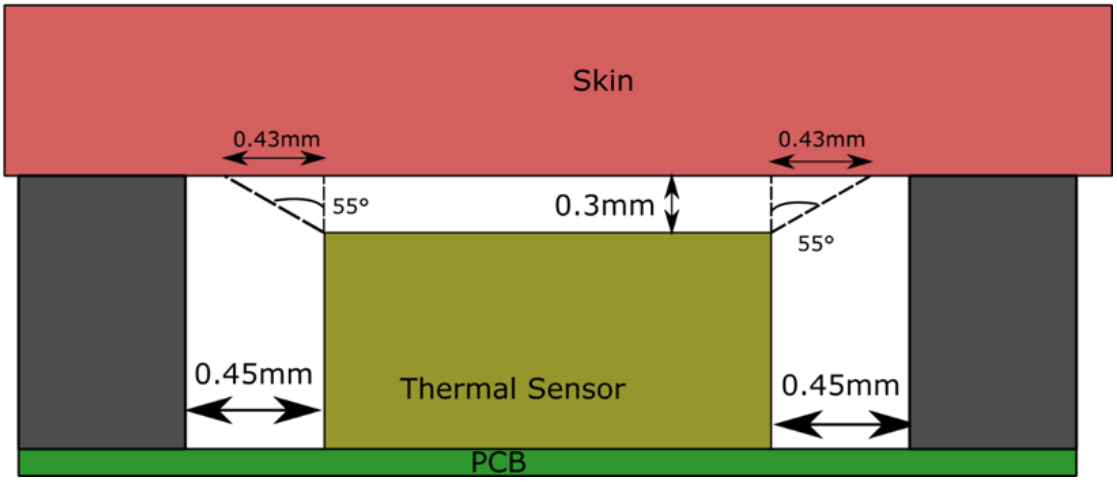

Figure 5.8.2-3.

Taking into account the optical barrier structure conditions and applying it to all of the four sub-sensors comprising the sensor system, as well as the required unobstructed viewing angles for the thermal sensor, we developed the following structure for the full sensor portion of the mechanical design seen in figure 5.8.2-4.

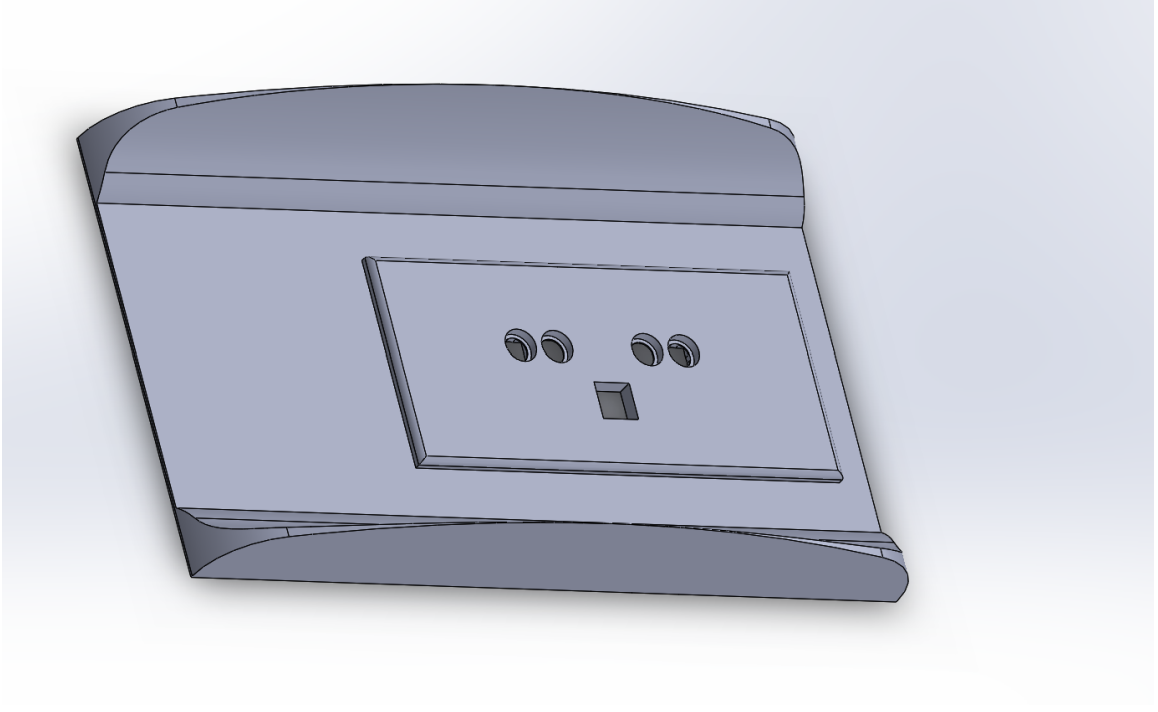

Figure 5.8.2-4.

6.0 Project Prototype Construction and Coding

Prototyping for this project was planned to be achieved by creating modular subsections of the final design which can be tested and modified individually. Several breakout boards were constructed to prototype the subsystems as shown below, such as the optical sensing system, which includes the array of photodiodes and LEDs in a rectangular arrangement. A breakout board was made dedicated to the photodiodes and LEDs so that the interaction between the geometric arrangement of the components and the quality of the signal acquired can be analyzed to make sure the device as a whole is able to achieve the most accurate possible readings. A separate board was then created to then test out the power conversion, and the breakout boards started coalescing into more integrated intermediate versions until we had the final product which has every subsystem previously modeled, built and tested.

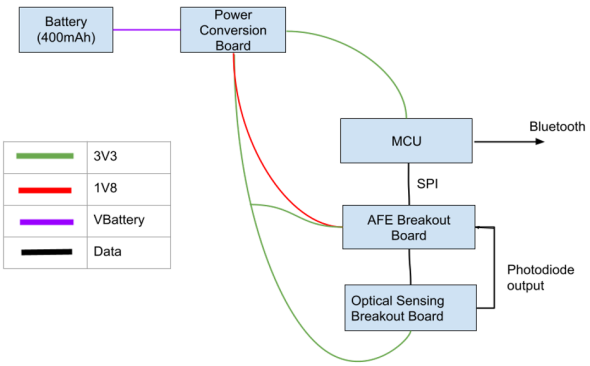

Figure 6.0-1 Testing power setup

6.1 Integration

The project's integration was broken up into different phases, with different subsystems being integrated at different times to eliminate extra variables when troubleshooting. Several Printed Circuit Boards were planned to be created and integrated beginning with just the optical module containing the photodiodes and then there would be a combination of the optical module with the AFEs which would be tested separately. On the other hand we individually tested the power delivery circuitry, and then integrated it into a model with the AFEs and optical units, and finally all the parts would be integrated into one seamless multi-layer PCB that can be housed in a wrist watch housing. Pictured below is the first PCB that was manufactured, as it is of utmost importance to figure out the layout of the optical units first. This board (Fig 6.1-1) features every electrical connection

of all the photodiodes and LEDs available on a pin, making it fully modular and easy to add into another design in a testing environment.

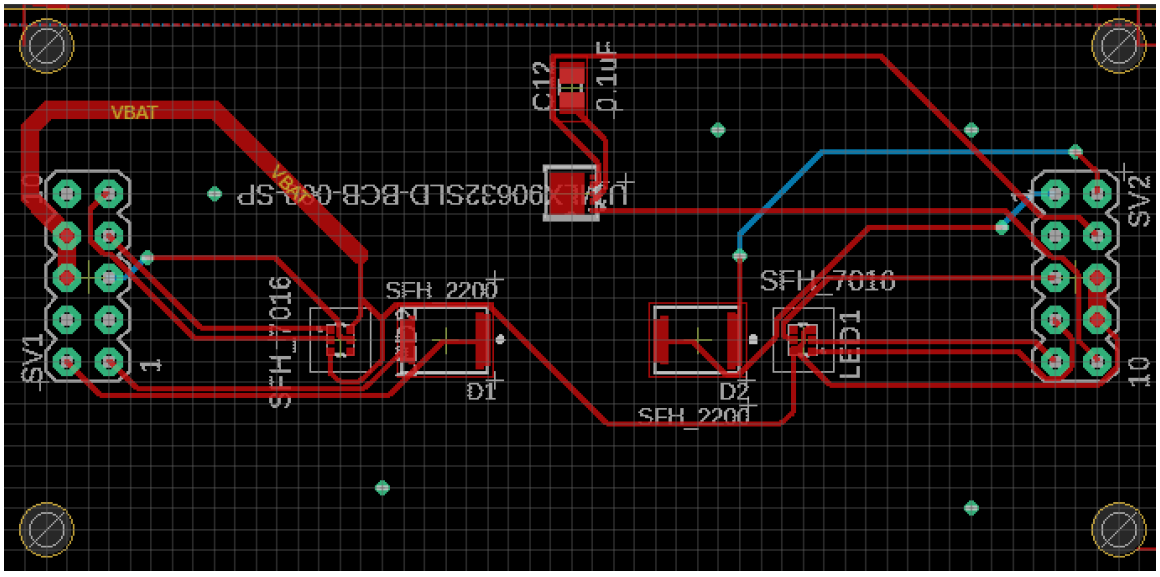

Figure 6.1-1. Sensor Board

The optical units were then integrated into a board that houses the AFEs and has a similar modular layout. Seen below in figure 6.1-2, the board that has the optical units and the AFE integrated were interfacing with the microcontroller using the I2C protocol, and deriving power through another set of pin headers. This system is then ready to be used with the arduino nano in a breadboard testing environment which allows us to rapidly test and prototype our systems. Ultimately we did not utilize this testing system and instead opted for buying the development board for the AFE4404 as soon as we could.

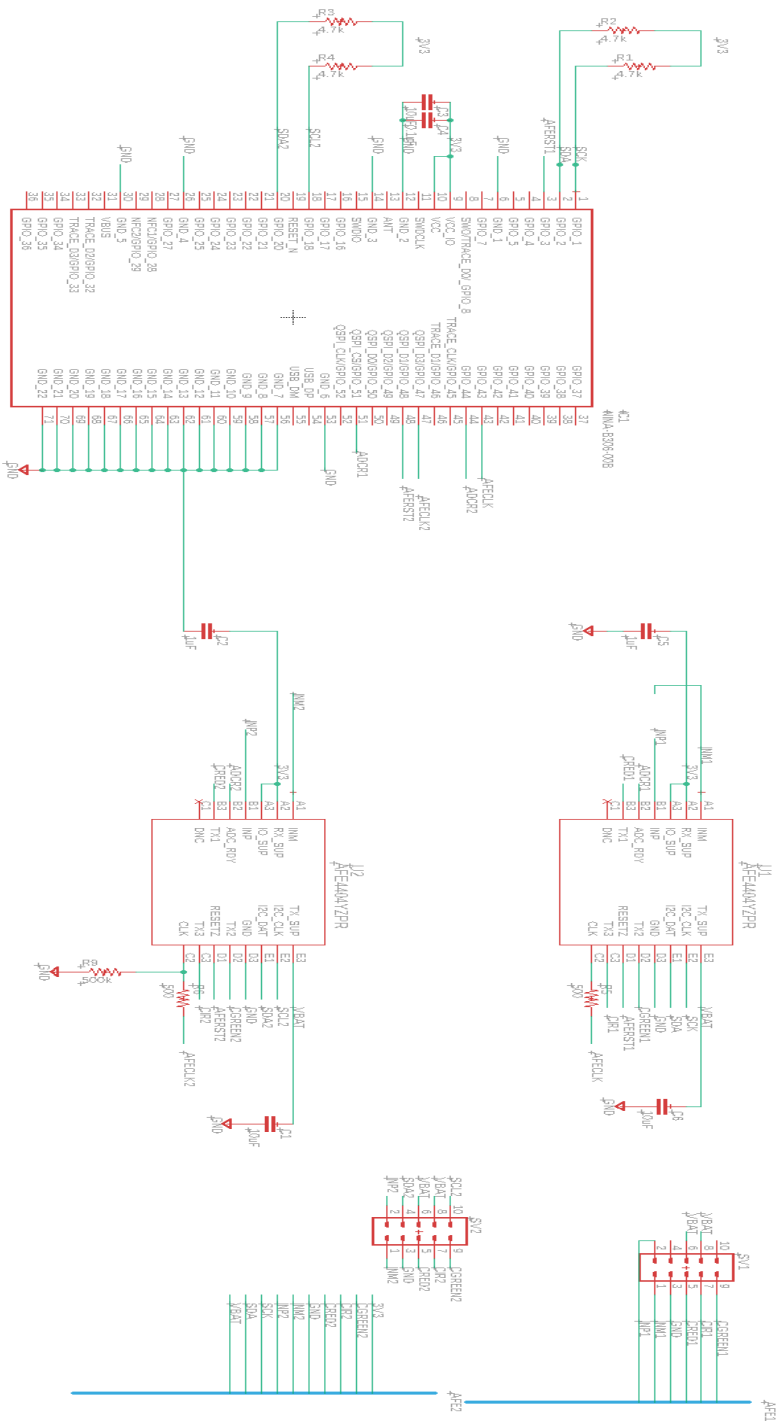

Figure 6.1-2.

6.2 PCB Vendor and Assembly

Delivering a finished Printed Circuit Board is a process that involves creating a schematic, translating it into a board layout, and exporting the Gerber file which contains details of how the PCB is to be constructed to the manufacturer who will then tune their machines to create the PCB. A PCB can be created in a variety of ways, including at home with materials that can be easily acquired at hardware stores. A homemade PCB solution is commonly created through the toner transfer method, wherein a copper laminate composed of a conductive copper outer layer, and an insulating fiberglass inner layer as pictured below (Fig 6.2-1), has ink traces transferred to it that will be etched. This process requires printing the layout of the PCB traces onto a piece of paper using a laser printer, and then ironing the paper onto the copper to transfer the toner, which will protect the copper on the traces from being etched. Once the paper has been removed using acetone and only the ink remains, the board is etched by submerging it into a mixture of Ferric Chloride and water, an example of how etching works can be seen below. The etching process will react with the outer copper layer and strip it away from the board, leaving only the copper protected by the ink. This quick method of making a Printed Circuit Board is by nature limited to the complexity that can be expressed through the projection of the printed paper to the copper sheet, the accuracy of the tools used such as the printer, and the amount of human error introduced when drilling holes manually and modifying other elements. This method, however, can be used to create quick prototypes to test out physical implementations of different systems and how a PCB realization may be different than expected.

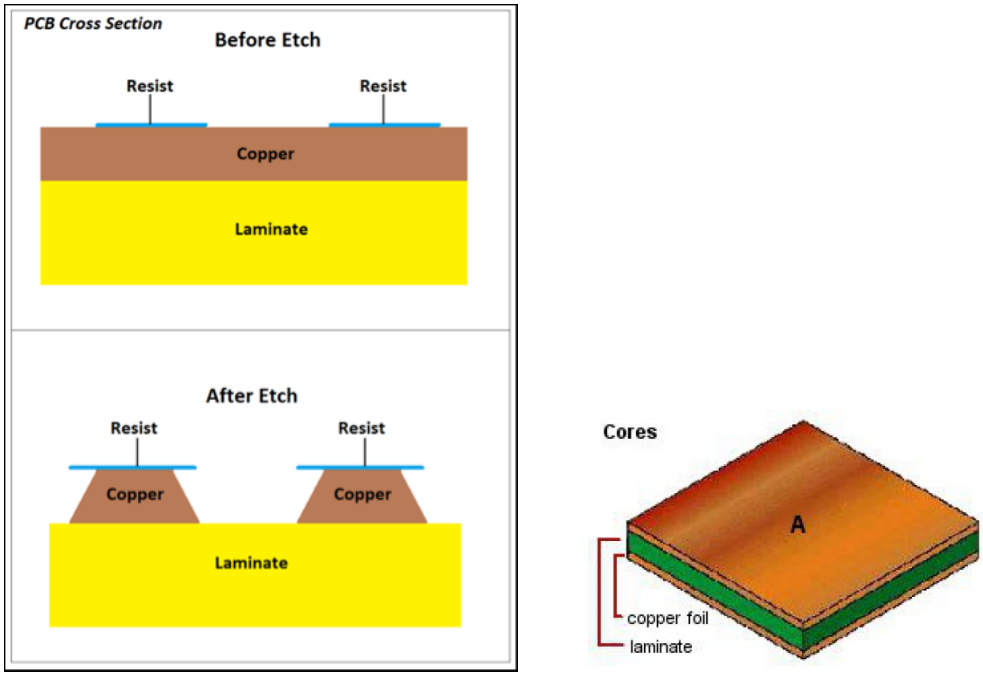

Figure 6.2-1. Courtesy of PCBPrime

For the final iterations of the device, the PCB must be created in a fail-safe manner, and that will include sending the Gerber files to a manufacturer that can create the necessary PCB to meet the physical requirements and constraints faced by this project. PCB manufacturers create PCBs using the same high-level concept discussed beforehand, however, the means by which they achieve these ends is vastly different, with automated tools and machines that inspect trace sizes, drill holes, and even control the etching process to a much greater degree than can be done at home. There were a variety of options when choosing where to get the PCB printed, to begin with there is the option of choosing an overseas manufacturer, which will present a lower cost, at the expense of taking much longer to machine and send the PCB to us. Domestic PCB manufacturers such as Advanced Circuitry International or Custom Circuit Boards tend to cost significantly more but provide a much faster turnaround and occasionally offer better customer service when issues with the design may arise.

When creating the PCBs required for this project, it was imperative to follow a few design principles, such as not routing at 90-degree angles and creating wide traces for signals which may carry higher current in order to reduce the resistance of the path, so that we can attain a PCB capable of transmitting all the power and data signals necessary without introducing significant interference. Corruption of the data signals being transmitted must be mitigated since we are dealing with delicate sensing components. The signal being output from the photodiode, for example, is tuned to a resolution of 5mV per step, so to obtain an accurate reading the board in general must transmit the power to the LEDs and the output from the photodiodes with millivolt precision.

To begin the PCB design, the correct footprints for all components had to be found. Using the Ultra Librarian repository along with SnapEDA, all the parts footprints were properly sourced and imported to EAGLE using a custom library created for this device. Once the necessary connections are made in the schematic for the device, the design enters the board planning phase, in which components must be placed carefully and oriented in a manner conducive to easy connections. The device we created features many components which must be connected on a small surface comparatively, which necessitates the use of more than one layer in the PCB. The multi-layer design in conjunction with the use of multiple extremely dense ICs, such as the AFE which has a ball grid array package, makes outsourcing the assembly of the PCB a lucrative idea, since assembling this by hand and with the tools we have at our disposal may not be possible.

Our two different PCBs were ordered together at PCBWAY, a chinese PCB manufacturer. Our final processing PCB, shown below, which hosted the microcontroller and the AFEs along with the voltage converter had to be manufactured by a company capable of printing a PCB with 3 mil wide traces. The requirements such as 3 mil traces and ultra small vias to route through a BGA component with a 0.5 mm pitch footprint made the manufacturing of one of our PCBs prohibitively expensive. Ultimately our two PCBs had all of their components soldered by hand using the tools available in the Senior Design Lab at UCF.

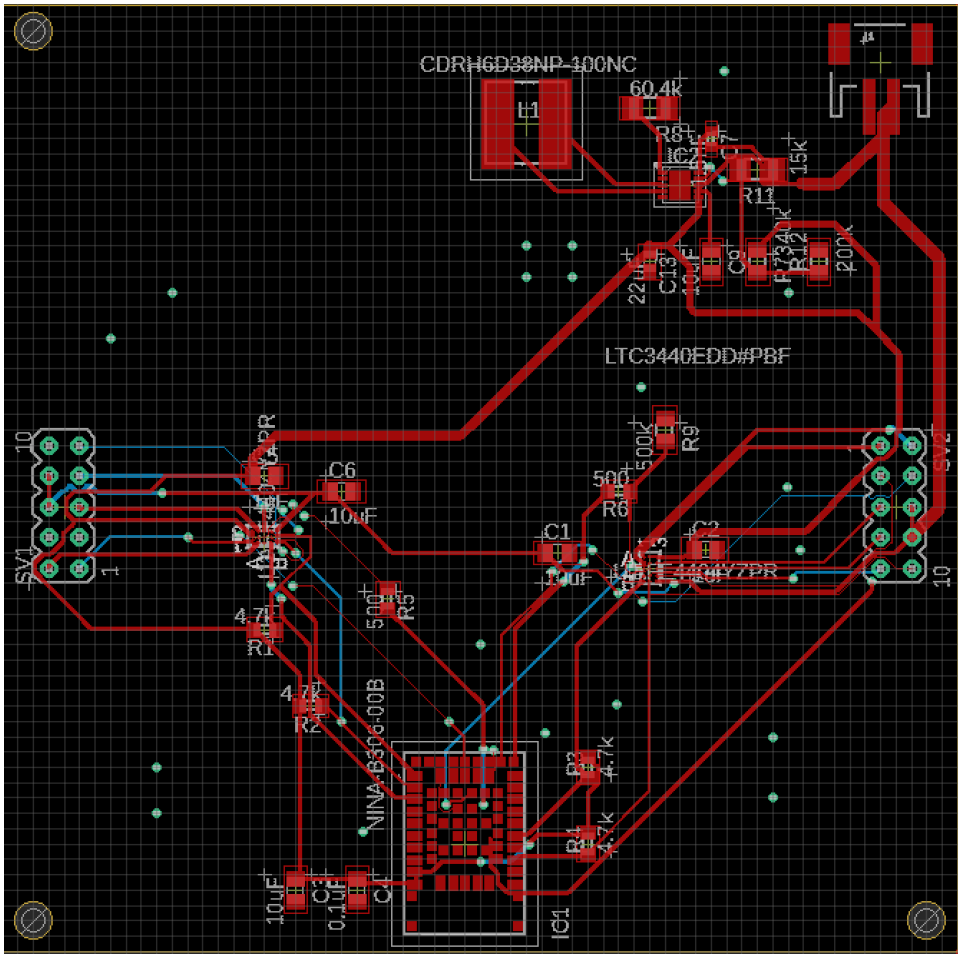

Figure 6.2-2. Processing PCB

7.0 Project Prototype Testing Plan

7.0.1 Hardware Debugging Interface

For the prototype we will be using an Arduino nano BLE. Unfortunately this off the shelf board does not come with a built-in debugging interface which the team has decided to be a crucial part of the development process. Though it does not come with the debugging interface it does come with breakout pins which can be soldered to a debugging interface.

Jlink is an extremely popular debug interface created by Segger that is used in the embedded system industry. Jlink is actually a JTAG interface emulator made specifically for arm cores. With the use of only 5 output pins we will be able to pause software as well as look into the memory of the system. Below is a

depiction of the pinout of the Arduino Nano as well as the pin descriptions in the corresponding table.

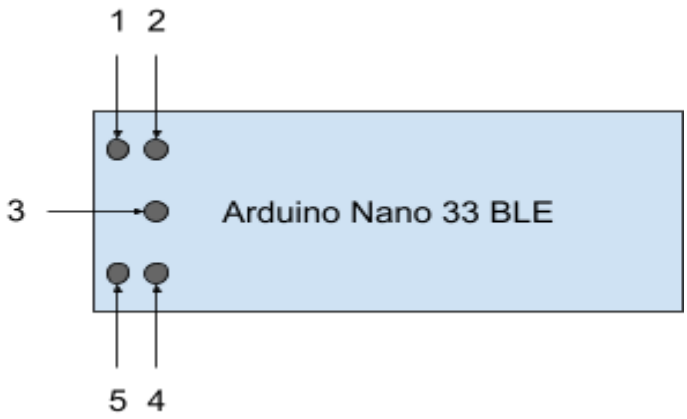

Figure 7.0.1-1.

Arduino Board	J-Link Pin Input
1	nRESET
2	GND
3	SWCLK
4	VTREF
5	SWDIO

Table 7.0.1-1.

7.1 Hardware Test Environment

Hardware testing become an indispensable tool in our development plan. Before introducing the procedures and tests we will conduct to develop our product, we will describe the equipment we plan to use for the respective tests.

7.1.1 Component Testing Environment

For the component testing, we will need to make use of a number of electrical and optical testing equipment from the undergraduate photonics laboratory. The table below (7.1.1-1) includes the name, function of the equipment we plan to use for the optical testing, as well as the components that shall be tested.

Equipment Name w/ Model	Function of Equipment	Components tested with Equipment
Optical Power Meter Main Module: (Newport: Model 1919-R) Sensor: (Newport: 918D-SL OD3R)	To measure the Radiant Flux of a source (Watts)	LEDs
Spectrometer (StellerNet: VIS-25)	To measure the spectrum of a source (Counts as a function of Wavelength)	LEDs
Optical Fiber	To guide light into the spectrometer	LEDs
Lenses and Lens Assembly	To collect and focus light onto a spot	LEDs and Photodiode
Digital Multimeter	To measure the forward current, forward voltage, and/or reverse voltage of a device. (Volts and/or Amps)	LEDs and Photodiode
Function Generator	To electrically modulate an input signal to a device.	LEDs (Later tests)
Oscilloscope	To measure the input and/or output signal of a device. (Volts)	LEDs (Later tests)
DC Power Supply	To supply DC power to a device. (Volts and/or Amps)	LEDs and Photodiode

Table 7.1.1-1.

7.2 Hardware Specific Testing

The hardware tests we will conduct can be divided into three types of tests: Component testing, in which we will test the components of a sub-system to ensure the work properly before integrating; Sub-module prototype testing, in which we will test a sub-module to assure that it is functioning according to our design; and Product testing, in which we will test the product to compare the performance with other devices as means to benchmark.

7.2.1 Component Testing

For the characterizing of the optical components we intend on using for the full product, we plan on running two tests on the LEDs and one test on the photodiode.

The first LED test will be used to characterize the radiant intensity of the device. For the procedure we will construct an LED driver circuit with a lens system to collect and focus emitted light onto an optical power meter. We will measure the forward Voltage and radiant intensity at three varying forward currents using a digital multimeter (DMM) and optical power meter, respectively. The forward current will be monitored using another multimeter and adjusted via the voltage

supply. The series resistor on the circuit will be fixed at 150 Ohms. A diagram of the set up can be seen in figure 7.2.1-1.

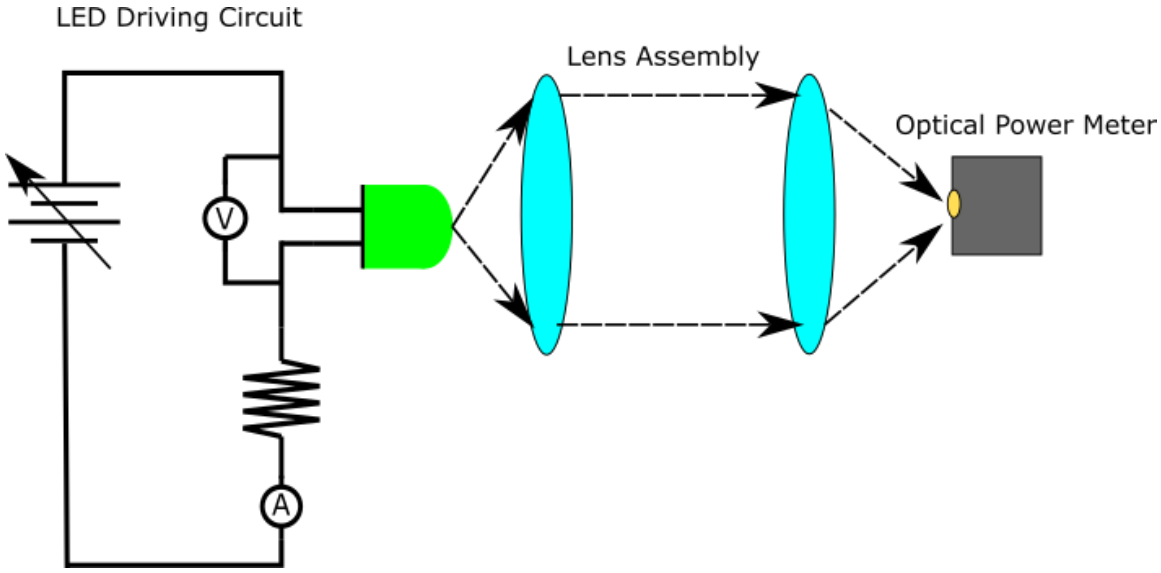

Figure 7.2.1-1.

For this LED test we expect to match the following inputs to their corresponding outputs taken from the datasheet as seen in table 7.2.1-1.

Variables	Green LED	Red LED	IR LED
Forward Current (Input)	Baseline: 10mA Step 1: 20 mA Step 2: <30 mA	Baseline: 20mA Step 1: 30 mA Step 2: <40 mA	Baseline: 20mA Step 1: 40 mA Step 2: <60 mA
Forward Voltage (Output)	Baseline: 2.3 V Step 1: 2.38 V Step 2: 2.42 V	Baseline: 1.92 V Step 1: 1.98 V Step 2: 2.22 V	Baseline: 1.7 V Step 1: 2.2 V Step 2: 2.7 V
Optical Power (Output)	Baseline: 1.8 mW/Sr Step 1: 4.0 mW/Sr Step 2: 6.0 mW/Sr	Baseline:4.3 mW/Sr Step 1: 6.3 mW/Sr Step 2: 8.4 mW/Sr	Baseline: 3 mW/Sr Step 1: 6 mW/Sr Step 2: 9 mW/Sr

Table 7.2.1-1.

The second LED test will be used to characterize the emission spectrum of the LED. We plan to use the same LED driver circuit and lens system to collect and focus emitted light onto an optical fiber that connects to a spectrometer. We will measure the emission spectrum and spectrum features (FWHM, centroid wavelength, peak wavelength) at 20 mA of base driving current (figure 7.2.1-2).

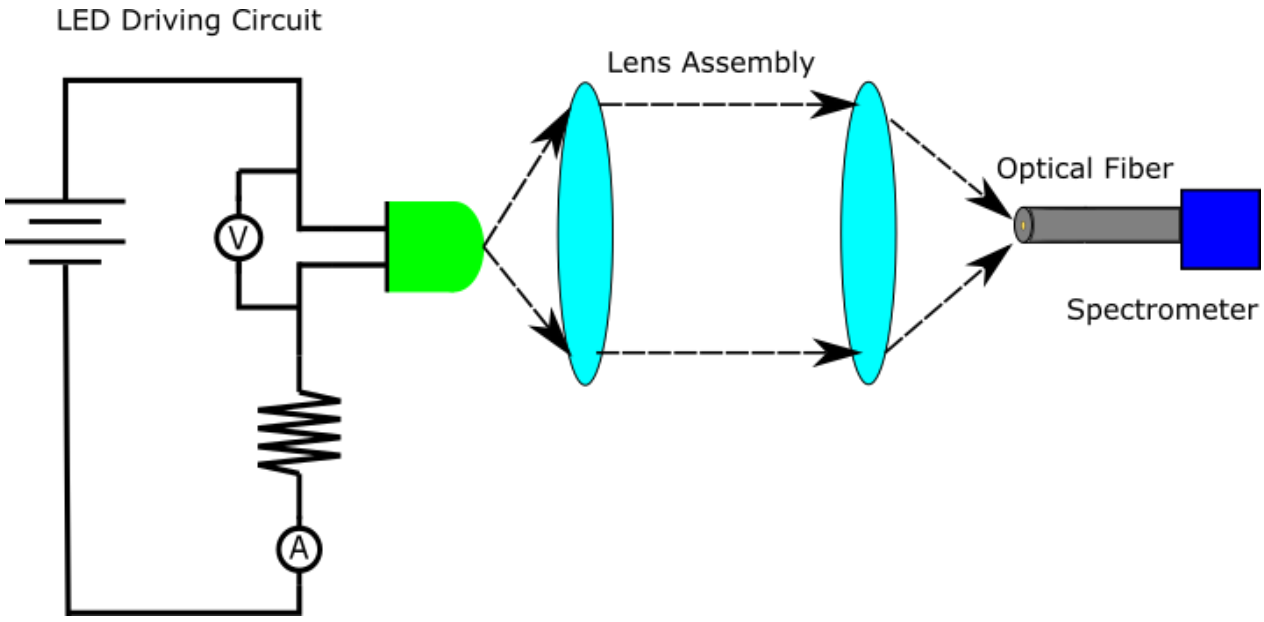

Figure 7.2.1-2.

For the spectral LED characterization test we expect to measure the following outputs (table 7.2.2-2) from previously stated inputs. The variation of spectral properties is indicated to not shift significantly by varying the current level so long as operation temperature does not exceed a certain threshold. Our application will not require high enough power consumption for this to occur, therefore no higher current test values are needed.

Variables	Green LED	Red LED	IR LED
Peak Wavelength (Output)	526.0 nm	660.0 nm	950.0 nm
Centroid Wavelength (Output)	530.0 nm	655.0 nm	940.0 nm
FWHM (Output)	32.0 nm	17.0 nm	42.0 nm

Table 7.2.2-2.

The photodiode test will be used to characterize the spectral response of the device. We plan to construct a multi-wavelength illumination with a lens system to collect and focus light onto a reverse-biased photodiode circuit with multimeter

probes attached. We plan to measure the spectral responsivity of the three working wavelengths (530nm, 660nm, 950nm) via the generated photocurrent. We plan to reverse bias the photodiode at 5 volts and use a 50 Ohm resistor (figure7.2.1-3).

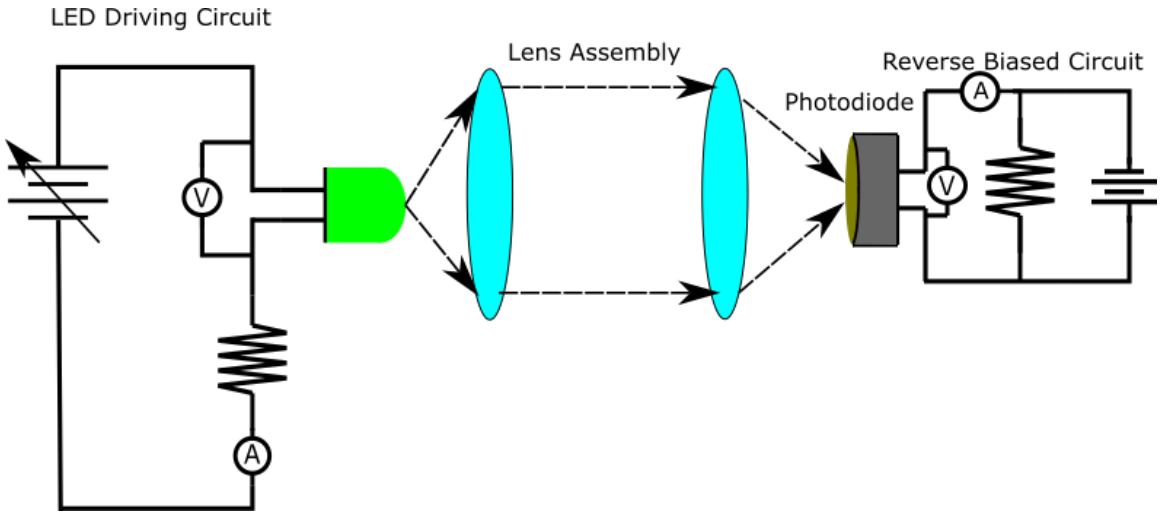

Figure 7.2.1-3.

For the photodiode spectral responsivity characterization test, we expect the following outputs (table 7.2.1-3) from a 2.0 mW optical power incident on the photodiode at the three working wavelengths. Assuming the relative responsivity from the specification sheet of the photodiode is valid.

Variables	Green Illumination	Red Illumination	IR Illumination
Photocurrent	0.588 mA	0.952 mA	1.330 mA

Table 7.2.1-3.

An issue that became apparent in the testing of the LED's radiant power was the issue of light collection. The collecting methods previously stated did not provide accurate results due to the large divergence of light rays. An integrating sphere could have resolved this issue if access was acquired.

7.2.2 Module Testing

Once we have gotten past the stage of testing individual components, we will be moving onto testing modules as a whole that can then slowly be integrated into the whole system. As previously discussed breakout boards have been made to test subsystems, the first system to be tested will be the optical modules, namely

the LEDs and Photodiodes in the specific geometric arrangement we wanted. As seen below in Figures 7.2.2-1 and 7.2.2-2 they are in a rectangular formation and the board was connected to a breadboard and manually wired to a transimpedance amplifier circuit that will feed into a microcontroller and give us the ability to analyze how well light is being captures, and whether the geometric arrangement significantly improves PPG signal acquisition.

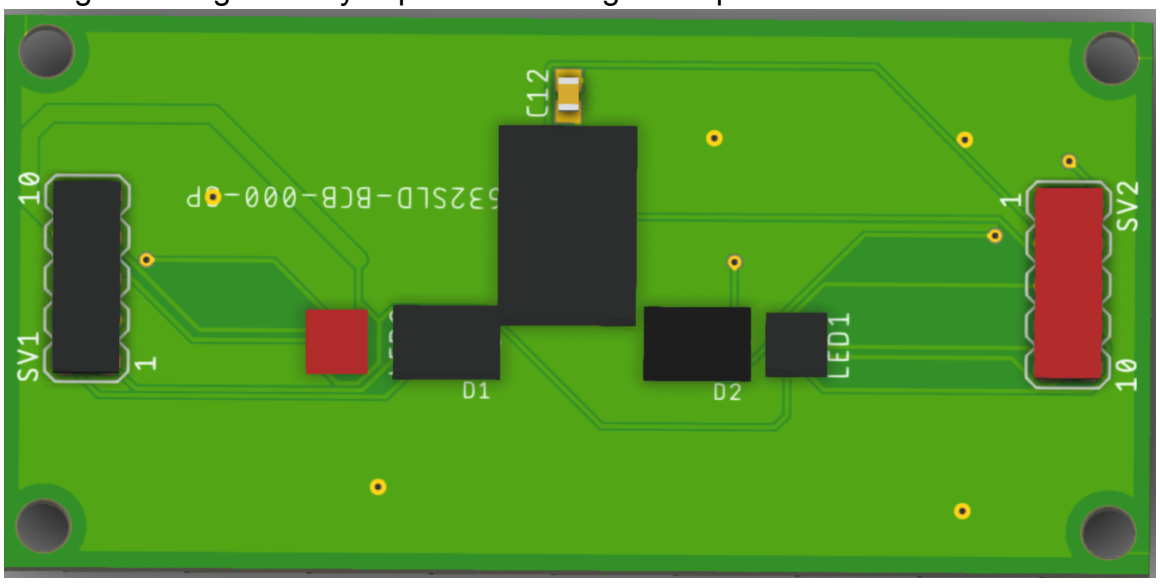

Figure 7.2.2-1.

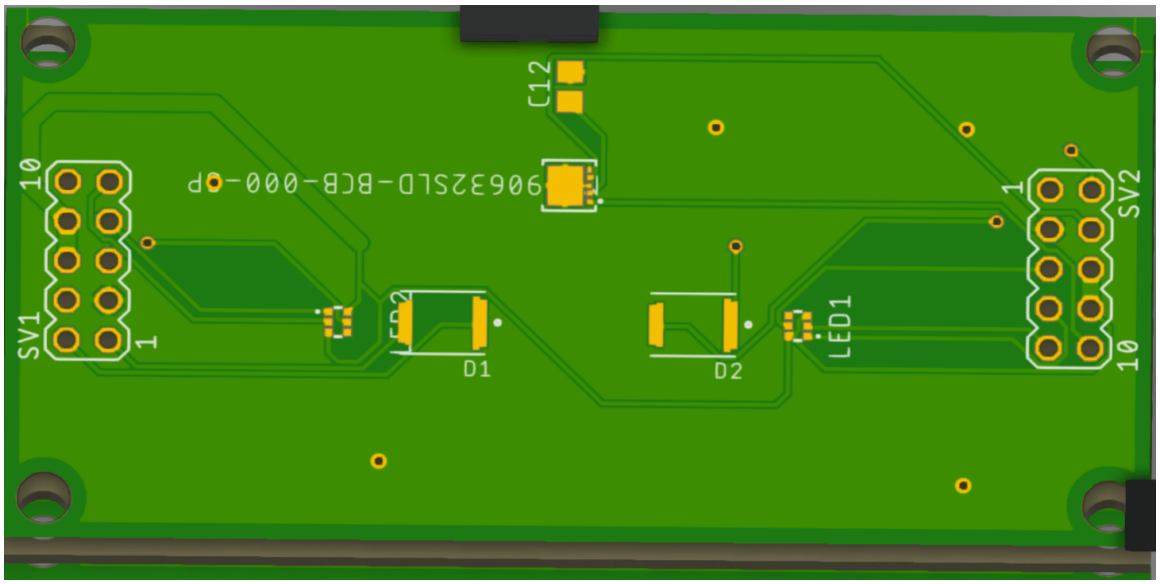

Figure 7.2.2.-2.

The breakout board featuring the optical units and the AFEs combined will then be used to test out how the signal from the photodiodes will be processed and sent. The AFE does some low level signal processing to remove the ambient lighting, which then has to be tested against the data we were getting from just

the optical units with no AFE driving them. This will once again be done on a testbench with a breadboard and the arduino nano, which will allow us to plot the ppg data live as we receive it from the AFEs using software on a PC.

7.3 Software Test Environment

Software testing will have to be split up to test functionality separately before being combined. Matlab functioned as an algorithm test environment and allowed us to even test our feature extraction algorithms to test the viability of this product. It also will allow us to have a benchmark to compare the signal processing algorithm's results given test data versus any simulated results or actual results on the mobile platform at the end.

For the rest of the applications functionality Android Studio allows the emulation of the phone environment to stage up the user interface and allow testing of the events tied to the UI and the data archiving systems. This will also allow us to confirm both the security and size of the archiving system before it has actual userdata. This emulation extends to devices that extend beyond the devices physically available for the context of the demonstrations allowing us to confirm hardware independence.

Testing the software environment related to the sensing device will rely on the development environment specific to the hardware configuration chosen. For this design Arduino Integrated Development Environment. This is an integrated development environment designed specifically to work with systems modeled after Arduino system-on-chip modules. Since this system is going to use a PCB designed after and components from an Arduino Nano BLE 33 software for the integrated circuit can be developed and tested directly in this environment.

7.4 Software Specific Testing

There are several pieces to the software testing of this system because it implements software that exists both on an integrated circuit and a mobile device. Further implementing the signal analysis portion the algorithm needs to be tested for efficacy prior to its implementation in the application. For this reason tests in multiple environments need to be designed to ensure accuracy of all of these systems.

The embedded system, acting as the sensor module will need to react to a given signal from the AFEs, inertial sensor, and the heat sensor to logically modify behavior. Further the sensor system will be informed from the application via the Bluetooth module on the next sensor run. The integrated environment will allow a test of the overall logic simulated given specific conditions provided to the system through the IDE itself. Logically a program can be designed to run the system

application disconnected from the external sensors and given specific results to simulate when the system meets specific conditions. In a similar vein the NANO can be manipulated to simulate motion to test the system's logic regarding the inertial sensor.

The application logic testing can be broken into three main components, the signal analysis portion, database logic testing and application UI logic testing. For the signal analysis algorithm, this can be tested in a platform independent environment, but it must also be tested as part of a Java application. Given known data and results, this can be tested independently and these results can also inform tests on the implemented software system.

7.4.1 Embedded Systems Filter Testing

The first piece of embedded software that needs to be tested is the digital filtering algorithm. The procedure for this is to open a UART comm port between the arduino microcontroller and a PC which will act as a data storage device. We can then write the data and read the data into a software that performs the peak detection algorithm. We will also perform a Forier transform on the data set and look at the cut off frequencies which should be at 100hz as shown in the signal conditioning algorithm in the design section. Because we can depend on the presence of additive white gaussian noise we should be able to see a negative slope in the power of the signal as we approach the cutoff frequency.

The mathematical function was designed and implemented in MatLab first. This allows datasets to be created and tested against prior to implementation on the embedded system. This allows for two separate tests to be run on the embedded system to confirm functionality. One test can be used to validate the implementation of the shaping algorithm on the embedded system implemented in C++ independent of any other system or the processing speed. This test would be limited to smaller datasets as there is a limitation in the memory space and registers available to be used. The next test would be to use the communication protocols built into the Arduino board. Although this is dependent on more systems, it allows the system to be tested at a rate which more closely resembles how the data will be received from the sensors.

The high level overview of the tests will be as shown in the image below, in figure 7.4.1-1. An onboard test will be completed, ideally without the UART connection to sample data to prove its accuracy and pave the way for a UART communicated test.

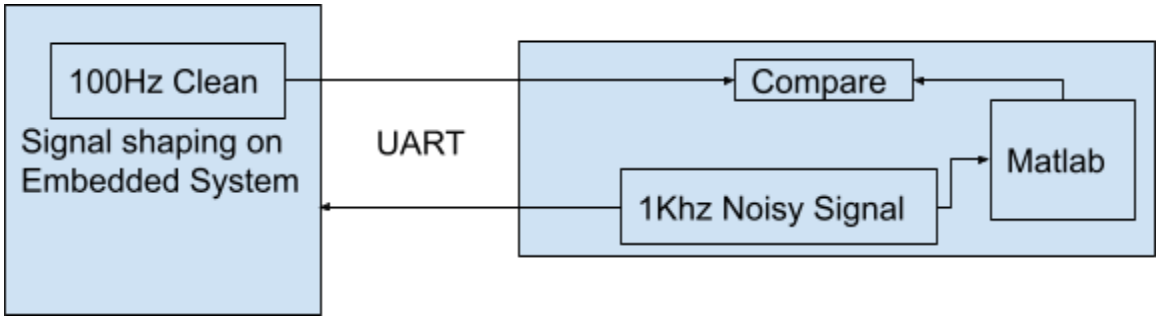

Figure 7.4.1-1.

First a function can be defined within the application space to cycle through values to be shaped. As the values are cycled through the shaping function, an output value will be generated that can be compared against designated values in a sample run through the MatLab. This can be done to shape data over most of the range of a 4 byte integer value range, however in theory the maximum value that can be used with this function would be 1/10th of the max value. This is because it relies on a summation and then averaging of the sensor values. This can be done to data even outside the scope of data that the sensors will be removed to ensure that it is mathematically sound when implemented on the embedded system. The output of this data will need to be sent form the device to an output sent through the bluetooth. Since this will emulate sensor data, it will be coded as if it was actual sensor data sent to the device. It will be visible in the database.

The next test would be a similar implementation only set to receive a stream of data. For this test the USB interface will be used to emulate a serial communication from the sensors. For this stage fixed arrays of pregenerated data can be fed through this interface as well as functions written to more closely resemble the expected datasets. Using a custom written random number generator to preprogram a function that generates 100 points of data in this range and sends through our communication interface. The output of this test will again be sent as a signal through the bluetooth interface to the application and stored where it can be compared. Since this test will not require rewriting to the embedded system except on failure, once the algorithm is set we can test 100 times off randomly generated data easily. The data will need to be stored on the computer it is generated so that it can also be run through MatLab.

These tests will allow us to ensure that the signals received from the AFEs can be shaped preemptively and data is processed as expected. This is a key to the design's implementation since the results need to be accurate before being sent to the application and it can be processed in time to prevent the need for local storage while receiving enough data points to take these biometrics.

7.4.2 Embedded Systems Workflow Testing

The control software in the embedded system will have a modified flow based on the information provided by the sensors, a signal shaping algorithm implemented in the flow, and by error reporting received by the Bluetooth module.

For sensors not integrated in the arduino system-on-chip, a control application can be developed to simulate the signals received by the system out of expected ranges in order to test the application flow. If connected to a breadboard, LEDs can be used to simulate the reporting produced by the LED indicator system.

The method being used here for optical sensing is subject to artifacting and noise from an excess of motion. Initial testing of application flow related to the inertial sensor is possible using one of the Arduinos the system's architecture is based on. Setting a control system to record data, a tester will pick up and manipulate the Arduino system on chip at varying speeds to simulate activity. This will allow the motion activated control system to be tested for reliability.

7.4.3 Wireless Communication Testing

The Bluetooth communication module is also integrated on the Arduino board. From this, the system can be tested by creating a software application that simulates the data signals expected by the sensors to be packaged and received by an awaiting connected Bluetooth system. Since the application flow is designed to take in the sensor data directly a program to simulate sensor data can be made, and processed through the packaging algorithm and sent through Bluetooth to the application. The data received by the paired Bluetooth device can be compared directly to the sample data imported.

The initial test for the communication system will be initializing data on the external bluetooth device. Simple test software will be written on the server to receive store and echo data sent to it from the external bluetooth device. By comparing the echoed data to the original echoed data we will be able to confirm the subsystem is working correctly. The process is depicted in Figure 7.4.3-1.

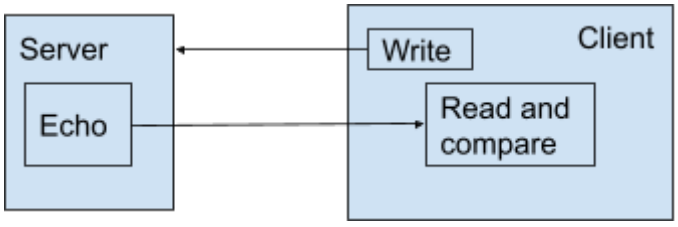

Figure 7.4.3-1.

Once we can confirm that the system is working with sample data we will then need to confirm that the bluetooth attribute protocols are working in the bluetooth stack. To do this we will create an attribute profile similar to one that will be used

on the final project and try to write to it from an external bluetooth device. We will then resolve the physical address and check it manually using the JLink debugger interface. The process is shown in Figure 7.4.3-2.

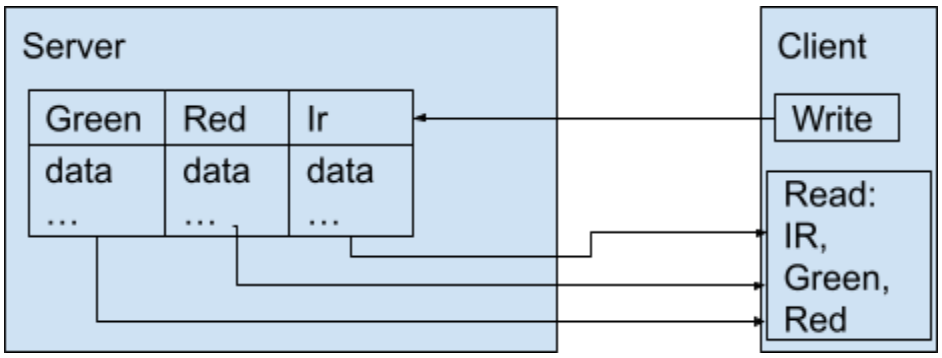

Figure 7.4.3-2.

If all of the above tests come back correctly we are able to confirm that the system is working and capable of serving its designated purpose in the working product.

To ensure that the hardware was able to be connected over Bluetooth, we used an application Nordic Systems released for testing bluetooth connections, NRF connect. This application allowed us to check that our UUID was being published correctly for each service and characteristic and allowed us to pull individual values from the peripheral device ensuring data quality. This is not sufficient for a full test however, as the sensing device has to be selected and characteristic changes cannot be monitored through the app without manually polling for the individual characteristic. Further testing was through our device and an external system. The external system was handled through either the NRF application, our mobile application, or an Arduino nano configured as a client to receive data rather than an Android device.

7.4.4 Logical Database Testing

The data storage system will have two functions that need to be tested to ensure the system will function properly. The first system that will need to be tested is the data input flow. Once data is received from the Bluetooth module it can be stored in a specific database table based on its results. Because the data is known prior to the transmission it will be clear if the database populates with the data as expected. Reviewing the automatically generated data such as data and time will be crucial as this metadata has to be appended at the time of writing to the database. Further reviewing the data which has been received will also be important as certain known values of input will result in certain metrics received for Biometrics measured.

The next system which needed testing is the ability to recall historical data by a given user. Implemented as part of the database initialization a subset of data for a debug user can be programmed. In this case the user will be named Demo and the password will be “a”. Logging in as this user on initial launch of the application allowed this data to be reviewed. Data was marked at several points along its trajectory into the database system. Data would report the user account and ID it was created for and a message was generated on successful insertion. Further review of the data could be completed with testing through the Android emulator when the resulting tables could be inspected for accuracy after the test. Several instances were run with 30 preset data points for each biometric.

Another test was devised to allow the accuracy of data points to be associated with the correct users and to be displayed when loading those individual users for this test the database was removed and allowed to rebuild using the function to populate new biometrics. In this test random biometrics were generated for two separate users. 365 sets of biometrics were generated for the user Demo and 15 were generated for the user Demo2. In this test the database was removed and the application was launched again with a new function integrated to create the sets of data mentioned. The results were viewed both in the application graph view by logging in with each user and through an external database viewer. This test was run 10 times to ensure data was integrated as expected. Each time the

biometrics were created in the parameters set and data was appropriately assigned to each user in question.

A final test of the database where the database was created with various levels of biometric data stored. Since realistically the bulk of data to be stored will be in the form of stored biometrics, 4 per scan, judging database size growth and application performance based on introduction of biometric data makes the most sense. This test would include regenerating the database with various amounts of biometric data populated and measuring application performance and data storage required to accommodate. This test was run 5 times for each level of biometrics and an average was taken to remove the chance of interruption due to unforeseen circumstances. To prepare for this test this was completed without measurement in an emulator to ensure the logic was sound. Once this was completed it was run on the device used for Demo-ing a Samsung Galaxy tab a sm-t280, the device the demonstration was to be run on.

Sets of Readings	First Time App Launch (s)	Subsequent App Launch (s)	User Data Load (s)	Graph Swap time (s)	Database Size on Disk
0	< 1 s	< 1 s	< 0.1 s	< 0.1 s	44 KB
20	< 1 s	< 1 s	< 0.1 s	< 0.1 s	44 KB
400	27.5 s	< 1 s	< 0.1 s	< 0.1 s	92 KB
3000	210.4 s	< 1 s	< 1.7 s	< 0.2 s	412 KB

7.4.5 Application Signal Analysis Pretest

The signal analysis of the sensor data is the most complicated and crucial software system to be tested in this system's design. Given the mathematical basis of the analysis the algorithms for shaping and analysis will be first designed and implemented in Matlab. Once the algorithm is designed, known good sets of data will be passed through in order to ensure the algorithm returns the correct results.

7.4.6 Signal Analysis Testing

The signal analysis algorithm also has to be written in a format which the mobile device can understand, in this case an Android mobile device. The native language of Java is explicit in its data types, so when running these complicated equations it is possible to lose accuracy. A sample dataset will be stored in the starting database to emulate the sensor data which may be received by the sensing device and sent to the application. This data will have results that end in biometrics calculated by the signal analysis pretest in MatLab. There are sample datasets available online to start with in comparison and further datasets can be

generated programmatically. So long as they are put through the MatLab Simulation a known value will come out that the results can be compared against.

The tests which will be run will include one pregenerated and pre tested set of data. 5 subsequent tests will be generated for a calculation cycle using a software function generator. All of these will be implemented in the database initialization code to be sampled for testing in the application after the fact.

7.4.7 Software Integration Testing

Next, to test the peak detection algorithm we will use the same process of using a PC as a data retention platform by reading from a UART com channel between the embedded system and the mobile device. Measuring the distance between N peaks and dividing by the period of time between the first and last peak we should extract the heart rate. The result will be compared to the result of a medically approved heart rate monitor to confirm the accuracy.

8.0 Administrative Content

The chapters prior to this one have all informed some research, or decisions in the implementation of the system. However, this is not the only consideration required for a project like this one. It is important to keep track of time and expenses as well. This chapter outlines the milestones that must be met for this project's timely completion and the costs incurred designing, testing, and implementing this design in particular.

8.1 Milestone Discussion

Chapter 8.1 is an outline of the planned milestones to reach and their expected dates over the course of designing this system. It is important to outline these milestones and expected dates to ensure the project deadline is met. Failure to meet timing for deliverables or meeting these intermediary goals could result in failure to complete the overall project in time.

8.1.1 Senior Design 1 Milestones

It was crucial to set and meet soft goals on the way through the design process of this system. In the below table 8.1-1 is a listing of the milestones that were used to complete the design of this system during the course of the Senior Design 1 course in spring of 2022.

Week #	Dates	Milestone

1	1/10/2022 – 1/14/2022	Form a group and formulate ideas
2	1/17/2022 - 1/22/2022	First group meeting
3	1/24/2022 – 1/28/2022	Meet bootcamp objectives and start on D&C V1.0
4	1/31/2022 – 2/4/2022	Finalize D&C V1.0
5	2/7/2022 – 2/11/2022	D&C V1.0 meeting Work on D&C V2.0
6	2/14/2022 – 2/18/2022	D&C V2.0 submission
7	2/21/2022 – 2/25/2022	Begin work on 60 page paper
8	2/28/2022 – 3/04/2022	30/60 pages
9	3/07/2022 – 3/11/2022	40/60 pages
10	3/14/2022 – 3/18/2022	50/60 pages
11	3/21/2022 – 3/25/2022	60/60 pages, Assignment due
12	3/28/2022 – 4/01/2022	Finalize research and design, achieve 80 pages
13	4/04/2022 – 4/11/2022	100 pages due
14	4/18/2022 – 4/22/2022	Refine paper, finish last 20 pages
15	4/25/2022 – 4/29/2022	Submit final report 120 pages Order PCBs

Table 8.1.1-1.

8.1.2 Senior Design 2 Milestones

These are the milestones expected to be completed in the design of this system during the course of the Senior Design 2 course in summer of 2022.

Week #	Dates	Milestone

1	5/16/2022 – 5/20/2022	Update meeting, order missing parts
2-3	5/23/2022 – 6/03/2022	Test sensor and data processing
4-6	6/06/2022 – 6/24/2022	Get App/UI finished
7-10	6/27/2022 – 7/22/2022	Finish prototyping/make final changes
11	7/25/2022 – 7/29/2022	Deliver presentation
12	8/01/2022 – 8/05/2022	Final report

Table 8.1.2-2. SD2 Milestones

The diagram below(figure 8.1.2-1) details the development and integration progress of this project. Due to the uncertainty in merging of subsystems the team thought this diagram coupled with a strict timelines was imperative to a successful outcome. To combat oversimplification the timeline will include system merging issues and course correction.

Starting from left to right there will be four main systems in development being led by each of the team members. There will be collaboration among the team however the main process should be under the responsibility of a single leading member. UI, Mobile Bluetooth Application, PCB Design, and AFE system development process were deemed independent of each other to push development in parallel independently of each other.

Once the four main systems are completed or in working state we will move into the interior of the flow diagram where we will be focussing on embedded software as well as the client side application in the bluetooth communication link. To specify further, the embedded software encompasses the BLE server application and the digital filtering/down sampling algorithm. Lastly we will merge the 2 main systems of the product completing our goals.

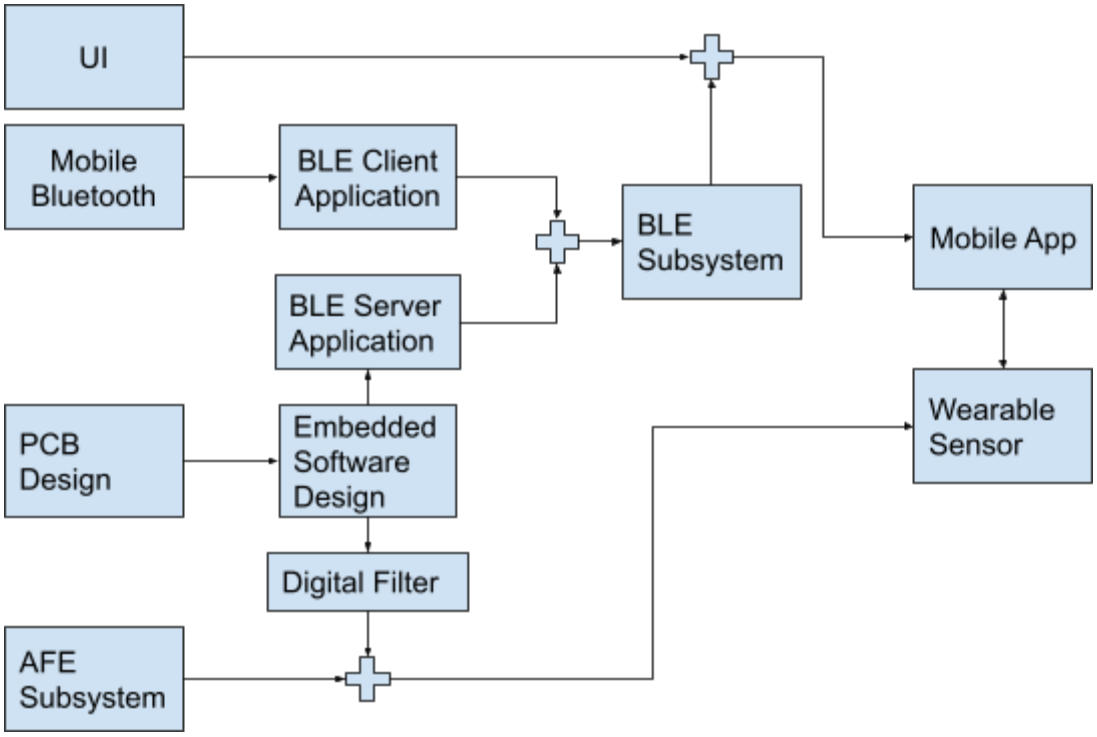

Figure 8.1.2-1.

8.2 Budget and Finance Discussion

The group had no sponsors and so this project will be financed entirely by the project group members. When creating a wearable device, cutting edge technology that is smaller than a common wristwatch is not feasible on a budget made with four students in mind, therefore we have chosen components that are light and affordable at the expense of not being smaller than market competitors. The team had agreed upon a maximum budget of $300 per person, with the aim to make this project under $150 per person. The high end of the budget estimate was intended to target reaching all of our goals, including the stretch goals. To implement just the core features and perhaps some advanced features, we aimed to keep the budget at the aforementioned $150 per person, but this was not reasonable. Decisions on what type of battery and power delivery system we use moderately affect our budget and convenience of the device. Between complications and availability of parts as well as unforeseen costs in our initial estimation, such as the evaluation board and steep PCB fabrication costs we exceeded our desired $300 per person system just to meet the original goals of the product. Without including costs of food or transportation for the team during the assembly, troubleshooting and testing of the systems our total ledger was approaching $1500. The breakdown of the costs planned or already incurred by the design of this system are listed below in table 8.2-1. The prices written that have yet to be incurred are an estimation based on the prices listed by vendors who could reasonably have the item or service in stock and available as of the

time of this writing. A breakdown of the cost for three expense categories (photonics, mechanical, electronics) can be seen in figure 8.2-1.

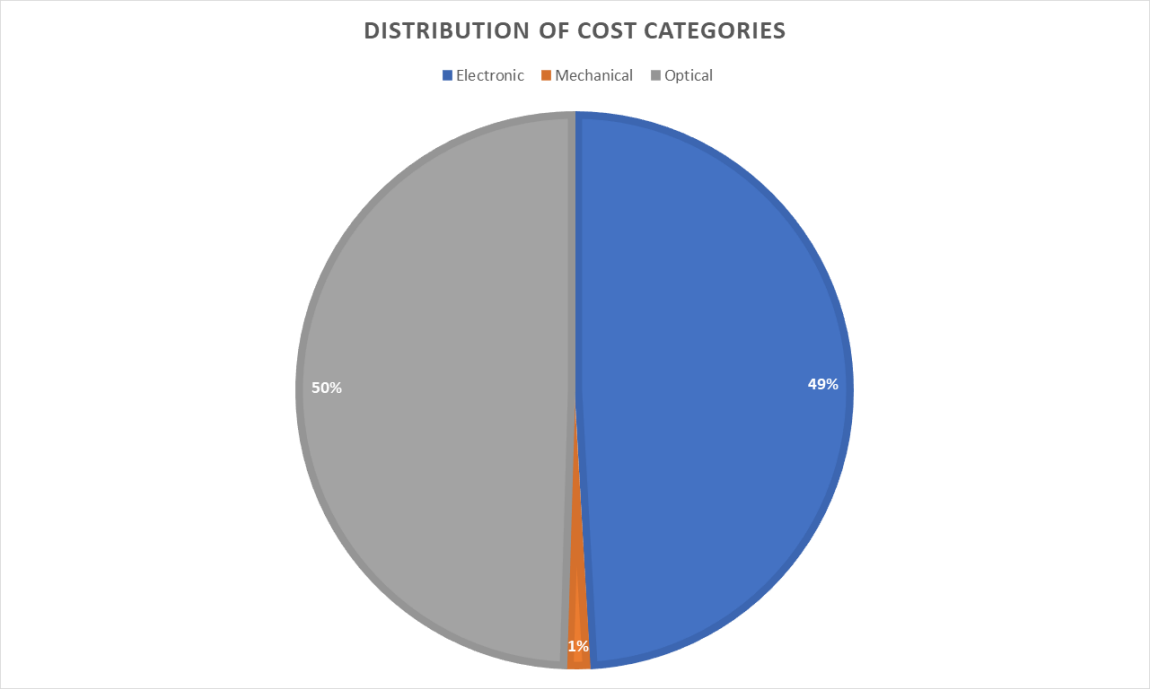

Figure 8.2-1.

Estimation of actual costs			
Item	Cost Per Item	Quantity	Total cost
Microcontroller Dev board	$20.00	2	$40.00
Wrist wearable Housing	$75.00	1	$75.00
Photo Diode(Demo)	$12.19	1	$12.19
Photo Diode	$1.09	4	$4.36
Battery	$10.00	2	$20.00
AFE4004 Eval board	$270.00	1	$270.00
PCB Printing - 2 Large Main PCB and 5 Smaller sensor boards	$240.00	1	$240.00

Arduino Nano BLE 33	$24.00	7	$168.00
LEDs(Demo)	$12.86	2	$25.72
LEDs(Full)	$2.12	3	$6.36
IMU	$2.66	5	$13.30
SMT JST 2 PIN	$1.00	1	$1.00
Battery charging circuitry	$7.00	1	$7.00
Buck boost converter	$7.75	1	$7.75
Resistors	$0.24	20	$4.80
Capacitors	$0.55	20	$11.00
Breadboard	$6.00	1	$6.00
PLA 3D Printer Filament	$20.00	1	$20.00
42BGA stencil from Protoboard and Photodiodes	$65.79	1	$65.79
Thorlabs - Optics polarizers and adhesives	$73.13	1	$73.13
AFE4004s and Photodiodes	$57.86	1	$57.86
Edmond optics glass windows	$141.23	1	$141.23
Electrical Components AFEs/ Adapter board Sensors / LEDs / Photodiodes	$271.00	1	$271.00
Total (Approx)			$1466.49

Table 8.2-1.

9.0 Usermanual and Troubleshooting

9.1 Hardware - the Sensing Device

9.2 User Application

Once the user device is attached to the user and ready to accept new data samples the user's next step is to load up the mobile application on their Android device. They will be greeted by a login screen.

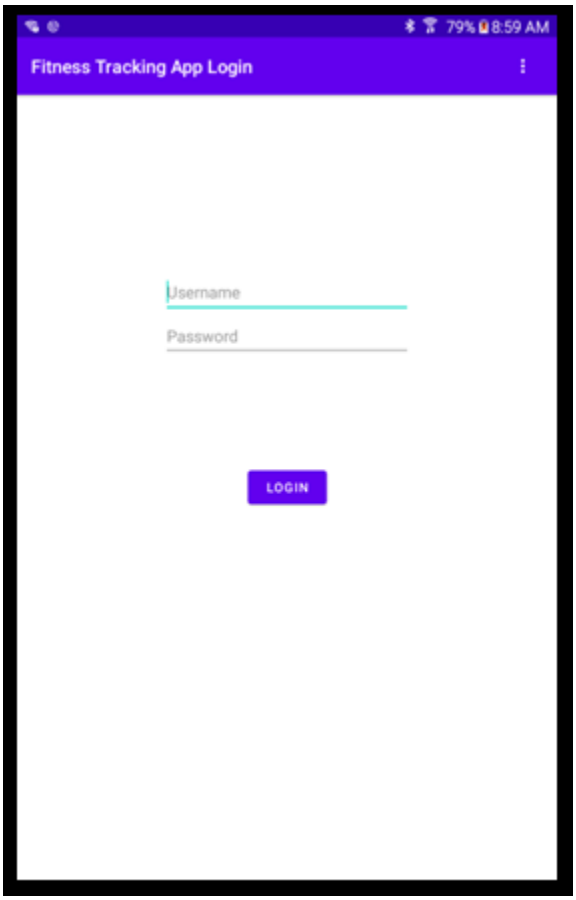

If the user has never logged in before, they will need to type a username and password, both case sensitive for a new data profile. Once they have completed typing both and are sure, they will press the Login button to bring them to the scan and history page.

If they are an existing user or wish to access an existing profile, the username must match an existing user and the password must be the corresponding password for this data profile. If the password does not match, the application will provide a user toast message indicating that the password is incorrect. If the user puts in a correct password of an existing profile, they will be directed to the next page, the scan and history page.

Once this page is reached the notice at the top of the page will request the user select a biometric or press the scan button to collect more data. If the user presses a biometric button the top label will update to that biometric and the last recorded value for this biometric will be displayed. It will also update the history graph below. It will indicate which biometric the unit it is measured in and all previously recorded values for this data profile in the graph.

In the above example, the user has 15 point of biometric data saved on their profile. They have selected Heart Rate as the biometric. These values range from a little over 82 BPM and up to 151 BM. Chronologically they are sorted with the first measurement saved all the way to the last. This graph is interactable, a user can zoom in by pressing two fingers on the screen touching the graph view and spreading them apart vertically. They can also swipe their finger left or right to move backwards or forwards in the timeline of measurements if the resulting graph is bigger than the view window.

If the user presses the scan button the app should receive 12 seconds worth of data from the sensing device, update the users biometrics saved. Once the user presses the biometric button they wish to see again, they will press the biometric

button again. Once the user is done looking at this data or they can either close the app or press the logout button to be returned to the login screen.

9.3 User Application Troubleshooting

If there is no data in a given data profile it is likely the user logged into an incorrect profile. The user must logout or close the application and attempt to log in with the correct credentials.

If the scan does not pick up a sensing device in range it will not be able to scan new data. This means that the graph will not update further and the last measured metric will not change.

If the data on the graph appears incorrect this can be because the device is not properly attached. The sensing device is sensitive to movement and requires having an even amount of pressure on the sensing unit. The biometrics in question are also configured to be acquired from the wrist, so attempting to use the device in another region of the body may not produce accurate results. Please make sure that the device is adequately strapped down and not in motion during sensing attempts.

Appendices I - Copyright Permissions

OSRAM Intellectual rights

From Section 5 Osram gives the right to use this information pulled from their site so long as it is either for personal or non-commercial purposes. This is accessed from their Services terms of use page (published at https://www.osram.com/cb/services/terms-of-use/index.jsp)

4. Intellectual Property Rights to the Information and Software published on the OSRAM Web Site
4.1 The information published on the OSRAM Web Site, including the editorial materials; informational texts; Software; documentation; databases; photographs; video and audio clips; downloads; illustrations; artistic designs and other graphical elements; materials; names; trademarks; and logos are the property of OSRAM or the licensors of OSRAM and are protected under national and international copyright law and/or intellectual property rights related to databases, trademarks, and other industrial property. You shall observe these rights and, in particular, you shall not remove alphanumeric codes, marks or copyright notices from the information, the Software or the documentation, nor from any copies thereof.

4.2 You may not systematically download, reproduce and/or disseminate the information on the OSRAM Web Site.

4.3 The word and figurative mark OSRAM, other product trademarks, illustrations and logos identify OSRAM products and are the registered property of OSRAM or its licensors. Trademark registrations may not yet have taken place in all relevant countries. These trademarks may only be used with the express permission of OSRAM GmbH. The OSRAM name may be used as a cross-reference, e.g. to link to this Web Site. OSRAM GmbH must be given prior notification of any such use.

5. Rights to Use the Information Posted on the OSRAM Web Site and the Software Provided on the OSRAM Web Site
5.1 OSRAM gives you the non-exclusive, revocable, non-transferable and non-sublicensable right to access the information and Software provided on the OSRAM Web Site and to use the information and Software for personal and non-commercial purposes. Above and beyond the personal and non-commercial use, you may not change; copy; reproduce; sell; lease; transmit; display; publish; license; process; use; supplement or otherwise exploit the information published on the OSRAM Web Site without the express consent of OSRAM GmbH.

5.2 Above and beyond the rights granted in item 5.1, nothing shall be construed as granting you, by implication or otherwise, any license or any right to use a patent, a trademark or any other intellectual property right of OSRAM. Nor is any license or any right to use a copyright or other rights related to the information published on the OSRAM Web Site granted thereby.

6. Additional Terms of Use for the Software Provided on the OSRAM Web Site
6.1 Above and beyond these Terms of Use, using the Software made available on the OSRAM Web Site may also be subject to Special Terms and/or Software Terms of Use. In case of contradictions, Special Terms and/or Software Terms of Use shall have precedence over these Terms of Use.

6.2 Software shall be made available to you free of charge in object code. There is a claim to surrender of the source code only with respect to the source codes of open source software, whose license conditions have precedence over these Terms of Use when open source software is passed on and require turning over the source code. In such a case, OSRAM shall make the source code available in return for the payment of incurred costs.

6.3 Unless mandatory law otherwise allows, you shall not modify the Software or its documentation nor disassemble, reverse engineer or decompile the Software or separate any part thereof. You may make one backup copy of the Software where necessary to secure further use in accordance with these Terms of Use.

Figure Thorlabs-2.

Thorlabs Intellectual rights

General Terms and Conditions

From Thorlabs general terms and conditions of sale, they authorize license to use supporting software products provided for use with Thorlabs' Products so long as they are used within the terms and conditions supplied with the product. This is found at (https://www.thorlabs.com/Images/PDF/LG-PO-001_Thorlabs_terms_and_%20agreements.pdf)

A screenshot of this section of the General terms and conditions is found below.

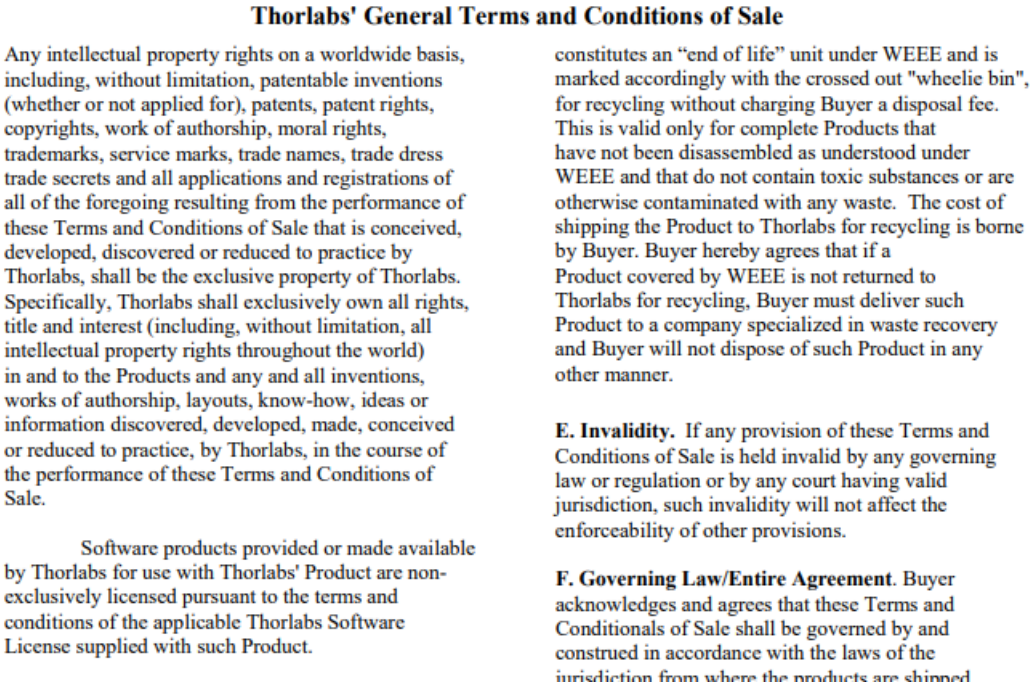

Thorlabs' General Terms and Conditions of Sale

Any intellectual property rights on a worldwide basis, including, without limitation, patentable inventions (whether or not applied for), patents, patent rights, copyrights, work of authorship, moral rights, trademarks, service marks, trade names, trade dress trade secrets and all applications and registrations of all of the foregoing resulting from the performance of these Terms and Conditions of Sale that is conceived, developed, discovered or reduced to practice by Thorlabs, shall be the exclusive property of Thorlabs. Specifically, Thorlabs shall exclusively own all rights, title and interest (including, without limitation, all intellectual property rights throughout the world) in and to the Products and any and all inventions, works of authorship, layouts, know-how, ideas or information discovered, developed, made, conceived or reduced to practice, by Thorlabs, in the course of the performance of these Terms and Conditions of Sale.

Software products provided or made available by Thorlabs for use with Thorlabs' Product are non-exclusively licensed pursuant to the terms and conditions of the applicable Thorlabs Software License supplied with such Product.

constitutes an "end of life" unit under WEEE and is marked accordingly with the crossed out "wheelie bin", for recycling without charging Buyer a disposal fee. This is valid only for complete Products that have not been disassembled as understood under WEEE and that do not contain toxic substances or are otherwise contaminated with any waste. The cost of shipping the Product to Thorlabs for recycling is borne by Buyer. Buyer hereby agrees that if a Product covered by WEEE is not returned to Thorlabs for recycling, Buyer must deliver such Product to a company specialized in waste recovery and Buyer will not dispose of such Product in any other manner.

E. Invalidity. If any provision of these Terms and Conditions of Sale is held invalid by any governing law or regulation or by any court having valid jurisdiction, such invalidity will not affect the enforceability of other provisions.

F. Governing Law/Entire Agreement. Buyer acknowledges and agrees that these Terms and Conditionals of Sale shall be governed by and construed in accordance with the laws of the jurisdiction from where the products are shipped

Figure Thorlabs-3.

Thorlabs LED528EHP Specification and Documentation

From the Thorlabs specification document which accompanies the LED528EHP the agreement for this product indicates that for use in military or life support applications permissions from the President of the Company must provide written permissions or is not otherwise granted.

There is a screenshot of this description from the specification sheet found at https://www.thorlabs.com/drawings/df144c21684b10b8-E1B008C9-F0B3-0DD3-CED87916A4B73562/LED528EHP-SpecSheet.pdf

Part 3. Precautions and Warranty Information

These products are ESD (electro static discharge) sensitive and as a result are not covered under warranty. In order to ensure the proper functioning of an LED care must be given to maintain the highest standards of compliance to the maximum electrical specifications when handling such devices. The LEDs are particularly sensitive to any voltage that exceeds the absolute maximum ratings of the product. Any applied voltage in excess of the maximum specification will cause damage and possible complete failure to the product. The user must use handling procedures that prevent any electro static discharges or other voltage surges when handling or using these devices.

Thorlabs, Inc. Life Support and Military Use Application Policy is stated below:

THORLABS' PRODUCTS ARE NOT AUTHORIZED FOR USE AS CRITICAL COMPONENTS IN LIFE SUPPORT DEVICES OR SYSTEMS OR IN ANY MILITARY APPLICATION WITHOUT THE EXPRESS WRITTEN APPROVAL OF THE PRESIDENT OF THORLABS, INC. As used herein:

1. Life support devices or systems are devices or systems which, (a) are intended for surgical implant into the body, or (b) support or sustain life, and whose failure to perform, when properly used in accordance with instructions for use provided in the labeling, can be reasonably expected to result in a significant injury to the user.

2. A critical component is any component in a life support device or system whose failure to perform can be reasonably expected to cause the failure of the life support device or system or to affect its safety or effectiveness.

3. The Thorlabs products described in this document are not intended nor warranted for usage in Military Applications.

Figure Thorlabs-4.

ThorLabs FDS100

This component has a similar agreement outlined in its spec sheet provided from the Thorlabs site at the following url.
https://www.thorlabs.com/drawings/df144c21684b10b8-E1B008C9-F0B3-0DD3-CED87916A4B73562/FDS100-SpecSheet.pdf

Below is a screenshot of the agreement requirements of Thorlabs products from that spec sheet.

Precautions and Warranty Information

These products are ESD (electro static discharge) sensitive and as a result are not covered under warranty. In order to ensure the proper functioning of a photodiode care must be given to maintain the highest standards of compliance to the maximum electrical specifications when handling such devices. The photodiodes are particularly sensitive to any value that exceeds the absolute maximum ratings of the product. Any applied voltage in excess of the maximum specification will cause damage and possible complete failure to the product. The user must use handling procedures that prevent any electro static discharges or other voltage surges when handling or using these devices.

Thorlabs, Inc. Life Support and Military Use Application Policy is stated below:

THORLABS' PRODUCTS ARE NOT AUTHORIZED FOR USE AS CRITICAL COMPONENTS IN LIFE SUPPORT DEVICES OR SYSTEMS OR IN ANY MILITARY APPLICATION WITHOUT THE EXPRESS WRITTEN APPROVAL OF THE PRESIDENT OF THORLABS, INC. As used herein:

1. Life support devices or systems are devices or systems which, (a) are intended for surgical implant into the body, or (b) support or sustain life, and whose failure to perform, when properly used in accordance with instructions for use provided in the labeling, can be reasonably expected to result in a significant injury to the user.
2. A critical component is any component in a life support device or system whose failure to perform can be reasonably expected to cause the failure of the life support device or system or to affect its safety or effectiveness.
3. The Thorlabs products described in this document are not intended nor warranted for usage in Military Applications.

Figure Thorlabs-5.

Figure Thorlabs-6.

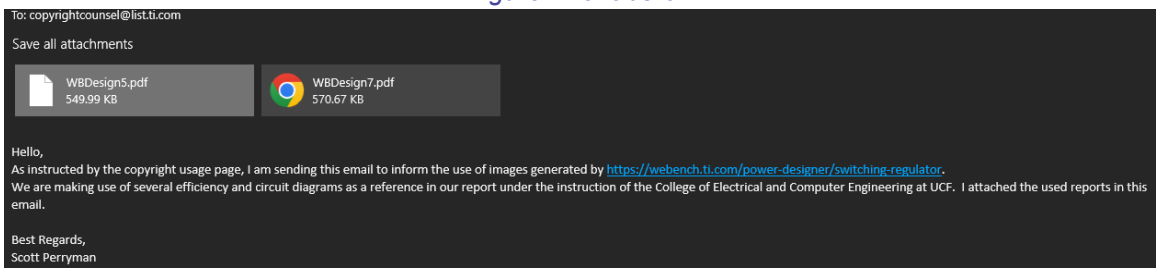

Figure Thorlabs-7.

http://www.apache.org/licenses/LICENSE-2.0

Unless required by applicable law or agreed to in writing, software
distributed under the License is distributed on an "AS IS" BASIS,
WITHOUT WARRANTIES OR CONDITIONS OF ANY KIND, either express or
implied.
See the License for the specific language governing permissions and
limitations under the License.

Apache License

Version 2.0, January 2004

http://www.apache.org/licenses/

TERMS AND CONDITIONS FOR USE, REPRODUCTION, AND DISTRIBUTION

1. Definitions.

"License" shall mean the terms and conditions for use, reproduction, and distribution as defined by Sections 1 through 9 of this document.

"Licensor" shall mean the copyright owner or entity authorized by the copyright owner that is granting the License.

"Legal Entity" shall mean the union of the acting entity and all other entities that control, are controlled by, or are under common control with that entity. For the purposes of this definition, "control" means (i) the power, direct or indirect, to cause the direction or management of such entity, whether by contract or otherwise, or (ii) ownership of fifty percent (50%) or more of the outstanding shares, or (iii) beneficial ownership of such entity.

"You" (or "Your") shall mean an individual or Legal Entity exercising permissions granted by this License.

"Source" form shall mean the preferred form for making modifications, including but not limited to software source code, documentation source, and configuration files.

"Object" form shall mean any form resulting from mechanical transformation or translation of a Source form, including but not limited to compiled object code, generated documentation, and conversions to other media types.

"Work" shall mean the work of authorship, whether in Source or Object form, made available under the License, as indicated by a copyright notice that is included in or attached to the work (an example is provided in the Appendix below).

"Derivative Works" shall mean any work, whether in Source or Object form, that is based on (or derived from) the Work and for which the editorial revisions, annotations, elaborations, or other modifications represent, as a whole, an original work of authorship. For the purposes of this License, Derivative Works shall not include works that remain separable from, or merely link (or bind by name) to the interfaces of, the Work and Derivative Works thereof.

"Contribution" shall mean any work of authorship, including the original version of the Work and any modifications or additions to that Work or Derivative Works thereof, that is intentionally submitted to Licensor for inclusion in the Work by the copyright owner or by an individual or Legal Entity authorized to submit on behalf of the copyright owner. For the purposes of this definition, "submitted" means any form of electronic, verbal, or written communication sent to the Licensor or its representatives, including but not limited to communication on electronic mailing lists, source code control systems, and issue tracking systems that are managed by, or on behalf of, the Licensor for the purpose of discussing and improving the Work, but excluding communication that is conspicuously marked or otherwise designated in writing by the copyright owner as "Not a Contribution."

"Contributor" shall mean Licensor and any individual or Legal Entity on behalf of whom a Contribution has been received by Licensor and subsequently incorporated within the Work.

2. Grant of Copyright License. Subject to the terms and conditions of this License, each Contributor hereby grants to You a perpetual, worldwide, non-exclusive, no-charge, royalty-free, irrevocable copyright license to reproduce, prepare Derivative Works of, publicly display, publicly perform, sublicense, and distribute the Work and such Derivative Works in Source or Object form.

3. Grant of Patent License. Subject to the terms and conditions of this License, each Contributor hereby grants to You a perpetual, worldwide, non-exclusive, no-charge, royalty-free, irrevocable (except as stated in this section) patent license to make, have made, use, offer to sell, sell, import, and otherwise transfer the Work, where such license applies only to those patent claims licensable by such Contributor that are necessarily infringed by their Contribution(s) alone or by combination of their Contribution(s) with the Work to which such Contribution(s) was submitted. If You institute patent litigation against any entity (including a cross-claim or counterclaim in a lawsuit) alleging that the Work or a Contribution incorporated within the Work constitutes direct or contributory patent

infringement, then any patent licenses granted to You under this License for that Work shall terminate as of the date such litigation is filed.

4. Redistribution. You may reproduce and distribute copies of the Work or Derivative Works thereof in any medium, with or without modifications, and in Source or Object form, provided that You meet the following conditions:

You must give any other recipients of the Work or Derivative Works a copy of this License; and
You must cause any modified files to carry prominent notices stating that You changed the files; and
You must retain, in the Source form of any Derivative Works that You distribute, all copyright, patent, trademark, and attribution notices from the Source form of the Work, excluding those notices that do not pertain to any part of the Derivative Works; and
If the Work includes a "NOTICE" text file as part of its distribution, then any Derivative Works that You distribute must include a readable copy of the attribution notices contained within such NOTICE file, excluding those notices that do not pertain to any part of the Derivative Works, in at least one of the following places: within a NOTICE text file distributed as part of the Derivative Works; within the Source form or documentation, if provided along with the Derivative Works; or, within a display generated by the Derivative Works, if and wherever such third-party notices normally appear. The contents of the NOTICE file are for informational purposes only and do not modify the License. You may add Your own attribution notices within Derivative Works that You distribute, alongside or as an addendum to the NOTICE text from the Work, provided that such additional attribution notices cannot be construed as modifying the License.

You may add Your own copyright statement to Your modifications and may provide additional or different license terms and conditions for use, reproduction, or distribution of Your modifications, or for any such Derivative Works as a whole, provided Your use, reproduction, and distribution of the Work otherwise complies with the conditions stated in this License.
5. Submission of Contributions. Unless You explicitly state otherwise, any Contribution intentionally submitted for inclusion in the Work by You to the Licensor shall be under the terms and conditions of this License, without any additional terms or conditions. Notwithstanding the above, nothing herein shall supersede or modify the terms of any separate license agreement you may have executed with Licensor regarding such Contributions.

6. Trademarks. This License does not grant permission to use the trade names, trademarks, service marks, or product names of the Licensor, except as required for reasonable and customary use in describing the origin of the Work and reproducing the content of the NOTICE file.

7. Disclaimer of Warranty. Unless required by applicable law or agreed to in writing, Licensor provides the Work (and each Contributor provides its Contributions) on an "AS IS" BASIS, WITHOUT WARRANTIES OR CONDITIONS OF ANY KIND, either express or implied, including, without limitation, any warranties or conditions of TITLE, NON-INFRINGEMENT, MERCHANTABILITY, or FITNESS FOR A PARTICULAR PURPOSE. You are solely responsible for determining the appropriateness of using or redistributing the Work and assume any risks associated with Your exercise of permissions under this License.

8. Limitation of Liability. In no event and under no legal theory, whether in tort (including negligence), contract, or otherwise, unless required by applicable law (such as deliberate and grossly negligent acts) or agreed to in writing, shall any Contributor be liable to You for damages, including any direct, indirect, special, incidental, or consequential damages of any character arising as a result of this License or out of the use or inability to use the Work (including but not limited to damages for loss of goodwill, work stoppage, computer failure or malfunction, or any and all other commercial damages or losses), even if such Contributor has been advised of the possibility of such damages.

9. Accepting Warranty or Additional Liability. While redistributing the Work or Derivative Works thereof, You may choose to offer, and charge a fee for, acceptance of support, warranty, indemnity, or other liability obligations and/or rights consistent with this License. However, in accepting such obligations, You may act only on Your own behalf and on Your sole responsibility, not on behalf of any other Contributor, and only if You agree to indemnify, defend, and hold each Contributor harmless for any liability incurred by, or claims asserted against, such Contributor by reason of your accepting any such warranty or additional liability.

END OF TERMS AND CONDITIONS

References

Castenda, D., et al. (2018). "A review on wearable photoplethysmography sensors and their potential future application in health care." Int J Biosens Bioelectron. **4**(4): 195-202.

Elgendi, M. (2012). "On the analysis of fingertip photoplethysmogram signals." Curr Cardiol Rev. **8**(1): 14-25.

Fine, J., et al. (2021). "Sources of inaccuracy in photoplethysmography for continuous cardiovascular monitoring." Biosensors **11**(126).

Ghamari, M., et al. (2016). "Design and prototyping of a wristband-type wireless photoplethysmographic device for heart rate variability signal analysis." Conf Proc IEEE Eng Med Biol Soc.: 4967-4970.

Organization, W. H. "Cardiovascular diseases." Retrieved 1/30/2022, 2022, from https://www.who.int/health-topics/cardiovascular-diseases.

Saha, S. "PPG-Signal-Processing." from https://github.com/ShoumikSaha/PPG-Signal-Processing.

Bluetooth Low Energy Protocol Stack — Bluetooth Low Energy Software Developer's Guide 3.00.00 Documentation. https://software-dl.ti.com/lprf/simplelink_cc2640r2_sdk/1.00.00.22/exports/docs/blestack/html/ble-stack/index.html#:~:text=The%20Bluetooth%20low%20energy%20protocol%20stack%20(or%20protocol%20stack)%20consists,two%20sections%20are%20implemented%20separately

"Why Is There A Global Semiconductor Chip Shortage and What Can We Expect? | GEP." GEP | Supply Chain & Procurement – Strategy, Software, Managed Services, https://www.gep.com/blog/mind/why-is-there-a-global-semiconductor-chip-shortage-and-what-can-we-expect

Yabuki, Ryosuke et al. "PPG and SpO2 Recording Circuit with Ambient Light Cancellation for Trans-Nail Pulse-Wave Monitoring System." 2019 IEEE Biomedical Circuits and Systems Conference (BioCAS) (2019): 1-4.

Maeda, Y., Sekine, M. & Tamura, T. Relationship Between Measurement Site and Motion Artifacts in Wearable Reflected Photoplethysmography. J Med Syst 35, 969–976 (2011).

Bestbier, Andre. (2017). Development of a vital signs monitoring wireless ear probe.

Texas Instruments, "AFE4403 Ultra-Small, Integrated Analog Front-End for Heart Rate Monitors and Low-Cost Pulse Oximeters" AFE4403 datasheet, May. 2014 [Revised April. 2021].

Texas Instruments, "AFE4404 Ultra-Small, Integrated AFE for Wearable, Optical, Heart-Rate Monitoring and Bio-Sensing" AFE4404 datasheet, June. 2015 [Revised Dec. 2016].

Han, S.; Roh, D.; Park, J.; Shin, H. Design of Multi-Wavelength Optical Sensor Module for Depth-Dependent Photoplethysmography. *Sensors* **2019**, *19*, 5441. https://doi.org/10.3390/s19245441

Analog Devices, “Multimodal Sensor Front End” ADPD4100/4101 datasheet, June. 2016.

Arduino, “Arduino Nano 33 BLE” Arduino 33 BLE datasheet, 2021

Nordic Semiconductor, “nRF52840” nRF52840 datasheet, Feb. 2019.

Raspberry Pi, “RP2040 Datasheet A microcontroller by Raspberry Pi” RP2040 datasheet, June. 2021.

STMicroelectronics, “”STM32F100x6” STM32F100x6 datasheet, Oct. 2009 [Revised Aug. 2018].

Texas Instruments, “AFE4403 Ultra-Small, Integrated Analog Front-End for Heart Rate Monitors and
Low-Cost Pulse Oximeters” AFE4403 datasheet, May. 2014 [Revised April. 2021].

“AG13, SG13, LR1154, SR44, 303, 357, A76, LR44 Battery Equivalents and Replacements.” Battery Equivalents and Replacements, https://www.batteryequivalents.com/ag13-sg13-lr1154-sr44-303-357-a76-lr44-battery-equivalents.html.

Shepard, Jeff, and Jeff Shepard. “The Difference between Primary and Secondary Battery Chemistries.” Battery Power Tips, 29 June 2021, https://www.batterypowertips.com/difference-between-primary-secondary-battery-chemistries-faq/.

“Market share of wearables unit shipments worldwide from 2014 to 2021, by vendor”, Federica Laricchia, Mar 17, 2022, Statista, https://www.statista.com/statistics/515640/quarterly-wearables-shipments-worldwide-market-share-by-vendor/#:~:text=Apple%20has%20the%20highest%20market,shares%20close%20to%2040%20percent. Accessed 3/21/2022

Baek, H. J., Shin, J., & Cho, J. (2018). The Effect of Optical Crosstalk on Accuracy of Reflectance-Type Pulse Oximeter for Mobile Healthcare. *Journal of Healthcare Engineering*, *2018*.